


Summer 2015

Gold nanoparticle enhancements in electroporation mediated DNA and RNA therapeutics

Shuyan Huang
Louisiana Tech University

Follow this and additional works at: <https://digitalcommons.latech.edu/dissertations>

 Part of the [Biomedical Engineering and Bioengineering Commons](#), and the [Chemical Engineering Commons](#)

Recommended Citation

Huang, Shuyan, "" (2015). *Dissertation*. 192.
<https://digitalcommons.latech.edu/dissertations/192>

This Dissertation is brought to you for free and open access by the Graduate School at Louisiana Tech Digital Commons. It has been accepted for inclusion in Doctoral Dissertations by an authorized administrator of Louisiana Tech Digital Commons. For more information, please contact digitalcommons@latech.edu.

**GOLD NANOPARTICLE ENHANCEMENTS IN
ELECTROPORATION MEDIATED DNA
AND RNA THERAPEUTICS**

by

Shuyan Huang, B.S., M.S.

A Dissertation Presented in Partial Fulfillment
of the Requirements of the Degree
Doctor of Philosophy

COLLEGE OF ENGINEERING AND SCIENCE
LOUISIANA TECH UNIVERSITY

August 2015

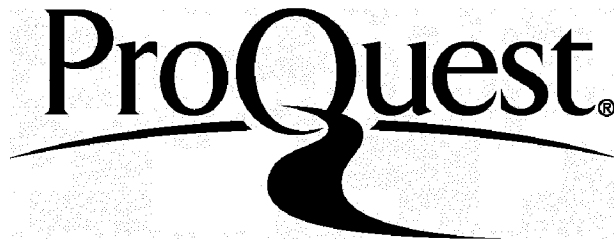
ProQuest Number: 3664524

All rights reserved

INFORMATION TO ALL USERS

The quality of this reproduction is dependent upon the quality of the copy submitted.

In the unlikely event that the author did not send a complete manuscript and there are missing pages, these will be noted. Also, if material had to be removed, a note will indicate the deletion.



ProQuest 3664524

Published by ProQuest LLC(2015). Copyright of the Dissertation is held by the Author.

All rights reserved.

This work is protected against unauthorized copying under Title 17, United States Code.
Microform Edition © ProQuest LLC.

ProQuest LLC
789 East Eisenhower Parkway
P.O. Box 1346
Ann Arbor, MI 48106-1346

LOUISIANA TECH UNIVERSITY

THE GRADUATE SCHOOL

MAY 11, 2015

Date

We hereby recommend that the thesis prepared under our supervision by
Shuyan Huang, B.S., M.S.

entitled Gold Nanoparticle Enhancements in

Electroporation Mediated DNA

And RNA Therapeutics

be accepted in partial fulfillment of the requirements for the Degree of

Doctor of Philosophy in Biomedical Engineering

Eng. Steve Jones

Supervisor of Thesis Research

Steven Jones

Head of Department

Biomedical Engineering

Department

Recommendation concurred in:

Steven Jones
Eng. Steve Jones
Jan M
Teresa A Murray

Advisory Committee

Approved:

J. P. ...

Director of Graduate Studies

Neil Hepburn

Dean of the College

Approved:

Sheryl S. Shauman

Dean of the Graduate School

ABSTRACT

Nonviral gene delivery methods have been explored as the replacement of viral systems for their low toxicity and immunogenicity. However, they have yet to reach levels competitive to their viral counterparts. Electroporation figured prominently as an effective nonviral gene delivery approach for its balance on the transfection efficiency and cell viability, no restrictions of probe or cell type, and operation simplicity. The commercial electroporation systems have been widely adopted in the past two decades but still carry drawbacks associated with the high applied electric voltage, unsatisfied delivery efficiency, and/or low cell viability. What we did was to improve electroporation performance by application of gold nanoparticles (AuNPs). By adding highly conductive AuNPs in an electroporation buffer solution, we demonstrated an enhanced electroporation performance (i.e., better DNA delivery efficiency and higher cell viability) on mammalian cells from two different aspects: the free, naked AuNPs reduced the resistance of the electroporation solution so that the local pulse strength on cells was enhanced; targeting AuNPs (e.g., Tf-AuNPs) were brought to the cell membrane to work as virtual microelectrodes to porate the cells with a limited area from many different sites.

The enhancement was confirmed with leukemia cells in both a commercial batch electroporation system and a home-made flow-through system using gWizGFP plasmid DNA probes. Such enhancement depends on the size, concentration, and the mixing ratio

of free AuNPs/Tf-AuNPs. An equivalent mixture of free AuNPs and Tf-AuNPs exhibited the best enhancement with the transfection efficiency increasing 2-3 folds with minimum sacrifice of cell viability. This new delivery concept – the combination of nanoparticles and electroporation technologies – could be widely applied in various *in vitro* and *in vivo* delivery routes of nucleic acids, anticancer drugs, or other therapeutic materials. In the second part of this dissertation, we further demonstrated its success in the enhancement of polyplex delivery of DNA. Specifically, AuNPs were used to carry polyplex (a chemical approach) while electroporation (a physical approach) was applied for fast and direct cytosolic delivery. AuNPs of various sizes were first coated with polyethylenimine, which were further conjugated with DNA plasmids to form AuNPs-polyplex. The hybrid nanoparticles were then mixed with cells and introduced into cell cytosol by electroporation.

In this hybrid approach, cationic polymer molecules condense and/or protect genetic probes, while AuNPs help fix polycations to reduce their cytotoxicity and promote the transfection efficiency of electroporation. The delivery efficiency was evaluated with model adherent cells (i.e., NIH 3T3) and suspended cells (i.e., K562) together with their impact on cell viability. We found that AuNP-polyplex showed 1.5-2 folds improvement on the transfection efficiency with no significant increase of toxicity when compared to free plasmid delivery by electroporation alone. Such a combination of physical and chemical delivery concepts may be further developed for the delivery of various therapeutic materials for both *in vitro* and *in vivo* applications. Thirdly, we tried nanoparticle enhanced delivery of small nucleotide including siRNA and miRNA as further proof of our concept. AuNPs are used to enhance the strength of the local electric

field and conjugated with the polyplex to reduce the cytotoxicity. The RNA release, expression, and their effect in regulating the target genes were justified.

APPROVAL FOR SCHOLARLY DISSEMINATION

The author grants to the Prescott Memorial Library of Louisiana Tech University the right to reproduce, by appropriate methods, upon request, any or all portions of this Dissertation. It is understood that "proper request" consists of the agreement, on the part of the requesting party, that said reproduction is for his personal use and that subsequent reproduction will not occur without written approval of the author of this Dissertation. Further, any portions of the Dissertation used in books, papers, and other works must be appropriately referenced to this Dissertation.

Finally, the author of this Dissertation reserves the right to publish freely, in the literature, at any time, any or all portions of this Dissertation.

Author 黄淑燕 S. Huang

Date 07/21/15

DEDICATION

This dissertation is dedicated to my whole family who has supported me during my studies all through these years.

TABLE OF CONTENTS

ABSTRACT.....	iii
DEDICATION.....	vii
LIST OF FIGURES	xii
ACKNOWLEDGMENTS	xvi
CHAPTER 1 INTRODUCTION.....	1
1.1 Research Hypothesis.....	1
1.1.1 Central Problems.....	1
1.1.2 Objectives	2
1.2 Approaches	3
1.3 Structure.....	4
CHAPTER 2 LITERATURE REVIEW.....	5
2.1 Motivations	5
2.1.1 Genetic Therapy for Diseases	5
2.1.2 Virus Vectors in Gene Delivery.....	6
2.2 Polymers in Gene Delivery.....	7
2.2.1 Poly-L-lysine.....	7
2.2.2 Polyethylenimine	8
2.2.3 Chitosan	10
2.2.4 Polyethylene Glycol.....	11
2.3 Application of Gold Nanoparticles in Gene Delivery	12
2.3.1 Historic Introduction.....	12

2.3.2	Synthesis and Modification of Gold Nanoparticles	13
2.3.3	The Applications of Gold Nanoparticles in Gene Delivery	14
2.4	Electroporation in Molecules Delivery	15
2.4.1	Introduction.....	15
2.4.2	Explanations to Electroporation	17
2.4.3	Electrical Factors in Electroporation	18
2.4.4	Non-electrical Factors in Electroporation	19
CHAPTER 3 GOLD NANOPARTICLE ENHANCED ELECTROPORATION IN MAMMALIAN CELL TRANSFECTION.....		21
3.1	Introduction.....	21
3.2	Materials and Methods.....	24
3.2.1	Materials and Reagents	24
3.2.2	Cell Culture	25
3.2.3	Thiol Modification of Transferrin.....	25
3.2.4	Preparation of Transferrin-AuNPs	26
3.2.5	Electroporation with Naked AuNPs.....	26
3.2.6	Electroporation with the Mixture of Naked AuNPs/Tf-AuNPs.....	27
3.2.7	Electroporation in Flow-Through Electroporation System.....	28
3.2.8	Determination of DNA Delivery Efficiency.....	28
3.2.9	Measurement of Cell Viability.....	29
3.2.10	AuNPs Imaging and Tracking <i>In Vitro</i>	29
3.2.11	Simulation on the Focusing Effect of AuNPs.....	30
3.3	Results and Discussion	31
3.3.1	AuNPs Enhancement on the Transfection of Mammalian Cells	31
3.3.2	Dependence of Electroporation Enhancement on the Concentration of AuNPs.....	36

3.3.3	The Dependence of Electroporation Enhancement on the Size of AuNPs ...	39
3.3.4	Enhancing Localized Electroporation with Transferrin-AuNPs.....	41
3.3.5	AuNP Imaging and Tracking <i>In Vitro</i>	45
3.3.6	Enhancement Performance of AuNPs in Fibroblast	46
3.4	Conclusions.....	50
CHAPTER 4 GOLD NANOPARTICLES ELECTROPORATION ENHANCED POLYPLEX DELIVERY TO MAMMALIAN CELLS.....		52
4.1	Introduction.....	52
4.2	Materials and Methods.....	54
4.2.1	Materials and Reagents	54
4.2.2	Preparation of AuNPs-polyplex.....	54
4.2.3	NIH 3T3 and K562 Cell Culture.....	54
4.2.4	Electroporation Setup and Procedure.....	55
4.2.5	Determination of AuNPs-polyplex Delivery Efficiency.....	56
4.2.6	Measurements of Cell Viability	56
4.2.7	Cellular Uptake of AuNPs-polyplex Nanoparticles.....	57
4.3	Results and Discussions.....	57
4.3.1	AuNPs-polyplex Size and Size Distribution.....	57
4.3.2	Cellular Uptake of AuNPs-polyplex via Electroporation	60
4.3.3	Plasmid DNA Delivery in NIH 3T3 Cells by AuNPs-polyplex	63
4.4	Conclusions.....	69
CHAPTER 5 GOLD NANOPARTICLE ENHANCED SMALL NUCLEOTIDE MOLECULE DELIVERY BY ELECTROPORATION TO MAMMALIAN CELLS ...		71
5.1	Introduction.....	71
5.2	Materials and Methods.....	73
5.2.1	Materials and Reagents	73

5.2.2	Preparation of AuNPs-polyplex.....	73
5.2.3	NIH 3T3 and K562 Cell Culture.....	74
5.2.4	Electroporation Setup and Procedure.....	75
5.2.5	Measurements of Cell Viability.....	75
5.2.6	AuNPs-polyplex Delivery Efficiency of Small Interfering RNA.....	75
5.2.7	AuNPs-polyplex Delivery Efficiency of microRNA.....	76
5.2.7.1	Total RNA Extraction.....	76
5.2.7.2	Reverse Transcription PCR.....	77
5.2.7.3	qRT-PCR Amplification.....	78
5.3	Results and Discussion.....	78
5.3.1	Gold Nanoparticle-Enhanced siRNA Delivery.....	78
5.3.2	Gold Nanoparticle-Enhanced miRNA Delivery.....	80
5.3.3	siRNA Delivery by AuNPs-polyplex.....	81
5.3.4	miRNA Delivery by AuNPs-polyplex.....	85
5.4	Conclusions.....	86
CHAPTER 6 CONCLUSIONS AND FUTURE WORK.....		88
6.1	Conclusions.....	88
6.2	Future Work.....	89
LIST OF PUBLICATIONS AND CONFERENCE PROCEEDINGS.....		91
BIBLIOGRAPHY.....		93

LIST OF FIGURES

- Figure 1-1:** Reaction scheme of Traut’s Reagent with molecules containing primary amines. 3
- Figure 3-1:** Schematic illustration on the mechanism of AuNPs enhancement on electroporation: (A) The pulse enhancement effect through minimizing the electric voltage consumed by the low conductive electroporation buffer during electroporation. By adding highly conductive AuNPs, more percentage of the overall electric voltage across the two electrodes is allocated on cells to have focused pulses when compared to the use of electroporation buffer alone; (B) localized electroporation when AuNPs are brought to the cell membrane through affinity binding with receptors there. The electric field is converged on the conductive AuNPs, and these AuNPs could serve as virtual electrodes to polarize only a limited area on the cell membrane when they stay nearby. 22
- Figure 3-2:** Gold nanoparticles enhancement on electroporation of K562 cells with a commercial batch electroporation (labeled as “BTX”) system and a home-made semi-continuous microchannel system (labeled as “microchannel”). Panel (A) exhibits fluorescence and phase contrast microscopic images of pGFP plasmid transfection through BTX, BTX with AuNPs, Microchannel, and Microchannel with AuNPs. The left side shows expression of GFP by the cells, and the right panel shows the cells under phase contrast microscopy. Panels (B) and (C) are the quantitative results of the transfection efficiency (B) and the cell viability (C). The concentration of AuNPs use here is 5X or 0.05 wt% (0.5 mg/mL). n = 6 and (***) represents $p < 0.005$ 32
- Figure 3-3:** Simulation of the electric field focusing effect of AuNPs in electroporation. (A) The model and mesh setup for one AuNP embedded in the membrane of a K562 cell. (B) The calculated electric field lines around the AuNP. (C) The electric field lines around a transient pore on the cell membrane in the presence of one AuNP present. 35

- Figure 3-4:** Dependence of the pulse enhancement on the size and concentration of free AuNPs: panels ((A)-(B)) are the cell viability (A) and the transfection efficiency (B) with an overall pulse strength of 625 V/cm and panels ((C)-(D)) are the results with an overall pulse strength of 475 V/cm (panel (C): the cell viability; panel (D): the transfection efficiency). The blue and red dashes refer to the cell viability and the transfection efficiency of electroporation with naked DNA at the optimal conditions (675 V/cm, single pulse of 10ms), respectively. 1X AuNPs refers to 0.01 wt% or 0.1 mg/mL gold content (n = 3). 37
- Figure 3-5:** Localized electroporation enhancement with Tf-AuNPs: (A) schematics of grafting Tf-AuNPs as virtual electrodes on the cell membrane, (B) the localized enhancement with Tf-AuNPs alone at various binding stages. The AuNPs used here are 20 nm with 1 X concentration (0.1 mg/mL). (n = 3) 42
- Figure 3-6:** The combined enhancement of the pulse strength focusing and localized electroporation effects using a mixture of free AuNPs and Tf-AuNPs of various mixing ratios with a total AuNPs concentration of 1 X (A) and 5 X (B) with the pulse strength of 625 V/cm and 475 V/cm. AuNPs of 20 nm were used here (n = 3). 44
- Figure 3-7:** The confocal microscope images of the cellular uptake of AuNPs before and after electroporation: ((A)-(B)) for free FNPs and ((C)-(D)) for Tf-FNPs. Images in panels (A) and (C) were taken before electroporation and panel (B) and (D) were after electroporation. FNPs of 10 X or 0.1 wt% (1.0 mg/mL) were used in all samples and Tf-FNPs were incubated with the cells for 4 hr. 46
- Figure 3-8:** The pulse enhancement of free AuNPs (5 nm) on NIH 3T3 cells: panels (A) present phase contrast and fluorescence microscopic images of cells after BTX electroporation with naked DNA alone, with 0.4 X, 1 X, and 2 X AuNPs, respectively. Panel (B) is the summary of the quantified cell viability by MTS assay and the transfection efficiency by flow cytometry. A single pulse with 10 ms pulse duration and 625 V/cm overall pulse strength was imposed for all samples and 1X AuNPs refers to 0.01 wt% or 0.1 mg/mL gold content. n = 3 and (***) represents $p < 0.005$ 48
- Figure 3-9:** The pulse enhancement of AuNPs for electroporation of NIH 3T3 cells with a commercial batch electroporation (labeled as “BTX”) system and a home-made semi-continuous microchannel system (labeled as “SFE”). Panels (A) and (B) are the quantitative results of the cell viability and transfection efficiency, respectively (n = 3). 49
- Figure 4-1:** Schematic illustration on the procedure of AuNPs-polyplex synthesis and delivery. 53

- Figure 4-2:** The AFM images of AuNPs-polyplex morphology with the original size of AuNPs of (A) 5 nm, (B) 10 nm, (C) 30 nm, and (D) 40 nm. Panel (E) is the traditional polyplex synthesized through the vortex mixing approach [4]. Panel (F) is the quantitative dynamic light scattering (DSL) particle size measurement. 59
- Figure 4-3:** Schematic of AuNPs-polyplex formation involving conjugation networking of multiple AuNPs with DNA probes. 60
- Figure 4-4:** Phase contrast and fluorescence microscopic images of distribution and fate of AuNPs-polyplex when mixing with NIH 3T3 cells (A-E) and immediately after electroporation (F-I): (A) untreated samples (negative control); (B) mixture of cells and naked DNA plasmids (green); (C) mixture of cells and FNP (red); (D) mixture of cells with FNP/PEI nanoparticles; (E) mixture of cells with FNP/PEI/DNA; (F) electroporation with DNA alone (green); (G) electroporation with FNP (red); (H) electroporation with FNP/PEI; and (I) electroporation with FNP/PEI/DNA. The 100 X objective was used. 62
- Figure 4-5:** Fluorescence and phase contrast microscopic images of pGFP plasmid transfection to NIH 3T3 cells by electroporation. 64
- Figure 4-6:** Fluorescence and phase contrast microscopic images of pGFP plasmid transfection to NIH 3T3 cells by polyplex and AuNPs-polyplex electroporation. 64
- Figure 4-7:** Quantitative measurement of electroporation enhanced AuNPs-polyplex delivery performance on 3T3 cells: (A) the flow cytometry results on transfection efficiency and (B) the cell viability via MTS assay. As comparison, results from electroporation with DNA alone, polyplex, and samples of a simple mixing of AuNPs and DNA are also shown. The error bars correspond to triplicate experiments made with independently produced batches. $n = 3$ and (***) represents $p < 0.001$ 66
- Figure 4-8:** The viability of NIH 3T3 cells when incubated with AuNP-polyplex and polyplex determined by MTS assay. PEI is the cationic polymer used here and the incubation was performed at various N/P ratios. The cell viability of commercial bulk electroporation (labeled as “BTX”) is also provided for comparison purpose ($n = 3$). 67
- Figure 4-9:** Comparison of AuNPs-polyplex electroporation was compared to traditional transfection approaches PEI/DNA polyplex at two different N/P ratios (6.6 and 10) and lipo2000 at two different dosages (“optimal” refers to the protocol recommended dosage; and “scaled up” refers to the case with increased lipo2000 dose to match the actual DNA amount use in electroporation) ($n = 3$). 69

Figure 5-1: AuNPs electroporation enhanced siRNA delivery: (A) fluorescence images and (B) intensity measurements on GFP expression level. n = 3 and (***) represents p < 0.001..... 69

Figure 5-2: Preliminary result for AuNPs enhanced miR-29b delivery in K562 cells: (A) mature miR-29b expression (all expression levels were normalized to bulk electroporation) (B) targeting genes expression. 81

Figure 5-3: AuNPs-polyplex electroporation enhanced siRNA delivery in 3T3 cells: (A) fluorescence images and (B) intensity measurement on GFP expression level. n = 3 and (*) represents p < 0.05, (***) represents p < 0.001. 83

Figure 5-4: AuNPs-polyplex electroporation enhanced siRNA delivery in 3T3 cells: (A) fluorescence images and (B) intensity measurement on GFP expression level, and (C) the luminescence measurement on luciferase expression level for free siRNA ("pMax + siRNA" and "pLuc + GL3") and siRNA from AuNPs-polyplex ("pMax + AuNP/PEI/siRNA" and "pLuc + AuNP/PEI/GL3"). n = 3 and p < 0.05, (***) represents p < 0.001 84

Figure 5-5: Preliminary result for AuNPs-polyplex enhanced miR-29b delivery in K562 cells: (A) mature miR-29b expression (B) targeting genes expression. "Au/PEI/miR29b incubation" stands for transfection with AuNPs-polyplex without electroporation. All expression level were normalized to untreated cells (control) 86

ACKNOWLEDGMENTS

In the past several years, I have had the honor of interacting with many people that assisted in various ways in my dissertation research. I am indeed very grateful to every one of them.

First, I would sincerely like to thank my advisor Dr. Shengnian Wang for his continuous support. He was always there to meet and talk about my ideas, research, and to ask pertinent questions to help me think through my problems. The research experience gained during this work could not be possible without his support, guidance and encouragement. Thank you for all your insight.

I am grateful to Dr. Eric J. Guilbeau, Dr. Steven A. Jones, Dr. Teresa A. Murray, and Dr. Jamie J. Newman for being my committee members. I appreciate all their encouragement, suggestions, and positive comments. Thank you all for allowing me to draw from your wealth of experience.

I am also grateful to Dr. James Spaulding, Ms. Debbie Wood, and Dr. Alfred Gunasekaran for their generous help and support. Thank you for all your time.

Special thanks to other members in Dr. Wang's group who assisted in this work – Juan Chen, Harshavardhan Deshmukh, Xuan Liu, Yang Lu, Kartik K. Rajagopalan, Vandhana Ramamoorthy, Fangfang Ren and Yingbo Zu. Thank you for the time and knowledge that we shared.

I would also like to acknowledge the support from my family and friends. They were always there cheering me up and stood by me through good and bad times. To my parents, thank you for letting me be away from you these years so I could pursue my dreams. Special thanks to my husband, Dr. Hui Xia, for standing by me through this journey. Your support was invaluable and will always be treasured. Thank you, Ms. Juan Chen, Dr. Emmanuel Ogbonnaya, Dr. and Mrs. Lee Kirby for your friendship and encouragement over the years. Thank you for being there whenever I need you most.

Finally, I would like to thank my country, China, which granted me the view of the world, the life and values of everything.

CHAPTER 1

INTRODUCTION

1.1 Research Hypothesis

1.1.1 Central Problems

A variety of non-viral strategies are becoming favorable alternatives to viral transduction, having a low risk of oncogenesis and inflammation [1, 2]. Potent therapeutic molecules are condensed or protected by cationic polymer or lipid via forming complexes (e.g. polymer-DNA complexes, lipo-DNA complexes) which help overcome multiple delivery barriers. Several molecules or probes, including plasmids, oligonucleotides, ribozymes, or small interfering RNAs, have been successfully tested with these strategies [3-15]. However, many of them showed slow and inefficient cellular uptake, high cytotoxicity, and/or low expression efficiency.

Simultaneously, physical gene delivery methods, electroporation in particular, have been explored with attractive features including surgery-like treatment, quick delivery response, and almost no restrictions on cell type and exogenous material properties. They have been widely used to reveal biological functions and transport at cellular level as well as to facilitate the delivery of various molecular probes. Conventional electroporation has been reasonably successful, but it has several major drawbacks, including high required voltages, large DNA consumption, low transfection efficiency, and/or cell viability.

1.1.2 Objectives

We hypothesized that the application of gold nanoparticles (AuNPs) in electroporation could improve the transfection performance of both electroporation and polyplex mediated DNA and RNA delivery strategies. With high conductivity, AuNPs could significantly reduce the potential drop consumed between the two electrodes needed in electroporation, and the local pulse strength on cells is highly focused. After tagging targeting molecules, AuNPs are brought to the cells to further limit the pulse induced polarization area within tiny spots on the cell membrane. In this way, the temporary permeable openings during electroporation will be greatly increased in number with each a limited size. This helps the following cell membrane recovery and the eventual cell survival rate.

Besides the enhancement of gold nanoparticles on electroporation, we also looked into their contribution to polyplex delivery. Because of their monodispersed size and consistent surface area and charge, gold nanoparticles help control the payload of cationic polymer on individual particles and the dimensions of hybrid polyplex nanoparticles. Together with good protection of DNA and RNA probes in the serum, such hybrid structure helps minimize the free cationic polymers in polyplex samples and fix those dissociated ones during cytoplasmic release. As captured cationic molecules are found to be much less toxic to their free counterparts; this help reduce the common cytotoxicity issues associated with polyplex delivery [16]. Because of the presence of AuNPs, electroporation is also adopted to promote direct cytoplasmic delivery of polyplex to bypass the traditionally slow and inefficient endocytosis-mediated delivery route of the polyplex.

1.2 Approaches

Based on these hypotheses, AuNPs with various sizes and aspect ratios were applied in electroporation. AuNPs conjugated with transferrin (AuNPs-Tf) of various ratios were mixed with cells before electroporation. AuNPs-Tf were prepared by incubating AuNPs with transferrin that was thiolated by Traut's reagent (Figure 1-1). This helps bring AuNPs to cells via conjugation of transferrin with transferrin receptors (TfR) on the cell membrane. The enhancement was evaluated in both a commercial batch electroporation system and a home-made flow-through system.

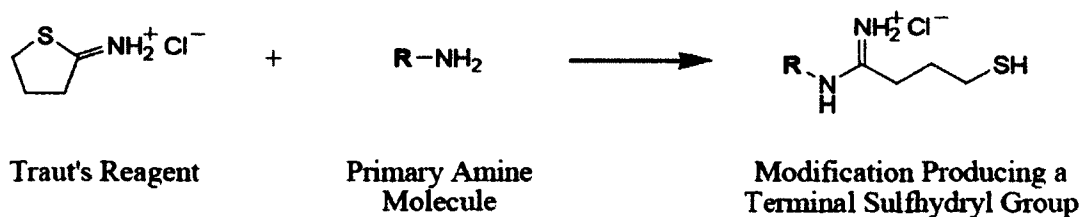


Figure 1-1: Reaction scheme of Traut's Reagent with molecules containing primary amines.

Polyethylenimine (PEI) was fixed on AuNPs by electrostatic interactions (AuNPs/PEI) via incubation of AuNPs and free PEI solution. The original citric acid terminated surface of AuNPs facilitates the deposition of PEI molecules through electrostatic interactions. Negatively charged DNA/RNA probes were conjugated to AuNPs/PEI to form AuNPs-polyplex.

We evaluated these hypotheses and concepts with model systems with DNA/RNA delivery to both adherent (e.g., NIH 3T3) and suspended cells (e.g., K562). The delivery enhancement was evaluated by measuring the cell viability and transfection efficiency of DNA and RNA probes.

1.3 Structure

Chapter 1 introduces the central problems and objectives for this research project- the research approaches and the organization of this dissertation are shown. Chapter 2 provides a literature review on relevant research work involving electroporation, polyplex, and other nanoparticles based DNA and RNA delivery. Chapter 3 demonstrates free and transferrin-grafted AuNPs enhanced electroporation in mammalian cell transfection. Chapter 4 demonstrates the advantage of AuNPs electroporation enhanced polyplex delivery to mammalian cells. Chapter 5 describes the AuNP enhanced RNA delivery to mammalian cells. Chapter 6 concludes the results of the dissertation and recommends some work worthy of further exploration.

CHAPTER 2

LITERATURE REVIEW

2.1 Motivations

2.1.1 Genetic Therapy for Diseases

In September of 1990, a four-year old girl with adenosine deaminase (ADA) deficiency became the first gene therapy patient at the NIH clinical center [17].

Thereafter, gene therapy has become the research focus in many pharmaceutical, medical, biochemical and chemical labs over the world. In general, the technique of gene therapy includes identifying suitable nucleic acid sequences and cell types, as well as developing feasible methods to deliver enough genetic probes into these cells, while the therapeutic range involves the diagnosis of genetic diseases, depression of tumor development, fighting against viral infections, and so forth. During the last 30 years, hundreds of gene therapy studies have been conducted, while more and more efforts (more than 70%) of genetic therapy were steered to cancer-related research [18].

Cancer development usually involves multiple alterations on the gene level of cancer cells [19]. The balance between oncogenes and tumor suppressor genes plays a pivotal role in carcinogenesis. The oncogenes facilitate cell proliferation, while tumor suppressor genes program apoptosis. Based on this understanding, anti-oncogenes and apoptosis related genes are usually used in cancer treatments.

Among various therapeutic strategies, how to deliver genes efficiently remain one of the major challenges. Naked nucleic acids could be successfully delivered into tumors [20, 21]; however, they can be easily cleared out and gain poor efficiency for systematic delivery [22]. Therefore, exogenous gene vehicles are needed with the purpose of protection. In general, those gene vehicles could be categorized as two groups: viral and non-viral systems. The viral delivery systems exhibit high efficiency while they also carry obvious limitations: viral vectors would be confronted by host immune responses and the size of inserted genetic materials is also limited by the carrier capacity [23]. The non-viral systems can avoid these limitations, while their delivery efficiency is not yet competitive to their viral counterparts.

2.1.2 Virus Vectors in Gene Delivery

In virus-mediated gene delivery, several viral vectors are popular, including retrovirus, adenovirus, herpes simplex virus (HSV), and adeno-associated virus (AAV). Retroviruses are small RNA viruses with DNA intermediate. They are developed by replacing the vital viral genes with therapeutic ones, which will be integrated into the host genome. Despite their high transfection efficiency, most retroviruses only infect actively dividing cells. This makes them not work well with tumors as all tumors contain some non-dividing or resting cells [21, 24]. Adenoviruses are viruses which carry double strands of DNA. They could infect both dividing and non-dividing cells. However, their transfection is transient since they cannot integrate into the host cell genome. Therefore, repetitive treatment is generally needed [25-27]. HSVs are usually utilized to deliver genes into brain tumors since they infect the ending of sensory nerves and migrate to the neuronal cells [28, 29]. AAVs can infect both dividing and non-dividing cells as

adenoviruses, while integrating into the host genome like retroviruses. AAVs are less toxic than other virus vectors, but they usually need helper viruses which may bring contamination problems [30-32].

2.2 Polymers in Gene Delivery

Recent research interest in the field of gene delivery has been shifted greatly from viral vectors to non-viral systems because of the associated vector size limitation and immunogenicity issues. Among those non-viral transfection systems, cationic polymer-based polyplex nanoparticles are attracting much attention with acceptable efficiency and biocompatibility.

2.2.1 Poly-L-lysine

Poly-L-lysine (PLL) is a natural cationic polymer that has been widely used as genetic probe carrier in early polyplex synthesis. The size of PLL in the polyplex composition ranges from less than 20 to more than 1000 amine groups, typically with a size of less than 100 nm [33-39]. The main role of PLL in polyplex is to condense negatively charged molecules (DNA or RNA) and bind proteins as target ligands. In 1989, Wu *et al.* reported the modification of PLL with asialoorosomuroid (ASOR) which targets liver specific receptors, resulting in organ specific drug delivery [40]. In 1998, Schaffer *et al.* conjugated PLL with epidermal growth factors (EGF), enabling delivery to cells expressing EGF receptors [41]. Thereafter, several ligands have been used to modify PLL [42-44].

Nevertheless, the application of PLL polyplexes has been limited because of its poor stability *in vivo* [44-46]. Protein binding and salt aggregation might be the reasons for the rapid clearance of PLL polyplexes from blood [43, 47]. Ward *et al.* showed that

poor solubility, leukocyte stimulation, macrophage capture and complement activation might also contribute to poor blood circulation of PLL polyplexes [48]. To improve the *in vivo* performance of PLL conjugates, PEG modification was performed to form a shell protecting polyplexes from proteins [49, 50]. The molecular weight of PLL has also been considered as a factor which influence its stability. Larger molecular weight resulted in better stability in blood and higher expression level [43, 48].

2.2.2 Polyethylenimine

Polyethylenimine (PEI) is a synthesized cationic polymer that could electrostatically conjugate negatively charged nucleic acids with primary amine groups. PEI could be synthesized as linear or branched with various molecular weight (e.g., 2, 4, 25, 50, 70, 800 kDa). PEI can facilitate the endosomal escape based on its buffering capacity. The osmosis swelling happens when pH drops in PEI containing endosomes, which is the so-called “proton sponge effect”, resulting in release of PEI-nucleic acids complexes into cytoplasm [4, 51, 52]. Research has demonstrated that the transfection efficacy and cytotoxicity depend on molecular weight, compactness and modification of PEI [53, 54].

The traditional method of PEI-polyplex preparation is a simple bulk mixing process in which the adding order of reagents greatly influences the transfection efficiency. It has been demonstrated that adding the PEI solution to the plasmid solution results in 10-fold more efficiency than the opposite [4, 55]. The reason is that a single copy of plasmid is complexed into a polyplex when plasmid is added to the PEI solution, whereas multiple copies of plasmids are incorporated into a polyplex in the opposite mixing order. Another consideration is the so-called “N/P ratio”, which is the ratio of the

molar ratio of nitrogen in the PEI to the phosphate in the nucleic acid. Studies have shown that plasmid is poorly condensed at N/P ratio around 3.3 leading to low transfection efficiency. Better efficiency could be achieved with an increase of N/P ratio; however, cell viability would be sacrificed [54, 56]. In our previous study, cytotoxicity became increasingly significant while N/P ratio was above 6.6 [57-61].

Aside from being an independent delivery vehicle, PEI is also used to coat other nanoparticles to improve their transfection performance. Duan *et al.* studied the complexation of PEI with quantum dots to deliver plasmids, and PEI (linear and branched with molecular weight of 0.423, 0.6 - 0.8, 1.2, 1.8 - 2, and 10 - 25 kDa) was chosen to enhance particle uptake and facilitate endosomal escape [62]. Xia *et al.* modified the surface of mesoporous silica nanoparticles with PEI and much higher affinity with nucleic acids was observed. The cellular uptake of those PEI coated particles was found significantly enhanced, which enabled efficient delivery and a more satisfied expression [63]. Several studies have also been done with PEI-coated magnetic particles. They were either synthesized in a PEI solution or mixed with it, resulting in covalent or electrostatic binding to PEI molecules. All of these strategies promoted gene delivery [64-68].

Besides magnetic particles, PEI coating of gold nanoparticles has also attracted great attention in recent years. Gold nanoparticle had already been used to deliver nucleic acids directly into the cells [69-73]. Elbakry *et al.* introduced a layer-by-layer strategy which provided a promising solution to the aggregation problem when AuNPs were assembled with nucleic acids [74]. Song *et al.* reported a new, simple method to prepare PEI-capped AuNPs by directly mixing HAuCl₄ solution with PEI [75]. The delivery of siRNA with these complex nanoparticles showed much higher efficiency and cell

viability compared to that when delivered with PEI alone. All of these studies indicate that the combination of PEI with AuNPs has great potential in gene delivery.

2.2.3 Chitosan

Chitosan is a biopolymer which is naturally produced by deacetylation of long-chain polymer, chitin [76, 77]. It is composed of two subunits, N-acetyl-glucosamine and D-glucosamine linked by β (1, 4)-glucosidic bonds. The amine groups in N-acetyl-glucosamine subunits, with a pKa value of around 6.5, provide high positive charge density from an acidic to a neutral pH range [78, 79]. Studies have shown that chitosan has good biocompatibility as well as the ability to increase the permeability of the cell membrane [80-82]. These properties enable chitosan as a favorable carrier for gene delivery.

Mumper *et al.* first reported the application of chitosan as a plasmid delivery carrier [83]. Thereafter, interests in chitosan have increasingly risen. Roy *et al.* prepared chitosan/DNA nanoparticles with diameters of 200-300 nm and successfully transfected HEK293 cells [84]. Richardson *et al.* demonstrated the protection effect of chitosan to plasmids from DNase *in vitro* [85]. There are also other studies on derived or modified chitosan for targeted transfection [86, 87].

Despite the gene condensation and protection functions, the transfection efficiency of chitosan complexes is relatively low [88]. The degree of acetylation and molecular weight of chitosan are the two main factors that influence its transfection efficiency. Some studies have already shown that plasmid binding efficacy and cellular uptake of chitosan complexes decreased with decreasing acetylation [89-92]. The influence of molecular weight could be explained by the chain entangle effect: the higher

the molecular weight, the easier for chitosan to entangle the free plasmids. As a result, chitosan with lower molecular weight is less efficient at conjugating and protecting plasmids, resulting in a low transfection [89, 92].

2.2.4 Polyethylene Glycol

The application of other cationic polymers in the polyplex is limited because of their cytotoxicity and poor *in vivo* stability. Polyethylene glycol (PEG) has been widely used as a copolymer in drug or gene delivery as an effort to overcome these limitations. Incorporation of PEG into polyplex formation, which is called PEGylation, has been reported to help increase stability of the particles, achieve extended circulation, and protect the carried probes from enzymes [59, 93-96].

Such an excellent feature of PEG is attributed to its popularity in copolymer construction. First, shielding the positive charges of polyplexes with PEG lowers the cytotoxicity and reduces the degradation of conjugated probes. The polymer-DNA/RNA complex is generally prepared with excess cationic polymers, which leads to a net positive charge. While it facilitates cellular uptake by interacting with negatively charged cell membrane, the high concentration of positively charged polyplex could induce cytotoxicity. At the same time, intracellular proteins could bind to the polyplex, resulting in rapid clearance and lower the delivery efficiency [47, 59, 97]. Kataoka *et al.* studied PEG-PLL block copolymer; the result showed that DNA was stable *in vitro* with the presence of DNase I in more than 60 min, while the transfection of DNA with this copolymer was higher than that with PLL only. In the *in vivo* tests with PEG-PLL complex, exogenous DNA was detected in the blood 30 min after the injection, while naked DNA was found degraded in 5 min [49, 98-100]. Petersen *et al.* investigated the

PEGylation of PEI and greatly reduced the cytotoxicity of PEI even if the transfection efficiency was not improved much [101]. Modifying the surface charge of nanoparticles with PEG could increase the water solubility since polymer-DNA/RNA complexes are kind of water resistant in their charge neutralized state [102]. A PEG-PLL dendrimer, synthesized by Choi *et al.* demonstrated that the water solubility of PEG-PLL-DNA complex was higher than PLL/DNA because of the introduction of PEG [103]. PEG could work as a molecule spacer between polymers and ligands to assist the binding of ligands to their receptors. Successful examples include the use of peptide conjugated PEG-PEI, lipoprotein conjugated PEG-PLL and folate conjugated PEG-PLL [104-106].

In spite of these advantages of PEG in polyplex formulation, some studies have shown that PEGylation reduced cellular uptake and decreased gene expression [93, 107, 108]. To minimize this negative influence of PEG, some cleavable copolymer configurations were further synthesized and explored [95, 109-112].

2.3 Application of Gold Nanoparticles in Gene Delivery

2.3.1 Historic Introduction

AuNPs are most stable nanoparticles with many favorable chemical and physical properties. This enables their applications in material science, electronics, or biomedical research. The extraction of gold started around the 5th century, and the early application of gold colloid was to make ruby glass or color ceramics. In 1857, Michael Faraday reported the reduction of an aqueous AuCl_4^- with phosphorus in CS_2 to form colloid gold which was of a deep red color [113]. However, the term “colloid” was not proposed until 1861 by Graham [114]. Various methods in the preparation of gold colloids were reported in the last century [115-127]. In the past twenty years, gold colloids (or AuNPs)

have attracted much attention as a non-viral drug or gene delivery carriers because of their good biocompatibility, large area volume ratio, controllable size and shape, and other favorable properties [69, 116, 128-143].

2.3.2 Synthesis and Modification of Gold Nanoparticles

The ease of surface modification led to an exciting development of AuNPs application in gene delivery. One of the most popular surface modifications of AuNPs is the citrate functionalization. Citrate-capped AuNPs could be steadily prepared with diameter ranges from 5 nm to 250 nm [116, 144]. Based on this well-established technique, studies investigated the relationship between the particle sizes and cell uptake. For example, Chan *et al.* reported that the size of the citrate-capped AuNPs did affect the cellular uptake amount [138]. Compared to AuNPs with diameters of 14 and 74 nm, AuNPs with diameters of 50 nm were more favorable for the internalization by HeLa cells. They supposed the non-specific binding of citrate-capped AuNPs with proteins contributed to the uptake [138]. Further studies also showed that binding some positively charged proteins (e.g., transferrin) could facilitate the particle internalization via endocytosis [137, 140]. Many other research work also used citrate functionalized AuNPs to construct more sophisticated complexes in order to increase the cellular uptake and affect cell response or target AuNPs to specific locations [71, 132, 145-147].

AuNPs of 1-3 nm stabilized by a monolayer of amine-terminated alkanethiolates could be synthesized with the Brust-Schiffrin method [148]. In physiological pH, positively charged amine groups could bind negatively charged nucleic acids. Retello *et al.* reported successful plasmids transfection by 2 nm AuNPs with the amine surface

groups [132]. Thomas et al. used PEI as amine provider in AuNPs synthesis and the resulting particles delivered plasmids more efficiently than PEI alone [69].

Other modifications of AuNPs involve the coating of peptides, antibodies and so forth. Feldheim *et al.* reported the conjugation of peptides to AuNPs, showing that peptides with both receptor-mediated endocytosis and nuclear localization signal facilitated the entry of AuNPs into the nucleus [147, 149, 150]. El-Sayed *et al.* demonstrated greater affinity of antibody modified AuNPs to cancerous cells, which may improve photothermal therapy [151]. In some cases, nucleic acids were thiolated for the attachment to AuNPs surface since gold has a high affinity to thiol groups.

2.3.3 The Applications of Gold Nanoparticles in Gene Delivery

Efficient delivery of nucleic acids often plays an important role in the treatment of various diseases [152, 153]. Its delivery involves the insertion of healthy copies of DNA or RNA probes in specific cells, which relies on either viral infection or nonviral membrane perturbation [154], but have safety concerns associated with oncogenesis, immunogenicity, and toxicity [2, 155]. Nonviral delivery approaches, including chemical and physical approaches, have been explored as replacements to natural viruses, but do not reach competitive levels to their viral counterpart [74, 143, 156-176]. Among nonviral approaches, gold nanoparticles (AuNPs) have been extensively explored in DNA or RNA delivery for their gold biocompatibility and unprecedented combination of therapeutic and imaging capability [74, 143, 162-165]. Through the unique gold-thiol chemistry and/or electrostatic interactions, AuNPs help improve the cellular uptake of molecular probes through similar internalization routes (i.e., endocytosis) as other nanoparticles. The long intracellular delivery barriers generally prevent many

nanoparticles from reaching the cytosol or nucleus, with the aid of cell penetrating peptides (CPPs), AuNPs-siRNA nanoconjugates were successfully demonstrated to reach cytosol directly to improve the delivery efficiency [166]. However, the low release extent of siRNAs from AuNPs still leads to poor transfection efficiency due to the high affinity of AuNPs and therapeutic agents [167].

2.4 Electroporation in Molecules Delivery

2.4.1 Introduction

Compared to nanoparticle-mediated delivery routes, physical approaches have been used in the past two decades to deliver drugs or gene probes directly to the desired intracellular locations (e.g., cytosol or nucleus) to attain impressive benefits in various biomedical research and clinic trials [168-176]. Among them, electroporation figures prominently for their balance of simplicity, transfection effectiveness, fewer restrictions on probe or cell type, and operation convenience [172].

Electroporation or electropermeabilization has been known for decades and received increasing attention over the last thirty years. Electroporation is the application of external electric pulses to induce transient and reversible breakdown of cell membranes to deliver a variety of molecule probes into the cells. Because it delivers drug or genetic bypassing endocytosis and endosomal escape, much more efficient transfection has been achieved with electroporation. The first report of reversible cell electroporation was in 1982 [170]. Thereafter, over the last decades, electroporation has been developing from a laboratory technique to a clinic application [174, 175, 177-197].

In electroporation, transient pores are formed during electroporation, and molecules present around the cells get access to the cytoplasm [194]. After the pulses,

cell membranes reseal within a time scale from seconds to minutes. The membrane breakdown is achieved when the transmembrane potential superimposed onto the resting potential is above a threshold [198]. The transmembrane potential initiated by the external electric field is usually estimated by:

$$\Delta V = \frac{3}{2} r E_{ext} \cos \theta [1 - \exp(-\frac{t}{\tau_m})] \quad \text{Eq. 2-1}$$

where r is the radius of the cell, E_{ext} is the field strength, θ is the angle between the normal to the membrane and the direction of the field [199-202]. τ_m is the membrane charging time constant, given by:

$$\tau_m = \frac{r \epsilon_m}{2d \frac{\sigma_i \sigma_e}{\sigma_i + 2\sigma_e} + r \sigma_m} \quad \text{Eq. 2-2}$$

where σ_i , σ_m and σ_e are conductivities of the cytoplasm, cell membrane, and extracellular medium, respectively, ϵ_m is the dielectric permittivity of the membrane, and d is the membrane's thickness [203]. Because of the “ $\cos \theta$ ” component in Eq. 2-1, electroporation induced permeabilization will first happen at points facing electrodes. A theory has been established in the last century that the permeabilized area is larger at the point facing the positive electrode and permeabilization degree is greater at the point facing the negative electrode. Small molecules incline to diffuse into the cell via the pole facing the positive electrode, while large, especially negative charged molecules (electrophoretic effect is involved) prefer to enter through the pole facing the negative electrode [204]. Also indicated by Eq. 2-1, cells with a smaller radius require stronger external electric field to trigger permeabilization, further illustrating that intracellular organelles with a much smaller radius will not be easily permeabilized by the field, which is just sufficient for cell membrane poration.

2.4.2 Explanations to Electroporation

The effort to illustrate the mechanism of electroporation has been made consequently [198, 205-211]. Considerable progress of understanding the electroporation process has been achieved (the most popular explanation is briefly described above), although it is far from being fully understood.

The intracellular liquid is rich in ions and therefore highly conductive. For animal cells, the external environment (either *in vitro* culture medium or *in vivo* fluids) is also conductive. However, the cell membrane, which is a lipid bilayer, is nonconductive and insulates the cell inside from the outside. Therefore, two opposite charges will be accumulated at both sides of the cell membrane when a cell is placed in an external electric field. This condition leads to a transmembrane potential. Some reports demonstrated that the transmembrane potential needs to be above a threshold for at least 30-40 μs to make a complete membrane structural change. There were rapid changes in the conductivity of the tissue in the electric fields, which might be the indication of electroporation [212, 213]. Therefore, compared to “electroporation”, “electroporation” is actually a more exact term to define the change of the cell in the electric field; the membrane permeability of the treated cells is increased so that otherwise non-permeant molecules (usually large or hydrophilic and cannot diffuse across intact membranes) have a better chance of entering into the cytoplasm [213-215].

Formation of large hydrophobic pores was the first electroporation theory proposed by Eberhard Neumann [170]. It was confirmed later, to some extent, by some simulation studies [216-220]. Besides, several other explanations exist for the change in permeability of the cell membrane. Teissie *et al.* pointed out that the permeability change

could result from the electrocompression force generated during the pulses with the assumption that the force brought the two lipid layers closer and disrupted the order of the bilayer [221]. Lopez *et al.* demonstrated the increased permeability came from the change in orientation of lipids polar head [222]. These explanations support the theory of electropermeabilization without the formation of pores.

2.4.3 Electrical Factors in Electroporation

According to Schwan's equation, referring to Eq. 2-1, the strength of the external electric field determines the surface area that could be porated [200]. Afterwards, with the increasing understanding of the dynamic structural changes in the cell membrane, studies have examined the importance of pulse duration [223, 224]. Thereafter, many investigators made efforts to optimize these two electrical parameters so as to maximize the efficiency of delivery [170, 178, 179, 181, 225-228].

To date, it has been generally agreed that combinations of high voltage (larger than 1000 V / cm) with very short pulse duration (less than 100 μ s) and low voltage (lower than 200 V / cm) with longer pulse duration (longer than 20 ms) lead to effective electroporation. Some studies found that the sequential use of high voltage pulses and low voltage pulses worked even better with a possible explanation that high voltage porated the cell membrane while low voltage facilitated gene movements via electrophoretic forces [200, 201]. Satkauskas *et al.* also showed the advantages of using short high voltage pulses and long low voltages together [229, 230]. Moreover, they demonstrated that it was not necessary for plasmids to be present during the high voltage electroporation, but they had to be involved before the low voltage pulses [229].

For specific cell types or tissues, choices between high voltage and low voltage, long duration and short duration, single pulse and multiple pulses, or single set, and a combination of high voltage and low voltage are always the considerations for efficiency transfection. These factors need to be optimized according to other conditions.

2.4.4 Non-electrical Factors in Electroporation

Non-electrical factors should also be considered when establishing electroporation protocols because of their obvious impact on electroporation efficiency. These factors include the type of cells, and the size and formulation of DNA/RNA. The electroporation performance is known as cell type dependent. Therefore, for *in vitro* transfection, specific electroporation protocol has been established through trial-and-error. However, there is little chance for *in vivo* studies to transfect a certain type of cells selectively. As such, properties and formulations of nucleic acids consist of the main factors that impact their delivery by electroporation.

For gene delivery, the most common property of DNA/RNA which will directly influence the transfection should be the sizes. In general, smaller nucleic acids enter cells via electroporation more easily than larger ones. This size dependence explains, to some extent, why some researchers cannot achieve the claimed efficiency with some nucleofactors when they use larger plasmids other than the suggested ones. Another factor that impacts gene delivery is the methylation. To date, the DNA plasmid we use in electroporation are usually generated from *Escherichia coli*, which are in a high methylation format. Spath *et al.* reported a negative impact of this methylation on transfection efficiency with electroporation to lactic acid bacteria [231]. Even though no evidence has been shown the same situation on mammalian cells, it is worthy of notice

that methylation of promoter or surrounding regions may induce repression in gene expression because methylated plasmids might be restricted by methyl-dependent restriction enzymes [232, 233].

Another factor that influences transfection efficiency is the formulation of DNA/RNA probes, which is the solution in which nucleic acid is suspended during electroporation. The most commonly used formulation is sodium chloride (150 mM) [234]. Other formulations involve OptiMem and some additives. Nicol *et al.* reported that formulations with the addition of glutamate had the potential to improve transfection efficiency with electroporation [235]. Other studies showed the improvement on electroporation performance with modified formulations [236-240]. Moreover, researches on the relationship between cell types and formulation additives have also been conducted [241, 242].

CHAPTER 3

GOLD NANOPARTICLE ENHANCED ELECTROPORATION IN MAMMALIAN CELL TRANSFECTION

3.1 Introduction

Current electroporation systems have been reasonably successful while still carrying several major drawbacks that are associated with the high applied electric voltage and/or the lack of uniformity of electric pulses on all treated cells. The low electrical conductivity of the electroporation solution (e.g., for PBS, it is ~ 1.5 S/m) leads to the consumption of a large percentage of the overall applied voltage allocated on treated cells is much lower than expected, as illustrated in Figure 3-1A. Because of the physiological condition requirements, increasing the ion strength (e.g., salt concentration) of the electroporation buffer is not allowed to avoid such additional voltage consumption. To achieve the desired probe transfection efficiency, harsh electroporation conditions (e.g., high-voltage pulses) are therefore necessary to ensure enough permeabilization to the majority of treated cells. These conditions make electroporation inevitably accompanied with unwanted effects (e.g., strong electrochemical reactions, gas bubble issue, and Joule heating), which are harmful to the survival of treated cells [175]. Current protocols are often established on the compromise between acceptable transfection efficiency and cell viability. The recent introduction of microtechnology in electroporation research is devoted to the reduction of these issues through closely

patterning electrode pairs [182-193, 243-247]. However, these designs often sacrifice some favorite features of electroporation systems, namely simplicity, low-cost, and operation convenience.

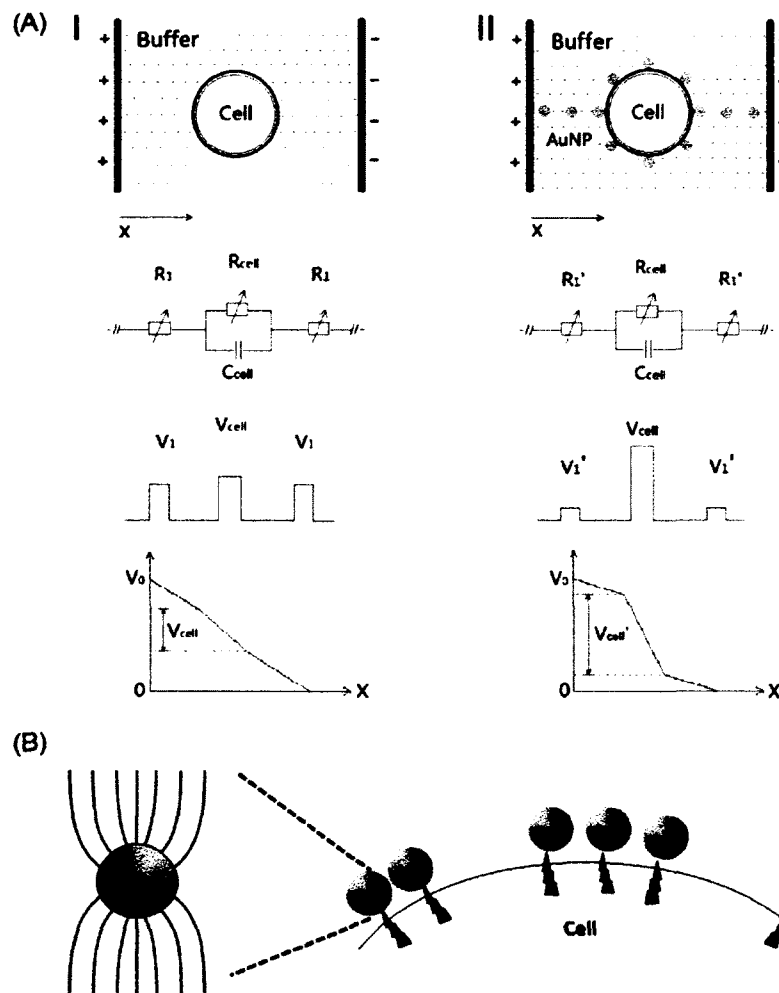


Figure 3-1: Schematic illustration on the mechanism of AuNPs enhancement on electroporation: (A) The pulse enhancement effect through minimizing the electric voltage consumed by the low conductive electroporation buffer during electroporation. By adding highly conductive AuNPs, more percentage of the overall electric voltage across the two electrodes is allocated on cells to have focused pulses when compared to the use of electroporation buffer alone; (B) localized electroporation when AuNPs are brought to the cell membrane through affinity binding with receptors there. The electric field is converged on the conductive AuNPs, and these AuNPs could serve as virtual electrodes to polarize only a limited area on the cell membrane when they stay nearby.

Here, we present a simple approach to enhance the transfection performance of electroporation that is compatible to most commercial electroporation instruments as well as the emerging micro/nanoelectroporation systems. In this new approach, free therapeutic probes (e.g., DNA plasmids) are directly introduced into cell cytosol through electroporation while AuNPs are added to locally enhance the electric pulse strength and control the poration area on the cell membrane with minimum operation changes. Because of the high conductivity of AuNPs ($\sim 4.5 \times 10^6$ S/m), the electric voltage consumed by it is greatly reduced so that most of the applied electric voltage is imposed on the cells. In addition, as the electric pulses converge in the vicinity of AuNPs, the particles work like many virtual microelectrodes when they are near the cells, with the focused field strength causing localized poration, as shown in Figure 3-1B. In contrast to bulk electroporation, where two large breakdown locations occur at the two poles of the cells facing the electrodes, electroporation with added nanoparticles is expected to cause multiple small poration sites on the cell membrane by AuNPs. The increased number of sites could benefit not only the recovery of the cell membrane and the survival of the cells, but also the uptake opportunity for the subjected probes from multiple sites.

To test our hypothesis on pulse focusing and localization effects of AuNPs, we added AuNPs to the electroporation solution, together with mammalian cells and DNA plasmids. Cells were then electroporated using both commercial bath-type electroporator (BTX 830 from Harvard Apparatus) and a home-made semi-continuous flow electroporator (SFE) [190, 247]. The pulse strength focusing was evaluated from two aspects: (i) electroporate cells in the presence of AuNPs under standard electroporation conditions, in which the cell viability should get worse as the electric pulse is focused by

AuNPs and cells received higher-than-optimal electric pulses; (ii) electroporate under less-effective conditions (i.e., low-voltage, more benign pulses), in which the focusing effect helps gain sufficient electrical strength for better transfection efficiency and/or cell viability. Human chronic leukemia cell line (K562 cells), a hard-to transfect cell line, was utilized in this investigation so that the localized electroporation with controlled polarization area and locations on the cell membrane could also be conveniently evaluated through ligand-receptor affinity binding. The electroporation enhancement evaluation was focused on the cell viability and transfection efficiency of a reporter gene (gWizGFP). Similar enhancement performance was also observed in NIH 3T3 cells, confirming the effectiveness of the enhancement roles AuNPs play in electroporation for both adherent and suspended cell lines.

3.2 Materials and Methods

3.2.1 Materials and Reagents

AuNPs of 5 nm, 10 nm, and 20 nm were obtained from Sigma-Aldrich. The concentration of 1X AuNPs refers to the stock solution, which has 0.01 wt% of Au (0.1 mg/ml) while the particle number varies with the size of AuNPs. Other concentrations of AuNPs were prepared by either concentrating or diluting from the stock solution. DNA plasmids with gWizTMGFP reporter were purchased from Aldevron, Inc. The plasmids are driven by modified cytomegalovirus promoter that is followed by the intron A from human CMV early gene and terminated by a highly efficient artificial transcription terminator. All other chemicals were purchased from Sigma-Aldrich and the cell culture reagents were purchased from Life Technologies (Carlsbad, CA) unless specified.

3.2.2 Cell Culture

K562 lymphoblast cells were also obtained from American Type Cell Culture (ATCC, Manassas, VA). K562 cells were cultured and maintained in RPMI 1640 media supplemented with 10% heat-inactivated fetal bovine serum (FBS), 100 U/mL penicillin, 100 g/mL streptomycin, and L-glutamine. For subculture, the desired amount of K562 cell suspension was transferred to a new Petri dish with the addition of the appropriate amount of fresh culture medium. All cultures were maintained at 37 °C with 5% CO₂ and 100% relative humidity.

NIH 3T3 cells were obtained from American Type Cell Culture (ATCC, Manassas, VA). They were grown and maintained in high-glucose DMEM supplemented with 10% newborn calf serum, 1% penicillin and streptomycin, 1% L-glutamine, and 1% sodium pyruvate. For subculture, culture medium was removed and discarded first. The cell layer was briefly rinsed with DPBS to remove the serum, which contains trypsin inhibitor. Then 1-2 mL trypsin-EDTA was added to a 100 cm² Petri dish. Cell culture was then observed under an inverted microscope until the cell layer was dispersed (usually 5-15 min). Eight to 9 mL complete growth medium was added and cells were aspirated by gently pipetting. An appropriate aliquot of the cell suspension was transferred to a new culture dish with addition of more growth medium to make a total volume of 10 mL for 100 cm² surface.

3.2.3 Thiol Modification of Transferrin

The desired amount of transferrin in 50 mM PBS buffer (with 5 mM EDTA, pH 8.0) was dissolved to make a concentration of 10 mg/mL. EDTA in PBS helps chelate divalent metals (e.g., Ca, Mg) in the solution, preventing the oxidation of sulfhydryls.

The Traut's Reagent was dissolved in deionized water to prepare the stock solution at a concentration of 2 mg/mL or 14 mM; 46 μ L Traut's Reagent stock solution was added to the transferrin solution (ten folds molar excess of the protein solution) and the mixture was incubated for 1h at room temperature. Then the solution was transferred to a dialysis cartridge (EMD Millipore, Amicon cartridge, Cat no. UFC805024) and centrifuged at a speed of $4,000 \times g$ for $20 \text{ min} \times 2$. The thiolated transferrin was collected from the top retentate by washing off with 50 mM PBS-EDTA solution, sterilized using 0.22 μ m Whatman filters, and stored in an aliquot at 4 $^{\circ}$ C.

3.2.4 Preparation of Transferrin-AuNPs

500 μ L of AuNPs aliquot of a desired size was centrifuged at $15,000 \times g$ for 10 min and supernatant was discarded. The AuNPs pellet was collected and dispersed in PBS (pH 7.4) to prepare AuNPs solutions of desired concentrations (0.001-0.1 mg/mL). The prepared AuNPs solution was mixed with sterilized thiolated transferrin solutions and incubated at 4 $^{\circ}$ C overnight. Then excess transferrin was removed by repeated centrifuge at $15,000 \times g$ for 10 min. The purified Tf-AuNPs solution was re-diluted in 250 μ L HBS solution and immediately used or stored at 4 $^{\circ}$ C in aliquot.

3.2.5 Electroporation with Naked AuNPs

NIH 3T3 cells or K562 cells were counted using hemocytometer to determine cell density, pelleted by centrifuging at $200 \times g$ for 5 min and then resuspended in fresh GIBCO OPTI-MEM I (a serum free medium) at desired densities of 0.5×10^6 - 0.5×10^7 cells/mL. Cell suspensions were then mixed with naked AuNPs of various concentrations (0.01 - 1.0 mg/mL) and sizes (5, 10, and 20 nm) along with 25 μ g DNA. Electroporation

with a commercial instrument (ECM 830, Harvard Apparatus) was done in electroporation cuvettes with a 2-mm gap, each containing a 100 μ L sample solution.

Here, the pulse strength focusing was evaluated from two aspects: (1) electroporate cells / AuNPs mixture at a standard electroporation protocol (single 10 ms pulse of 125 V/2 mm cuvette), in which the cell viability was supposed to get worse as the focused pulse cells received were higher than optimal; (2) electroporate cells / AuNPs mixture at more benign conditions (single 10 ms pulse of 95 V/2 mm cuvette), in which the focusing effect helped gain sufficient electrical strength for better transfection efficiency and similar or better cell viability. After electroporation, samples were transferred to 6-well cell culture plates, incubated in a fresh medium for another 24 hr, and then harvested for analysis.

3.2.6 Electroporation with the Mixture of Naked AuNPs/Tf-AuNPs

Cell samples were prepared with similar concentrations in GIBCO OPTI-MEM I medium, same as in section 3.2.5. Tf-AuNPs and cells were first incubated for 0.5-4.0 hours. Immediately before electroporation, naked AuNPs were added in to obtain a total of 100 μ L of cell suspension. The amount of naked AuNPs was adjusted to make appropriate mixing ratios of naked AuNPs and Tf-AuNPs (e.g., ~ 50% / 50%) and total gold concentrations (0.1 – 0.5 mg/mL) in the mixture. According to previous studies, it takes ~4 hr of incubation to accomplish complete affinity binding of transferrin to the transferrin receptors on the cells. For enhancement of the mixture of AuNPs / Tf-AuNPs, cells and AuNPs were incubated for 0.5 - 4 hr to check the difference [248]. The same electroporation protocols established in section 4.2.5 were used here. After

electroporation, samples were transferred to 6-well cell culture plates, incubated in fresh medium for another 24 hr, and then harvested for analysis.

3.2.7 Electroporation in Flow-Through Electroporation System

Cell samples were prepared with similar concentrations in GIBCO OPTI-MEM I medium, same as in section 4.2.5, and then pumped through the serpentine microchannel (length \times width \times depth = 37.5 mm \times 150 μ m \times 150 μ m) at a prespecified flow rate (1.8 mL/h). Electric pulses (76 pulses with each at 16 V, 10 ms) were added simultaneously through embedded Pt electrodes. In this system, cell suspension flowed through the microchannel in which the Pt electrodes also served as two-sided walls of the flow channels. When cells were pumped through, electric pulses were imposed in such a way that most cells only received one pulse inside the flow channel. This condition was accomplished by appropriately choosing the pulse frequency and the flow rate of cell suspension in the microchannel. Cells were then flushed out with Opti-MEM I medium and transferred to 6-well plates which were preloaded with a cell culture medium, incubated in a fresh medium for another 24 hr, and then harvested for analysis. Detailed SFE operation procedure can be found in our early publication [190].

3.2.8 Determination of DNA Delivery Efficiency

The transfection efficiency of gWizTMGFP plasmids was evaluated both qualitatively by visualizing the number of cells with green fluorescence within a representative area selected from the entire culture surface under an inverted fluorescence microscope (Olympus, Japan) and quantitatively by counting cells using a four-color flow cytometry system (FACS Calibur, BD Biosciences, CA) 24 hr post transfection. Briefly, an amount of 1.5×10^6 cells/mL was collected and the percentage of GFP-positive cells

was calculated quantitatively via flow cytometer. The unstained samples were run first to adjust the voltage setting and compensation of the flow cytometer. Then the tested samples were processed by CellQuest. At least 10,000 events were collected for each sample.

3.2.9 Measurement of Cell Viability

The cell viability was evaluated by an MTS cell proliferation assay (Promega, Madison, WI). Briefly, the cells in 100 μ L/well of the medium were transferred to a 96-well plate and incubated; 20 μ l of CellTiter 96 AQueous One solution (Promega, Madison, WI) was added to each well, and the cells were incubated at 37 $^{\circ}$ C for another 1 hr. Absorbance was measured at 492 nm on an automated plate reader (Elx 800, Biotek, VT). Normally grown cell samples were used as negative control whose viability was set to 100%. Data points were represented as the mean \pm standard deviation (SD) of triplicates, unless otherwise indicated.

3.2.10 AuNPs Imaging and Tracking In Vitro

The distribution, cellular binding, and uptake of AuNPs in K562 cells were examined by laser scanning confocal microscopy. The cells was washed twice with 1X PBS after mixing with red fluorescence of AuNPs (from Nanopartz, Inc.), followed by fixation with 4% paraformaldehyde for 30 min. Nuclei were stained with 20 μ M of DAPI for 5 min at room temperature. Cells from each sample were then mounted on cover glass slides. Images of phase contrast, red and blue fluorescence channels were taken on a Zeiss 510 META Laser Scanning Confocal microscopy (Carl Zeiss MicroImaging, Inc., NY) and then the merged images were produced using the LSM Imaging software. As AuNPs are well known to quench the fluorescent signal from

proximal fluorescent probes, a sandwich design of AuNPs (from Nanopartz, Inc., having fluorophores separated from the gold surface with polymer spacer) was used to circumvent this problem. Fluorophore labeled AuNPs with a CH₃ group terminated surface (FNPs, 10 nm for AuNP core) were used to represent free, naked AuNPs used in electroporation experiments. To visualize and track Tf-AuNPs, carboxylated AuNPs (FNP-COOH) were utilized. FNP-COOH nanoparticles (1 mg/mL in PBS) were first incubated with 1-Ethyl-3-(3-dimethylaminopropyl) carbodiimide (20 mg/mL in PBS) for 15 min at room temperature. Transferrin solution (0.4 mg/mL in PBS) was then added and incubated at room temperature for 24 hr to obtain FNPs with transferrin targeting probes (Tf-FNPs). Tf-FNPs particles were then purified by repeated centrifugation and resuspension in PBS for three times prior to the binding with transferrin receptors (TfR) on K562 cell surface.

3.2.11 Simulation on the Focusing Effect of AuNPs

A commercial finite-element methods (FEM) software, COMSOL (Mathworks, Natick, MA), was used to calculate the electric field around the cell in the presence of a single AuNP. We considered an axially symmetric model with one AuNP ($d = 20$ nm) embedded in the cell membrane (5 nm in thickness). A K562 cell ($D = 15$ μ m) was placed at the center of the left side boundary (the symmetrical axis) in the computation domain (60 μ m \times 20 μ m). A polar angle (θ) with respect to the electric field direction was defined and the AuNP was placed at the top of the cell where $\theta = 180^\circ$. An electric field ($E = 475$ V/cm) was assigned across the top and bottom of the computation domain and the right side boundary was set as the insulated wall. A three-layer cell model, divided as the external medium, the cell membrane, and the cell cytoplasm, was set up here [191, 249].

The electric field distribution around the nanoparticle and the cell was calculated by solving the Laplace equation using COMSOL:

$$\nabla \cdot (\sigma \nabla V) = 0 \quad \text{Eq. 3-1}$$

where σ is the electrical conductivity and V is the electrical potential. The electric field strength was then determined by $E = -\nabla V$. In this three-layer cell model, the electrical conductivity of buffer, cytoplasm, membrane, and gold particle was set as 0.8, 0.2, 5×10^{-7} , and 4×10^7 S/m, respectively.

3.3 Results and Discussion

3.3.1 AuNPs Enhancement on the Transfection of Mammalian Cells

We first electroporated K562 cells in both a commercial batch electroporation (labeled as “BTX”) system and a home-made semi-continuous microchannel system (labeled as “microchannel”), adopting the pulse conditions which were previously optimized with gWizTMGFP plasmids alone: 125 V (625 V/cm), single 10 ms pulse for the BTX system and 16 V (1067 V/cm), multiple 10 ms pulses for the microchannel system. Transfection was successful in all four cases: BTX without AuNPs, microchannel without AuNPs, BTX with AuNPs, and microchannel with AuNPs. Many cells in each case expressed green fluorescence protein (GFP) 24 hr after electroporation (Figure 3-2A). More quantitative comparison was done by counting the percentage of GFP positive cells (Figure 3-2B) and cell viability (Figure 3-2C). Efficiency of pGFP transfection from the microchannel was generally much better than that from BTX (BTX: $27.5 \pm 1.9\%$, SFE: $51.6 \pm 4.5\%$), which is consistent with our earlier observations [191, 247]. After adding AuNPs (5 nm at a concentration of 5X or 0.5 mg/ml), the transfection

percentage was significantly increased to $50.8 \pm 6.7\%$ for BTX electroporator and to $61.1 \pm 4.8\%$ for microchannel electroporator, respectively.

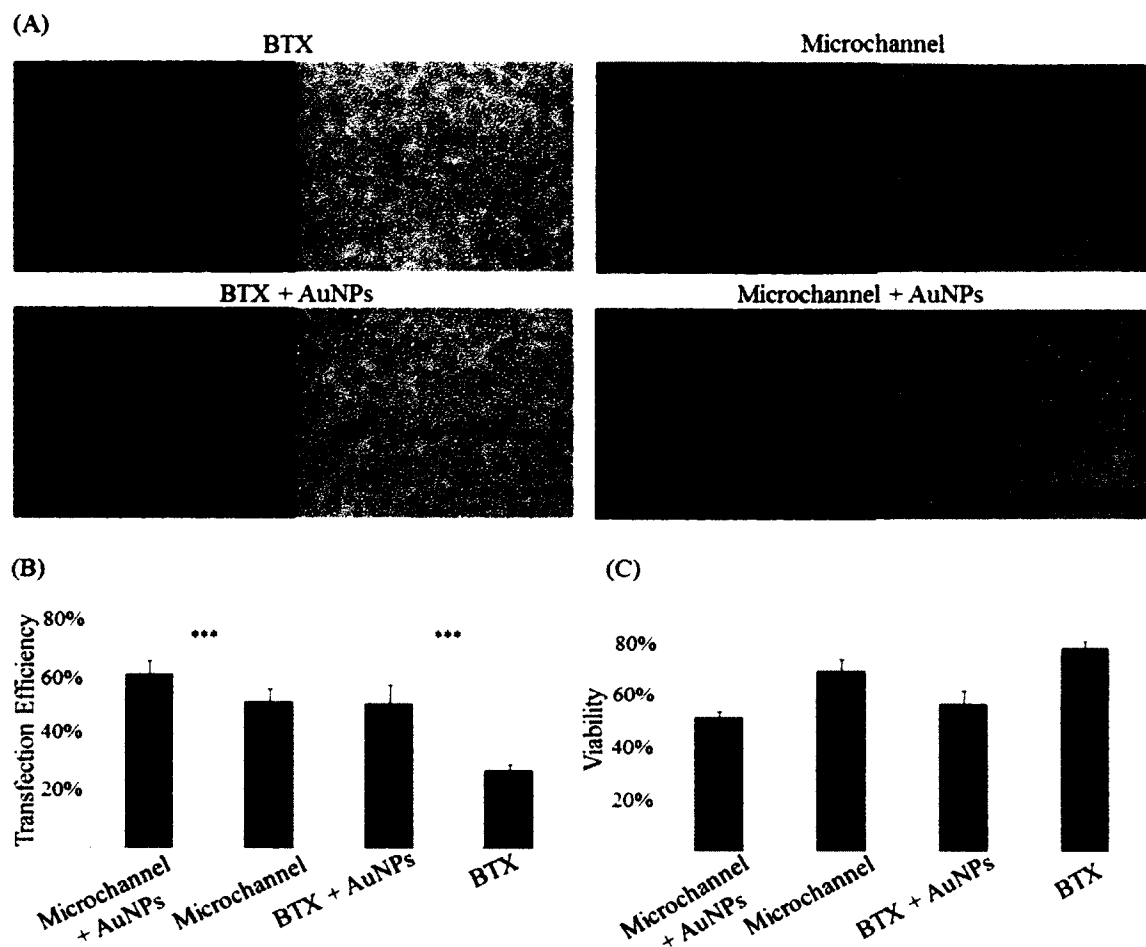


Figure 3-2: Gold nanoparticles enhancement on electroporation of K562 cells with a commercial batch electroporation (labeled as “BTX”) system and a home-made semi-continuous microchannel system (labeled as “microchannel”). Panel (A) exhibits fluorescence and phase contrast microscopic images of pGFP plasmid transfection through BTX, BTX with AuNPs, Microchannel, and Microchannel with AuNPs. The left side shows expression of GFP by the cells, and the right panel shows the cells under phase contrast microscopy. Panels (B) and (C) are the quantitative results of the transfection efficiency (B) and the cell viability (C). The concentration of AuNPs use here is 5X or 0.05 wt% (0.5 mg/mL). $n = 6$ and (***) represents $p < 0.005$.

Some loss on the cell viability was observed (from $78.9 \pm 2.9\%$ to $57.4 \pm 5.1\%$ for BTX electroporator and from $69.9 \pm 4.7\%$ to $52.1 \pm 2.3\%$ for microchannel electroporator), as shown in Figure 3-2C. This loss is not surprising considering the focusing effect of AuNPs could shift away the electric pulses from the desired strength. As mentioned earlier, K562 cells in Figure 3-2 were excited at electroporation conditions optimized in the absence of AuNPs. Considering the high conductivity of AuNPs, their addition greatly reduced the resistance contributed by the buffer solution so that most electric voltage imposed between the two electrodes was allocated to the cells. The actual pulse strength on the cell membrane was therefore mitigated to a higher-than-optimal level, resulting in over perturbation to the treated cells. Such harsh conditions increased the percentage of irreversible breakdown of the cell membrane, making the loss of the cell viability inevitable. As this pulse strength focusing effect is generated from the presence of free AuNPs in the electroporation buffer, the cell transfection efficiency can be improved (when reversible breakdown still dominates) or worsen (when irreversible breakdown becomes the dominant-cells might have probes successfully delivered while not getting the subjected transgenes expressed prior to lysis), depending on the concentration and size of the added AuNPs.

From the data shown in Figure 3-2C, the field focusing level for 5 nm AuNPs at a concentration of 5X (0.5 mg/ml) belonged to the first case (i.e., reversible breakdown still dominated). The transfection of gWizTMGFP was improved while accompanied with lower cell viability. Nevertheless, this experiment confirmed the electric field focusing effect of AuNPs to electroporation. (Note: the transfection percentage is defined as the number of transfected cell divided by the number of total living cells 24

hr post transfection in each sample, and the cell viability is measured as the ratio of the living cells in each sample to that in the negative control samples.) These definitions might differ from some others used in literature (divided by the number of cells initially used or cells surviving right after transfection) and emphasize the fate of all survived cells, though they sometimes show low values of transfection (or the cell viability) for their large number of the total living cells.

Our FEM simulation confirmed the enhancement effects of AuNPs to electroporation. The electrical potential distribution is plotted by colorful contours while the electric field lines through the buffer, the AuNP, and the cells are shown by blue lines in Figure 3-3. Because of the high conductivity, the electric field is clearly focused near the AuNP. Such localized focusing effect could also help attract charged DNA molecules from the surrounding area towards the focusing spot and enrich them there. As transient pores will form later at the same location, we also compared the total current passing through the pore with and without the AuNP present. It was found that the current was enhanced 34% (from 1.77 nA to 2.38 nA) when a AuNP was around (Figure 3-3C). This enhancement suggests that the charged DNA plasmids could transport faster with AuNPs in close proximity and more of them could be delivered into the cells before the resealing of the cell membrane.

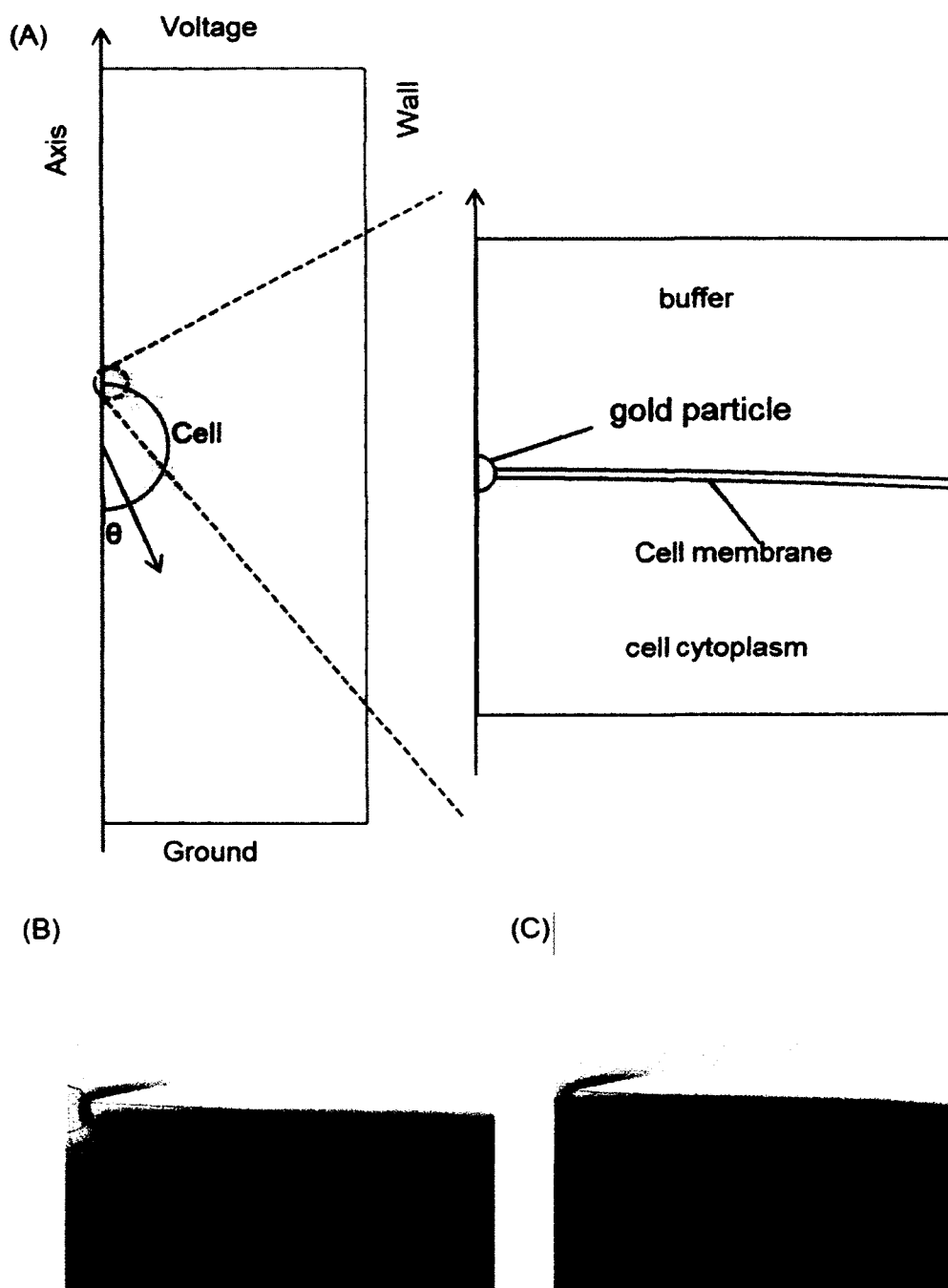


Figure 3-3: Simulation of the electric field focusing effect of AuNPs in electroporation. (A) The model and mesh setup for one AuNP embedded in the membrane of a K562 cell. (B) The calculated electric field lines around the AuNP. (C) The electric field lines around a transient pore on the cell membrane in the presence of one AuNP present.

As the presence of AuNPs greatly affects the pulse strength on treated cells, the size and number of AuNPs presented around each cell are critical to the electric pulse strength focusing level and the resulting electroporation performance (the transfection efficiency and cell viability). In the following sections, we evaluated the dependence of the pulse strength focusing effect on the size and concentration of AuNPs.

3.3.2 Dependence of Electroporation Enhancement on the Concentration of AuNPs

AuNPs of various concentrations (0.1 X–10 X of the stock solution) were used to evaluate the pulse strength focusing effect using the BTX electroporator. Similar to the aforementioned results, when electroporating cells at their standard pulse conditions (625 V/cm, single 10 ms pulse), the transgene expression enhancement generally sacrificed some of the cell viability with the increase of the AuNPs concentration (Figure 3-4A). After adding 5 nm AuNPs at a concentration of 0.1 X–1 X (1X = 0.1 mg/mL AuNPs), the cell viability retained at the same level ($71.9 \pm 51\%$ – $68.9 \pm 29\%$) as in electroporation with naked DNA. However, that value dropped gradually when more concentrated AuNPs solutions (2.5 X–10 X) were used. Such cell viability loss endorsed the field enhancing effect of free AuNPs mentioned earlier. Because the buffer resistance was reduced when adding AuNPs, the local pulse strength on the cells was focused. When starting from the standard pulse conditions, some treated cells were over-perturbed to lethal levels. When increasing the concentration of AuNPs, this pulse focusing effect got continuously enhanced and more cells were over-polarized or died. As a consequence, the cell viability dropped.

A threshold concentration of AuNPs existed for this pulse-focusing effect: it did not become obvious until the number of AuNPs reached a certain level (e.g., 1X, $7.91 \times$

10^{13} particles/ml for 5 nm AuNPs). Further increase in the pulse strength focusing effect led to loss of cell viability, but it was beneficial to the improvement of the transfection efficiency. For 5 nm AuNPs, the transfection efficiency increased from $\sim 25\%$ (bulk electroporation with DNA only) to the maximum enhancement of $\sim 51\%$ at the concentration of 5 X (0.5 mg/mL or $\sim 3.96 \times 10^{14}$ 5 nm AuNPs/ml) when increasing AuNPs concentration and started decaying afterwards due to the significant loss on the cell viability (Figure 3-4B).

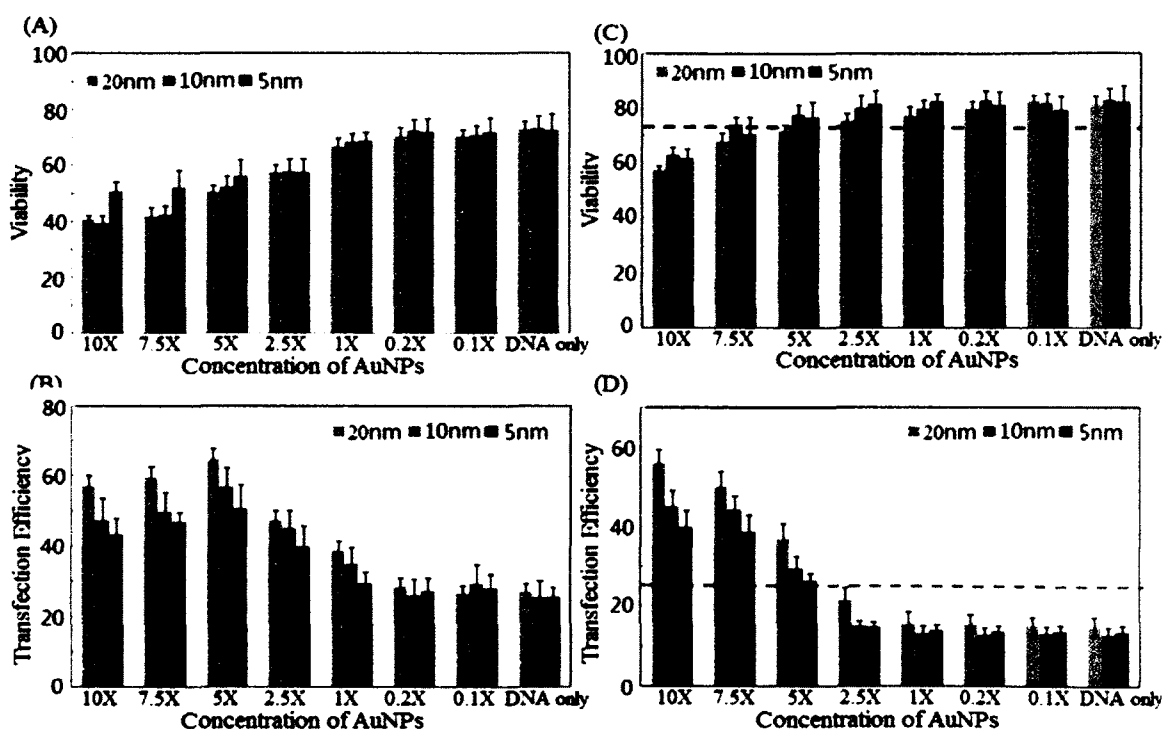


Figure 3-4: Dependence of the pulse enhancement on the size and concentration of free AuNPs: panels ((A)-(B)) are the cell viability (A) and the transfection efficiency (B) with an overall pulse strength of 625 V/cm and panels ((C)-(D)) are the results with an overall pulse strength of 475 V/cm (panel (C): the cell viability; panel (D): the transfection efficiency). The blue and red dashes refer to the cell viability and the transfection efficiency of electroporation with naked DNA at the optimal conditions (675 V/cm, single pulse of 10ms), respectively. 1X AuNPs refers to 0.01 wt% or 0.1 mg/mL gold content ($n = 3$).

As the electric pulses were generally over-focused when concentrated AuNPs were introduced at standard electroporation protocols, such enhancement might be more beneficial when more benign conditions are used (at these conditions, transfection with naked DNA alone is less effective as the consequence). At these conditions, the cell viability is certainly high and the enhancement is mainly contributed to the improvement on the transfection efficiency of molecular probes. During our investigation, to ensure the local pulse strength was still effective for the majority of the cells, we lowered the overall electric voltage (while keeping the pulse duration unchanged) to a minimum field strength that was just enough to transfect a statistically meaningful number of cells with DNA probes alone. For K562 cells, this minimum condition was 475 V/cm (95 V when tested with 2 mm BTX cuvettes) with a $13.6 \pm 15\%$ transfection efficiency of naked DNA using the BTX electroporator. As shown in Figure 3-4C, for all three sizes of AuNPs, similar cell viability ($\pm 10\%$) was achieved within a broad concentration range of AuNPs (0.1 X–10 X). Different from the enhancement performance at standard conditions, continuous increase on the transfection efficiency was achieved for all cases (Figure 3-4D). Such improvements were not only significant when compared to that using naked DNA (i.e., $\sim 14\%$) at the same pulse condition, but also much better than the best performance the BTX electroporator could achieve with naked DNA (i.e., $\sim 25\%$). This additional gain on the transfection efficiency at benign electroporation conditions confirmed from another viewpoint the focusing effect of free AuNPs-low-voltage pulses could be focused to high enough levels to provide the needed transmembrane field strength for better transfection efficiency ($40.0 \pm 4.1\%$ for 5 nm, $45.2 \pm 4.0\%$ for 10 nm,

56.1 ± 3.3% for 20 nm). More important, such delivery enhancement was attained with no or little sacrifice of the cell viability for the application of low-voltage pulses.

3.3.3 The Dependence of Electroporation Enhancement on the Size of AuNPs

Besides the concentration effect, the size of AuNPs also contributes to the reduction of the buffer resistance and the pulse strength focusing level on the cells. Moreover, the size of AuNPs could affect the poration area on the cell membrane if AuNPs are brought close enough. As shown in Figure 3-1B and Figure 3-3B, AuNPs converge the electric field on their two poles and hang around the cells. The particles work as many tiny virtual electrodes with focused pulses pointing towards the cell membrane. This focusing could induce the polarization on the cell membrane within a limited area (i.e., localized poration), which has been found to be beneficial for the electroporation performance [185, 186, 191]. Therefore, the electroporation enhancement with various sizes of AuNPs reflects a combination of the pulse strength focusing effect and localized electroporation benefits. Three different sizes of AuNPs (5 nm, 10 nm, and 20 nm) were tested here and their effects on the transfection efficiency and the cell viability are included in Figure 3-4. Similar to AuNPs of 5 nm, AuNPs of 10 nm and 20 nm exhibited similar concentration dependence on the transfection efficiency and the cell viability. As the concentration of AuNPs in Figure 3-4 were calculated based on the weight percentage of added AuNPs, their buffer resistance reduction effect or the pulse strength focusing level should be similar when the particle concentration is constant. In other words, at the same concentration of AuNPs, the enhancement difference for cases in Figure 3-4 reflected mainly the contribution of various particle sizes to the localized electroporation benefit.

The enhancement difference on the transfection efficiency among various sizes of AuNPs was marginal at low AuNP concentrations and became significant only when more concentrated AuNPs were used. For 625 V/cm pulses, the effective AuNP concentration started from 1 X AuNPs, and for 475 V/cm pulses, it started from 2.5 X, due to their different pulse strength focusing levels and localized electroporation situations. This effect of concentration is reasonable as the pulse strength focusing effect was weak at low AuNPs concentrations. Similarly, localized electroporation was very limited at low AuNPs concentrations, as only a small portion of the total free AuNPs could aggregate around the cells. In excess of the threshold AuNPs concentration, their contributions on the field focusing effect and localized poration became more pronounced so that the benefit on the transfection efficiency improvement showed up. The larger the size of AuNPs, the better transfection efficiency was achieved. Large AuNPs of a relative lower concentration could also help gain better transfection efficiency than small AuNPs at a higher concentration. For example, electroporation with 2.5 X and 5 X AuNPs of 20 nm help achieve similar or even better pGFP transfection than 5 X and 7.5 X AuNPs of 5 nm, respectively (Figure 3-4B and D). Among various particle sizes, the cell viability difference at the same pulse strength focusing level (i.e., the same AuNPs concentration) was marginal in most cases. Therefore, these AuNPs (5 to 20 nm) are appropriate for the electroporation enhancement without extra addition to the cell toxicity.

However, these results also suggested that, with free AuNPs (i.e., AuNPs that are randomly dispersed in the electroporation buffer), the electroporation enhancement was mainly decided by the pulse strength focusing effect or the concentration of AuNPs.

Localized poration only became beneficial at high AuNPs concentration when sufficient AuNPs were present around the cells during electroporation. However, this easily leads to over-perturbation if added AuNPs are all free AuNPs. To further enhance the localized poration effect, a sufficient number of AuNPs must be brought close to cells through some pre-concentration approaches.

3.3.4 Enhancing Localized Electroporation with Transferrin-AuNPs

As many transferrin receptors (TfR) are available on the cell membrane of K562 cells, AuNPs were conveniently brought to the cells by grafting transferrin (Tf) molecules on their surface [250]. This grafting was done with the help of the high affinity of sulfhydryl groups to the gold surface [251]. Specifically, sulfhydryl groups were introduced to transferrin molecules by converting a small proportion of their primary amine groups to sulfhydryl groups with Traut's reagent. The modified transferrin with sulfhydryl groups were then incubated with free AuNPs to form transferrin AuNPs (Tf-AuNPs), as shown in Figure 3-5A. To evaluate how this transferrin-targeting mechanism affected the localized electroporation, we incubated Tf-AuNPs of 1 X with K562 cells for various incubation times and compared their performance on transfection enhancement. As shown in Figure 3-5B, the best improvement occurred in samples having 4-hr incubation time and the transfection efficiency reached $41.7 \pm 3.2\%$ when compared to that of BTX with naked DNA ($26.4 \pm 1.9\%$) and BTX with free AuNPs ($34.4 \pm 2.9\%$). Some 50% or less enhanced performance resulted from the gradual depletion of mobile AuNPs in the electroporation buffer because of Tf-AuNPs grafting on the cell membrane. As a consequence, though localized electroporation was improved, the pulse focusing effect from free AuNPs diminished.

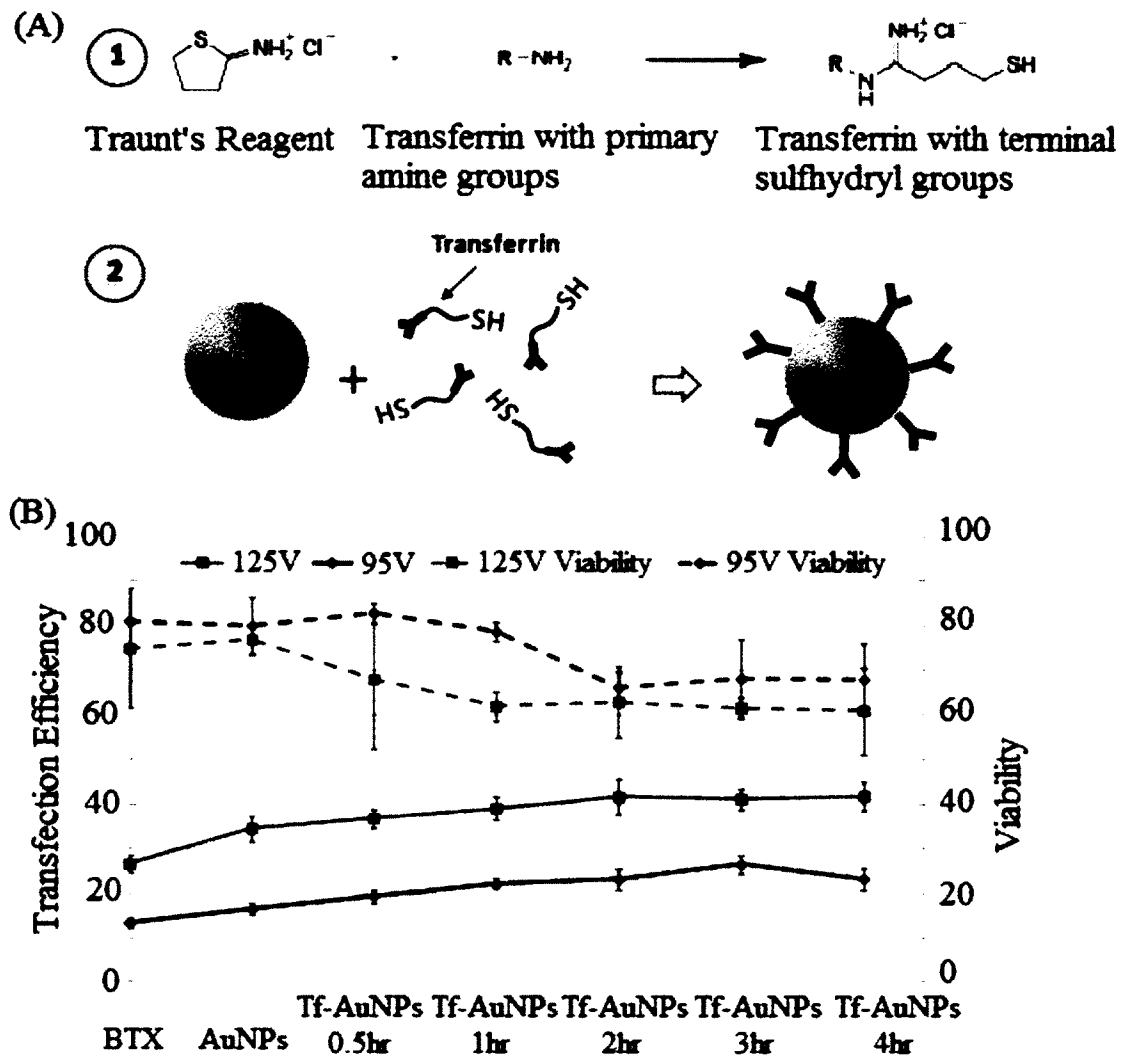


Figure 3-5: Localized electroporation enhancement with Tf-AuNPs: (A) schematics of grafting Tf-AuNPs as virtual electrodes on the cell membrane, (B) the localized enhancement with Tf-AuNPs alone at various binding stages. The AuNPs used here are 20 nm with 1 X concentration (0.1 mg/mL). (n = 3)

To retain both the pulse strength focusing and localized electroporation advantages, we added free AuNPs to Tf-AuNPs at various mixing ratios (0%, 25%, 50%, 75%, and 100% Tf-AuNPs). Based on other pioneering work on transferrin targeting, it took about 4 hr incubation to accomplish complete affinity binding of

transferrin to the TfRs on the cells [248]. Therefore, we first incubated K562 cells with Tf-AuNPs for 4 hr and then added the needed quantity of free AuNPs right before electroporation. As shown in Figure 3-6A, such a combination showed better enhancement of the transfection efficiency under the standard electroporation conditions with only 1 X total AuNPs (free AuNPs + Tf-AuNPs) while the actual improvement varied with their mixing ratio: a sustained increase was seen on the transfection efficiency when more Tf-AuNPs were added until reaching a 50%/50% mixture of free AuNPs and Tf-AuNPs (the transfection efficiency reached $58.2 \pm 1.8\%$), followed by some declines. This combination provides ~ 2.5 folds increase on the DNA transfection when compared to electroporation with naked DNA only. Considering the low concentration of AuNPs used here (only 1 X), the electroporation enhancement with a combination of free AuNPs and Tf-AuNPs seems more effective than that using free AuNPs or Tf-AuNPs alone.

The best enhancement came from an appropriate balance on the pulse strength focusing and localized electroporation advantages AuNPs offered. It is worth mentioning that such a transfection efficiency improvement was achieved without sacrificing much of the cell viability (Figure 3-6A). At more benign conditions (475 V/cm), the enhancement was not very obvious, consistent with the free AuNPs enhancement result at low concentrations (0.1 X–1 X). This insufficient pulse focusing level cannot provide the desired transmembrane potential to polarize the majority of the cells. When more AuNPs were introduced (e.g., 5 X for the total AuNPs concentration), the enhancement on the transfection efficiency became significant for pulses of both 625 V/cm and 475 V/cm and the equivalent mixture of

free AuNPs and Tf-AuNPs still offered the best transfection efficiency (Figure 3-6B). However, because of the over-focusing effect, obvious loss of the cell viability was found for the case with the pulse strength of 625 V/cm, consistent with our earlier observations.

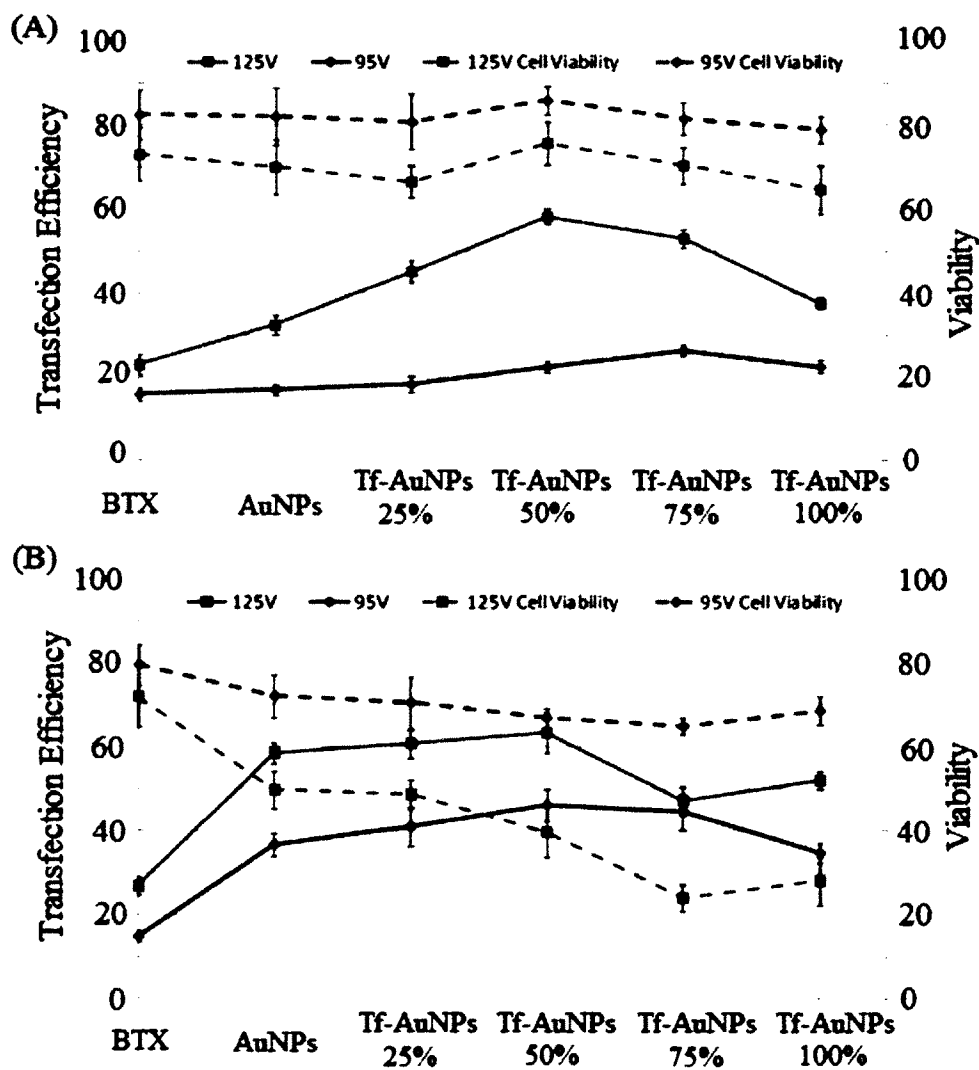


Figure 3-6: The combined enhancement of the pulse strength focusing and localized electroporation effects using a mixture of free AuNPs and Tf-AuNPs of various mixing ratios with a total AuNPs concentration of 1 X (A) and 5 X (B) with the pulse strength of 625 V/cm and 475 V/cm. AuNPs of 20 nm were used here (n = 3).

3.3.5 AuNP Imaging and Tracking In Vitro

We tracked the cellular uptake of AuNPs before and after electroporation for both free, naked AuNPs and Tf-AuNPs using confocal microscope and the results were shown in Figure 3-7. As free AuNPs were mixed with cells right before electroporation, the short contact time did not provide enough time to allow endocytosis-based uptake of AuNPs and no obvious fluorescently labeled AuNPs (FNPs) were observed (Figure 3-7A). After electroporation, many FNPs were clearly found in the cell cytoplasm (Figure 3-7B), indicating that AuNPs transported into the cells after electroporation. As all samples were fixed shortly after electroporation, we believe the majority of FNPs were taken through the transient openings on the cell membrane, not the endocytosis process. As mentioned in our FEM simulation, AuNPs around transient pores could enhance the cellular uptake of DNA plasmids because of the increase of electrical current (see Section AuNPs Enhancement on the Transfection of Mammalian Cells). Figure 3-7 C and D showed the distributions of Tf-FNPs before and after electroporation (Note: Tf-FNPs alone, not a mixture with free FNPs were used here). The accumulation of Tf-FNPs on the cell membrane was clearly found in the samples without electroporation treatment (Figure 3-7C), confirming the formation of ligand-receptor bonds after incubation. After electroporation, FNPs were also found in the cell cytoplasm (Figure 3-7D), consistent with what was exhibited in free FNPs electroporation. However, unlike in the free FNPs electroporation sample, many Tf-FNPs were also found on the cell membrane or regions nearby, suggesting that at least some Tf-AuNPs conjugates and the coupling of Tf-TfR could survive the electroporation process.

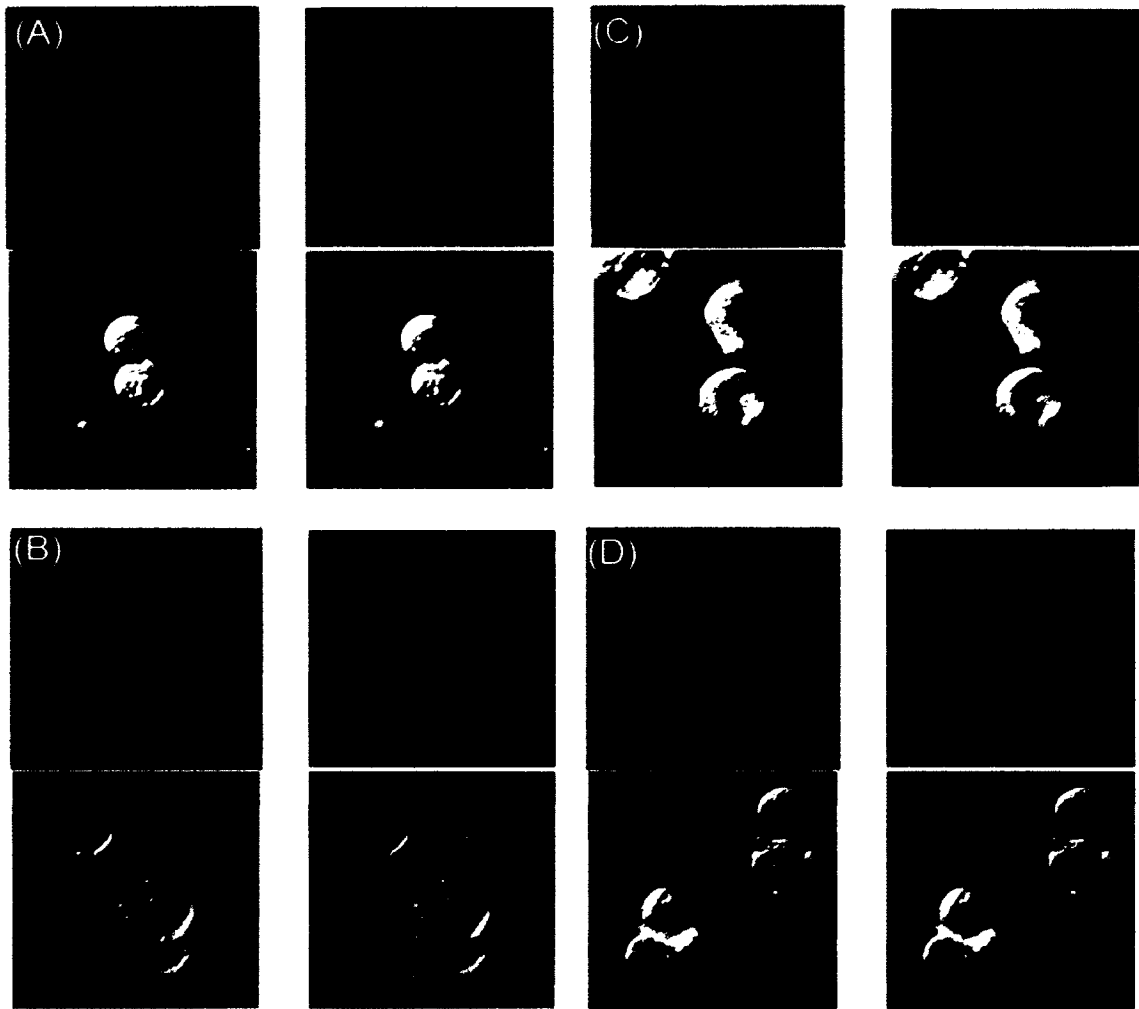


Figure 3-7: The confocal microscope images of the cellular uptake of AuNPs before and after electroporation: ((A)-(B)) for free FNPs and ((C)-(D)) for Tf-FNPs. Images in panels (A) and (C) were taken before electroporation and panel (B) and (D) were after electroporation. FNPs of 10 X or 0.1 wt% (1.0 mg/mL) were used in all samples and Tf-FNPs were incubated with the cells for 4 hr.

3.3.6 Enhancement Performance of AuNPs in Fibroblast

Leukemia cells K562 was selected in the aforementioned experiments on the basis that it is hard to transfect the suspension cell line. At the same time, we also tested with an adherent cell line – NIH 3T3 fibroblast.

Firstly, AuNPs of various concentrations (0.1 X – 2 X of the stock solution) were used to evaluate the pulse strength focusing effect with NIH 3T3 cells. Similar to the aforementioned results with K562, the transgene expression enhancement generally sacrificed some of the cell viability with the increase of the AuNPs concentration when electroporating cells at their standard pulse conditions (625 V/cm, single 10 ms pulse), as shown in Figure 3-8B. The cell viability tended to drop at higher AuNP concentrations (starting from 1 X). Such cell viability loss endorsed the field enhancing effect of free AuNPs mentioned earlier, that is, some treated cells were over-perturbed to lethal levels. The transfection efficiency increased from ~ 25% (bulk electroporation with DNA only) to the maximum enhancement of ~ 45% at the concentration of 2 X (0.2 mg/mL or ~ 1.58×10^{14} 5 nm AuNPs/ml).

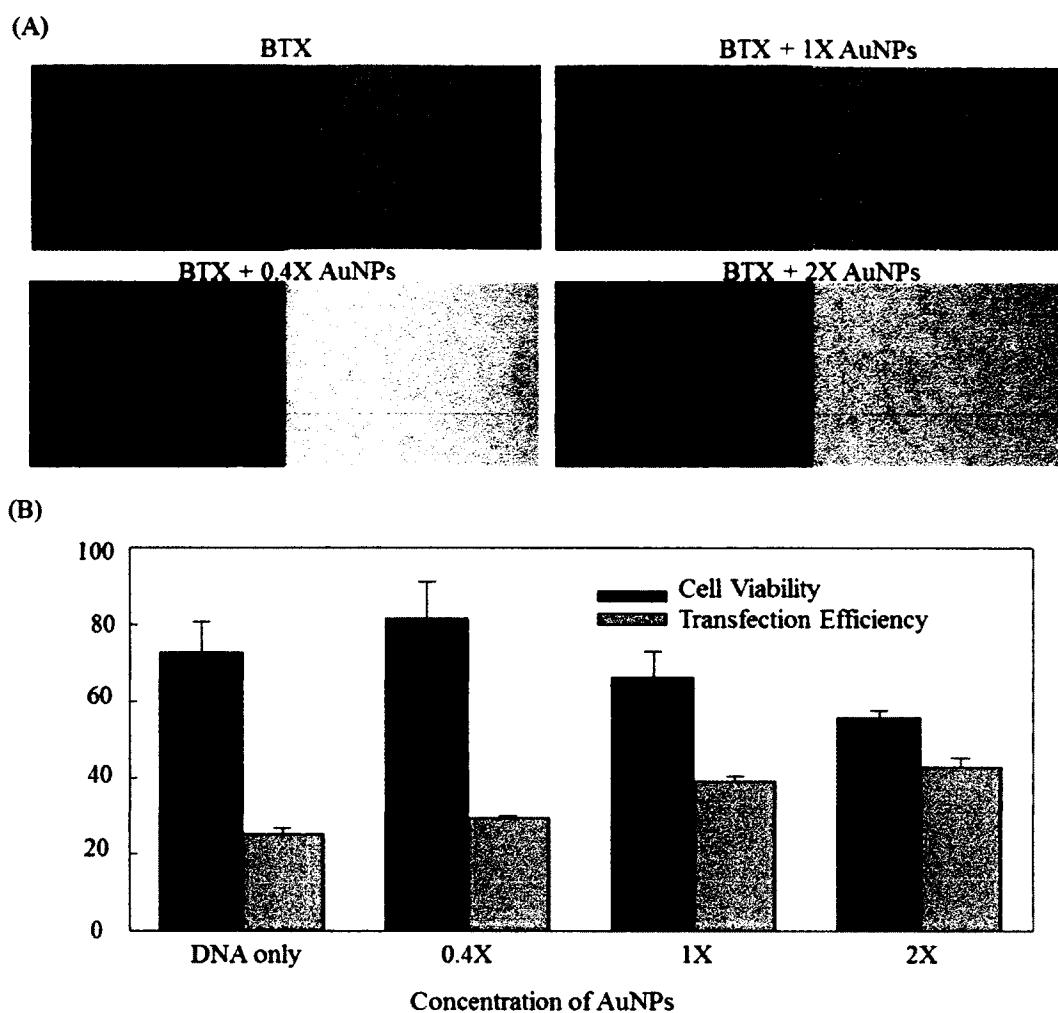


Figure 3-8: The pulse enhancement of free AuNPs (5 nm) on NIH 3T3 cells: panels (A) present phase contrast and fluorescence microscopic images of cells after BTX electroporation with naked DNA alone, with 0.4 X, 1 X, and 2 X AuNPs, respectively. Panel (B) is the summary of the quantified cell viability by MTS assay and the transfection efficiency by flow cytometry. A single pulse with 10 ms pulse duration and 625 V/cm overall pulse strength was imposed for all samples and 1X AuNPs refers to 0.01 wt% or 0.1 mg/mL gold content. $n = 3$ and (***) represents $p < 0.005$.

Secondly, two different sizes of AuNPs (5 nm and 20 nm) were tested with both commercial batch electroporation (BTX) and home-made semi-continuous microchannel system (SFE); their effects on the transfection efficiency and the cell

viability are included in Figure 3-9. According to our previous observation, the enhancement difference on the transfection efficiency among various sizes of AuNPs was marginal at low AuNPs concentrations and became significant only when concentrated AuNPs were used. Moreover, the larger the size of AuNPs, the better transfection efficiency was achieved. Here, we chose to test with 1 X, 5 X 5 nm and 5 X 20 nm AuNPs. The transfection efficiency grew with the increase of the particle size and concentration, while cell viability was reasonably scarified. Similar trends on the transfection efficiency and cell viability were found, consistent with those of K562 cells. This confirms the broad effectiveness of the enhancement roles AuNPs play in electroporation.

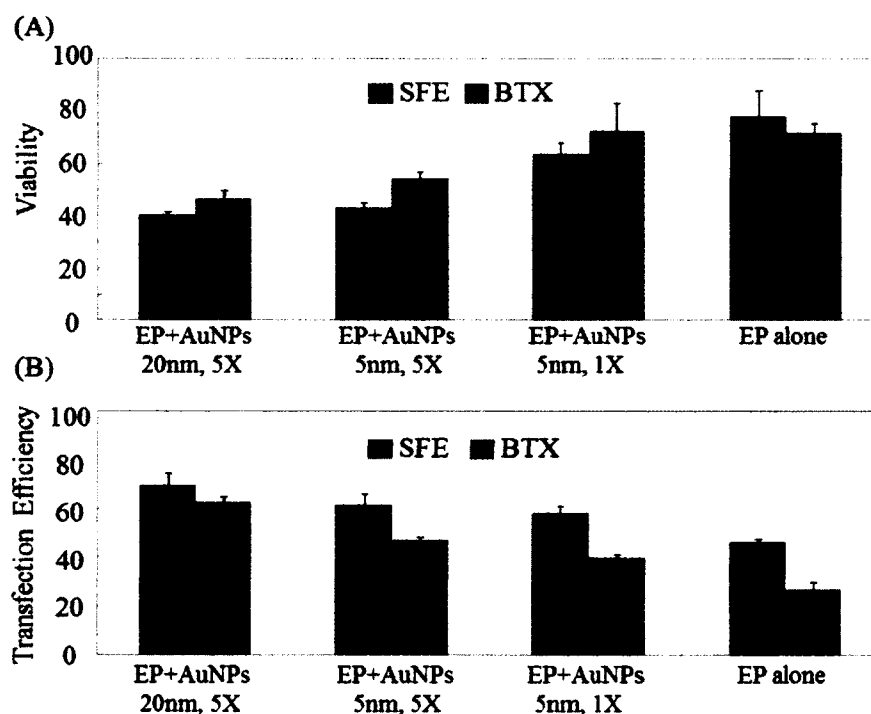


Figure 3-9: The pulse enhancement of AuNPs for electroporation of NIH 3T3 cells with a commercial batch electroporation (labeled as “BTX”) system and a home-made semi-continuous microchannel system (labeled as “SFE”). Panels (A) and (B) are the quantitative results of the cell viability and transfection efficiency, respectively (n = 3).

3.4 Conclusions

AuNPs were used to enhance *in vitro* delivery of DNA probes for both batch-type and flow-through electroporation systems. Highly conductive free AuNPs were added to the electroporation buffer to reduce the solution resistance so that the pulse strength on the cells could be enhanced. Tf-AuNPs were brought to K562 cells through affinity binding with TfR receptors on the cell membrane, serving as many virtual microelectrodes to polarize cells locally from various sites, each affecting only a limited area. In this way, electroporation was enhanced with better transfection efficiency and the same or higher cell viability. With DNA plasmids carrying a gWizTMGFP reporter gene, we confirmed the pulse strength focusing effect after adding free AuNPs in the electroporation buffer and investigated its dependence on the particle size, concentration, and electroporation conditions. The enhancement difference among various sizes was not significant until higher concentrations were used, and the best transfection was achieved with 20 nm nanoparticles. At 125 V, a threshold concentration of AuNPs existed for pulse-focusing effect and the transfection efficiency increased to maximum at a concentration of 5 X. At 95 V, transfection efficiency was continuously increasing with concentration. We also observed the contributions of localized electroporation with Tf-AuNPs.

An equivalent mixture of free AuNPs and Tf-AuNPs was found to provide the best enhancement performance while the optimal concentration of AuNPs was decided by the original pulse conditions. This study offers a new approach to improve the delivery efficiency of nucleic acids or anticancer drugs through the combination of nanoparticles and electroporation technologies. AuNPs were adopted here for their low

cost and easy accessibility while other forms of gold nanostructures, such as nanorod, nanoshell, or nanowires, in principle, could be used for similar purposes. As these gold nanomaterials have been widely explored in sensing, imaging, diagnosis, and therapeutic applications, our approach demonstrates a new function of these nanomaterials and/or broadens their potentials for multiple-function applications in drug discovery and clinical practice.

CHAPTER 4

GOLD NANOPARTICLES ELECTROPORATION ENHANCED POLYPLEX DELIVERY TO MAMMALIAN CELLS

4.1 Introduction

Polyplex serves as the favorable alternative to their virus-mediated counterparts and have been successfully tested for both *in vitro* and *in vivo* delivery of plasmids, oligonucleotides, ribozyme, and small interfering RNAs [3-15]. However, many of these systems still suffer insufficient delivery efficiency and cell viability, which often ties with their poor nanoparticle quality, slow and inefficient cellular uptake with endosome escape, and serious cytotoxicity from free cationic molecules after the unpacking of lipoplex or polyplex. As captured cationic molecules are much less toxic than their free counterparts, nanoparticles have been introduced to help fix cationic polymer [74]. AuNPs are favored in these applications for their good biocompatibility and multiple functionalities (i.e., targeting, therapeutic, and imaging) [74, 143, 162-165, 252]. However, issues like ineffective cellular internalization remain.

Herein we introduce the use of electroporation to bypass the slow and inefficient endocytosis process by directly delivering therapeutic probes into cell cytosol. A simple combination of lipoplex nanoparticles and electroporation has been explored early in the delivery of oligonucleotides in the format of lipoplex [247, 253]. However, negative impacts on both the delivery efficiency and the cell viability were found [253]. We

believe that the destroyed complex structure during electroporation released a large number of free cationic molecules, which significantly lower the overall cell viability. To avoid a similar situation, we first immobilized the cationic polymer on AuNPs and then allowed conjugation with negatively charged therapeutic probes to form AuNPs-polyplex complex. In addition to the help on retaining cationic polymer on the surface, the presence of AuNPs also enhances the electroporation performance with focused electric pulses and localized poration [254], which was proven beneficial for not only the recovery of treated cells to gain high cell viability, but also the uptake of probes from multiple sites to facilitate the cytosolic delivery. Specifically, cationic polymer, polyethylenimine (PEI), was immobilized on AuNPs by electrostatic interactions (Figure 4-1). DNA plasmids were then conjugated with PEI molecules to form AuNPs-polyplex. The complex nanoparticles were then mixed with cells for electroporation. The delivery enhancement was evaluated by the cell viability and the transfection efficiency.

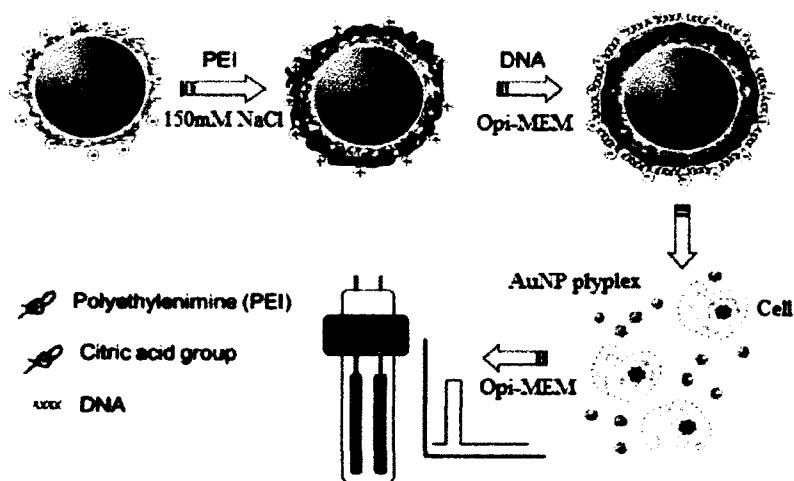


Figure 4-1: Schematic illustration on the procedure of AuNPs-polyplex synthesis and delivery.

4.2 Materials and Methods

4.2.1 Materials and Reagents

Branched PEI (MW = 25 kDa), AuNPs of 5 – 40 nm were obtained from Sigma-Aldrich. The concentration of 1 X AuNPs refers to the stock solution, which has 0.01 wt% of Au (0.1 mg/mL) while the number of particles varies with the size of AuNPs. Other concentrations of AuNPs were prepared by either concentrating or diluting from the stock solution. DNA plasmids with gWizTMGFP was purchased from Aldevron (Fargo, ND). All other chemicals were purchased from Sigma-Aldrich and the cell culture reagents were purchased from Life Technologies (Carlsbad, CA) unless specified.

4.2.2 Preparation of AuNPs-polyplex

To prepare AuNPs/PEI polyplex, 500 μ L 0.5 mg/mL PEI (pH 7.0) was added to 500 μ L 0.01 wt% of AuNPs. The original citric acid terminated surface of AuNPs facilitates the deposition of PEI molecules through electrostatic interactions. The incubation was performed at room temperature for 20 min and the extra PEI was removed by centrifuging at 15,000 \times g for 10 min. The PEI-coated AuNPs were resuspended in a desirable amount of PBS (pH 7.0) and 5 μ L of nucleic acid solution (with a concentration of 5 mg/mL) was added to AuNPs/PEI of varying concentrations. The resulting mixture was mixed by pipetting and further incubated at room temperature for 20 min.

4.2.3 NIH 3T3 and K562 Cell Culture

NIH 3T3 cells were obtained from American Type Cell Culture (ATCC, Manassas, VA). They were grown and maintained in high-glucose DMEM supplemented with 10% newborn calf serum, 1% penicillin and streptomycin, 1% L-glutamine, and 1% sodium pyruvate. For subculture, culture medium was removed and discarded first. The

cell layer was briefly rinsed with DPBS to remove the serum which contains trypsin inhibitor. Then 1-2 mL trypsin-EDTA was added for a 100 cm² Petri dish. Cell culture was then observed under an inverted microscope until the cell layer was dispersed (usually 5-15 min); 8 to 9 mL of complete growth medium was added and cells were aspirated by gently pipetting. Appropriate aliquot of the cell suspension was transferred to a new culture dish with an addition of more growth medium to make a total volume of 10 mL for 100 cm² surface. K562 lymphoblast cells were also obtained from American Type Cell Culture (ATCC, Manassas, VA). K562 cells were cultured and maintained in RPMI 1640 media supplemented with 10% heat-inactivated fetal bovine serum (FBS), 100 U/mL penicillin, 100 g/mL streptomycin, and L-glutamine. For subculture, a desired amount of K562 cell suspension was transferred to a new Petri dish with the addition of an appropriate amount of fresh culture medium. All cultures were maintained at 37 °C with 5% CO₂ and 100% relative humidity.

4.2.4 Electroporation Setup and Procedure

NIH 3T3 or K562 cells were counted with hemocytometer to determine cell density, centrifuged at 200 × g for 5 min and then resuspended in fresh GIBCO OPTI-MEM I (a serum free medium) at the desired densities of 0.5 × 10⁶ - 0.5 × 10⁷ cells/mL. Cell suspensions were then mixed with AuNP-polyplexes of various concentrations and sizes while the amount of DNA plasmids was fixed at 25 μg/sample. Electroporation was done with a commercial instrument (ECM 830, Harvard Apparatus) in cuvettes with a 2-mm gap, each containing a 100 μL sample solution. The standard electroporation condition (single 10 ms pulses of 125 V / 2 mm cuvette) was applied with a single

unipolar pulse. After electroporation, the samples were transferred to 6-well cell culture plates, incubated in a fresh medium for another 24 h, and then harvested for analysis.

4.2.5 Determination of AuNPs-polyplex Delivery Efficiency

The transfection efficiency of gWizTMGFP plasmids was evaluated both qualitatively by visualizing the number of cells with green fluorescence within a representative area selected from the entire culture surface under an inverted fluorescence microscope (Olympus, Japan) and quantitatively by counting cells using a four-color flow cytometry system (FACS Calibur, BD Biosciences, CA) 24-h post transfection. Briefly, an amount of 1.5×10^6 cells/mL was collected and the percentage of GFP-positive cells was calculated quantitatively via the flow cytometer. The unstained samples were run first to adjust the voltage setting and compensation of the flow cytometer. Then the tested samples were processed by CellQuest. At least 10,000 events were collected for each sample.

4.2.6 Measurements of Cell Viability

The cell viability was evaluated by an MTS cell proliferation assay (Promega, Madison, WI). Briefly, the cells in 100 μ L/well of medium were transferred to a 96-well plate and incubated. Twenty microliters of CellTiter 96 AQueous One solution (Promega, Madison, WI) was added to each well and the cells were incubated at 37 °C for another 1 h. Absorbance was measured at 492 nm on an automated plate reader (Elx 800, Biotek, VT). Normally, grown cell samples were used as negative control whose viability was set to 100%. Data points were represented as the mean \pm SD of triplicates, unless otherwise indicated.

4.2.7 Cellular Uptake of AuNPs-polyplex Nanoparticles

The distribution of AuNPs-polyplex in 3T3 cells was examined using an inverted fluorescent microscope. As AuNPs are well known to quench the fluorescent signal from the proximal fluorophores, a sandwich design of fluorophore-labeled AuNPs (FNP from Nanopartz, having Alexa Fluor 546) with fluorophores separated from the gold surface by polymer spacers were used to circumvent this problem. Plasmids were stained with YOYO-1 iodide (Life Technology) with a ratio of 100 bp/dye. The mixture of cells with nucleic acids, AuNPs, or AuNPs-polyplex were washed twice with $1 \times$ PBS (pH 7.0), followed by fixation with 4% paraformaldehyde for 30 min. Nuclei were stained with $20 \mu\text{M}$ of 4', 6-diamidino-2-phenylindole (DAPI) for 10 min at room temperature. Cells from each sample were then mounted on cover glass slides. Images of the phase contrast, green (nucleic acids), red (AuNPs), and blue (nuclei) fluorescence channels were taken on an Olympus 1×51 inverted microscope (Olympus) with a $100 \times$ objectives.

Note that in our nomenclature, symbols such as “A/B” or “A – B” means materials A and B are conjugated together through electrostatic interactions after incubation; “A + B” means A and B are simply mixed without incubation before further treatment.

4.3 Results and Discussions

4.3.1 AuNPs-polyplex Size and Size Distribution

Current polyplex delivery vehicles have not yet shown competitive delivery advantages over natural virus-based counterparts. This result is at least partially attributed to their heterogeneous assembly conditions and poor synthetic quality of nanoparticles (i.e., relatively large variations in size, structure, and component quantity). As in our

AuNPs-polyplex synthesis, cationic polymer molecules (i.e., PEI) were first immobilized on the surface of AuNPs; their amount in individual AuNPs-polyplex should be more uniform than those synthesized through dynamic complexation of freely charged agents. This further determines the total dosage of genetic probes, which are condensed on AuNPs-polyplex later on. Therefore, the introduction of AuNPs in the polyplex not only helps fix free or dissociated polycations on a solid surface, but also provides better management on molecule assembly and multiple-agent packaging. As a consequence, nanoparticles of better quality are produced.

As shown in atomic force microscopy (AFM) images in Figure 4-2, more homogeneous morphology was found for AuNPs-polyplex than polyplex synthesized via vortex mixing (Figure 4-2E) [4]. Their size was also much smaller and more uniform, which was further confirmed with quantitative measurements using dynamic light scattering (Figure 4-2F). Except for AuNPs-polyplex synthesized from 5 nm AuNPs, the average size of AuNPs-polyplex with various original sizes lies between 100 and 200 nm, an appropriate size range of nanoparticles for efficient cellular uptake. As the size of DNA plasmids used in this study is much bigger than that of AuNPs, each DNA molecule is suspected to interact with multiple AuNPs-PEI nanoparticles simultaneously (Figure 4-3). Therefore, clusters (or aggregates from conjugation networking) of AuNPs-PEI-DNA, instead of many individual AuNPs-polyplex nanoparticles with the assembly structure schematically shown in Figure 4-1, are more likely to form. With smaller size and higher mobility, AuNPs of 5 nm allow easier occurrence of such conjugation networking than other AuNPs with larger original size. As a result, such stable clusters

might become the dominated population when small AuNPs are used in AuNPs-polyplex synthesis.

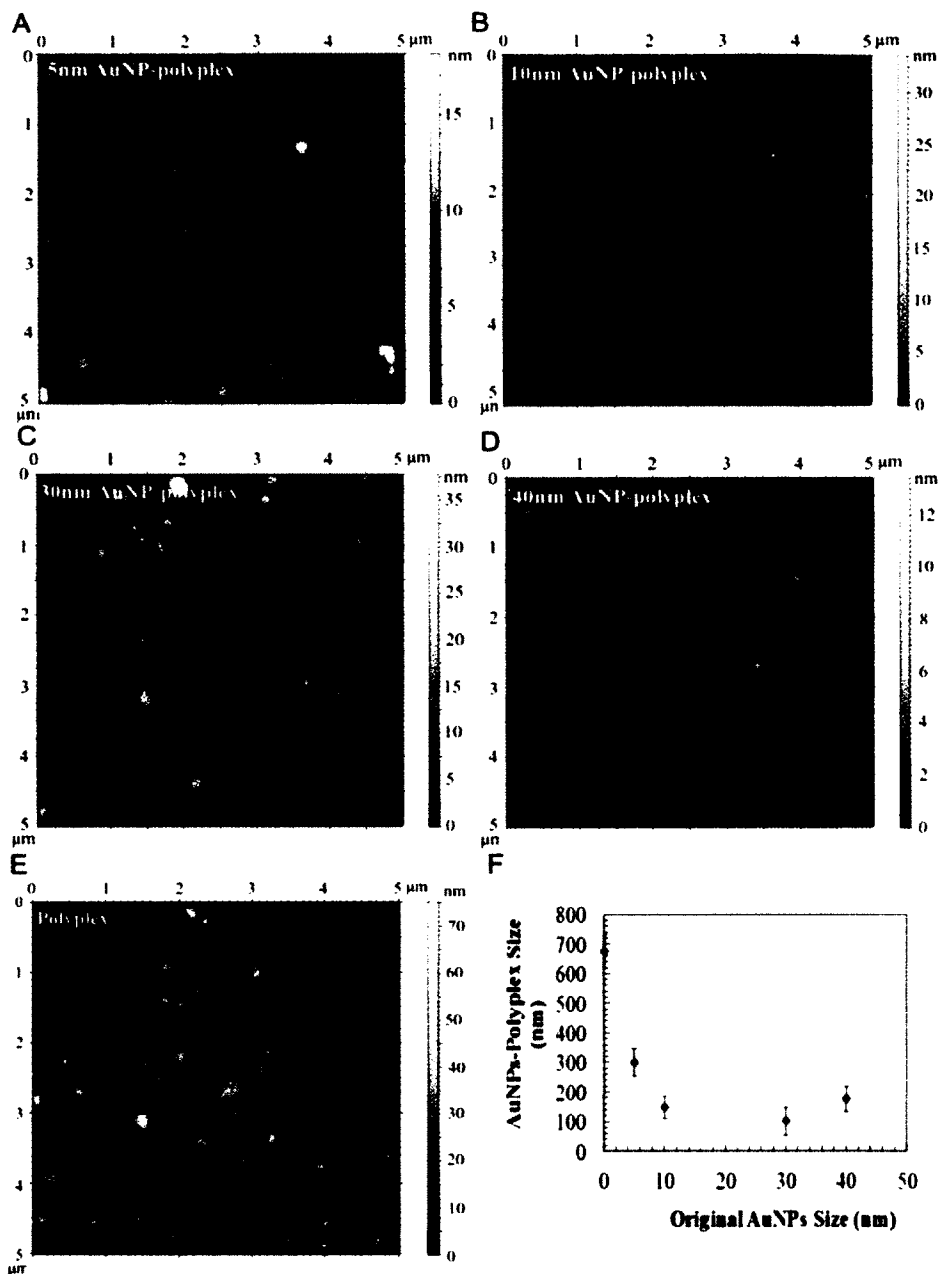


Figure 4-2: The AFM images of AuNPs-polyplex morphology with the original size of AuNPs of (A) 5 nm, (B) 10 nm, (C) 30 nm, and (D) 40 nm. Panel (E) is the traditional polyplex synthesized through the vortex mixing approach [4]. Panel (F) is the quantitative dynamic light scattering (DLS) particle size measurement.

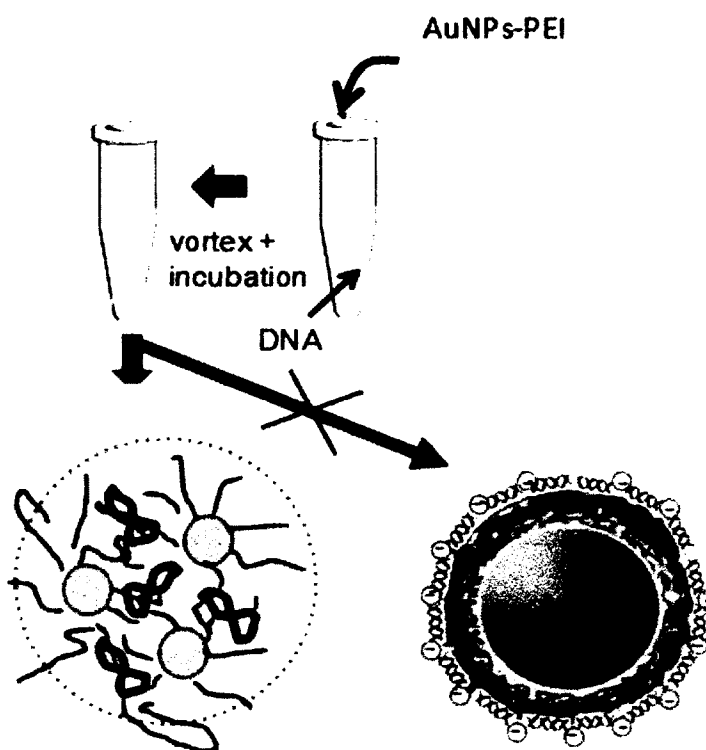


Figure 4-3: Schematic of AuNPs-polyplex formation involving conjugation networking of multiple AuNPs with DNA probes.

4.3.2 Cellular Uptake of AuNPs-polyplex via Electroporation

To verify that PEI molecules remain on AuNPs during electroporation, fluorescence probes were tagged to track the locations and fate of AuNPs-polyplex during the cellular uptake. As AuNPs quench fluorescent signal from proximal fluorophores, FNP with polymer spacer separating fluorophores from the gold surface was utilized. These nanoparticles are also carboxylated to match similar interaction capacity as those with citric acid terminated surface. After conjugating with PEI molecules, fluorophores are pushed back to the gold surface, and therefore, the fluorescent signal of

FNP is quenched again unless most immobilized PEI molecules are gone. When DNA plasmids are condensed on FNP, the PEI layer underneath serves as the new thick spacer so that the YOYO-1 labeled DNA probes become visible and are used to track the uptake of AuNPs-polyplex.

Compared to the untreated sample (Figure 4-4A), samples of simply mixing cells with YOYO-1 labeled DNA plasmids (Figure 4-4B) or FNP (Figure 4-4C) have weak fluorescent spots visible. This weakness is attributed to their tiny particle size and limited fluorescent signal when staying as individual nanoparticles. After the nanoparticles were capped with a layer of PEI, even such weak fluorescent signals disappeared (Figure 4-4D), which confirmed that the original fluorophores were pushed back close to the gold surface. As the PEI layer serves as the new spacer layer, the condensed DNA plasmids labeled with YOYO-1 exhibited a similar fluorescent signal as free DNA plasmids (showing weak green fluorescence spots in Figure 4-4E), indicating that the location of AuNPs-polyplex was mainly outside the cells. After electroporation, stronger fluorescent signals were generally seen in electroporated cells with naked plasmids and FNP as nanoparticles accumulated in the cells (Figure 4-4 F and G). No fluorescent signal was observed for the sample using PEI-coated FNP (Figure 4-4H), though similar accumulation of AuNPs-PEI nanoparticles was clearly observed in the phase contrast image. This suggests that the electric pulses did not break the interactions between AuNPs and PEI molecules. For YOYO-1 labeled AuNPs-PEI-DNA polyplex, a strong green fluorescent signal was shown inside the cells (Figure 4-4I). As the samples were fixed immediately after electroporation, this fluorescence clearly indicates the similar quick and direct cytosolic delivery of plasmids by electroporation.

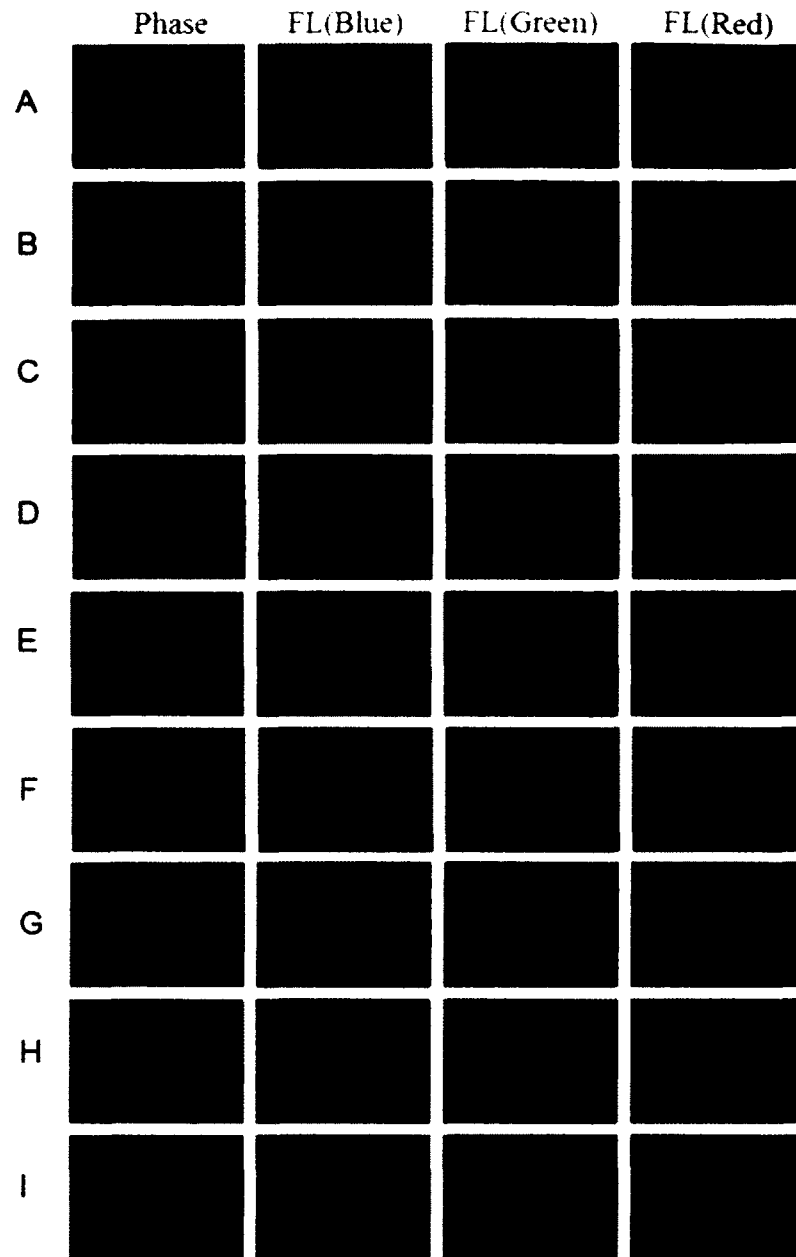


Figure 4-4: Phase contrast and fluorescence microscopic images of distribution and fate of AuNPs-polyplex when mixing with NIH 3T3 cells (A-E) and immediately after electroporation (F-I): (A) untreated samples (negative control); (B) mixture of cells and naked DNA plasmids (green); (C) mixture of cells and FNP (red); (D) mixture of cells with FNP/PEI nanoparticles; (E) mixture of cells with FNP/PEI/DNA; (F) electroporation with DNA alone (green); (G) electroporation with FNP (red); (H) electroporation with FNP/PEI; and (I) electroporation with FNP/PEI/DNA. The 100 X objective was used.

4.3.3 Plasmid DNA Delivery in NIH 3T3 Cells by AuNPs-polyplex

We further explored the delivery of DNA plasmids from AuNPs-polyplex by electroporation. The electroporation was done with NIH3T3 cells with a BTX system using gWiz™GFP plasmids and the following pulse scheme was applied: 125 V (625 V/cm), single 10 ms pulse. Successful transfection was observed 24 h after electroporation in all four cases: electroporation with DNA alone (no AuNPs), with AuNPs + DNA, with polyplex (no AuNPs), and with AuNPs-polyplex, as shown in Figure 4-5. However, a simple combination of electroporation and polyplex showed a significant negative impact on both the delivery efficiency and cell viability (Figure 4-5B), which is consistent with an earlier observation for lipoplex delivery using a similar approach [253]. The poor quality and loose structure of the polyplex might have been destroyed to release a large number of free cationic PEI molecules. These free positively charged macromolecules, together with additional harsh electric pulses, further lowered the overall cell viability and transfection when compared to the electroporation of naked plasmids (Figure 4-5A). Electroporation of polyplex and AuNPs-polyplex with various N/P ratios was conducted as additional proof. As shown in Figure 4-6, with the increase of the N/P ratio, which was an increase in the amount of PEI, more dead cells were observed for polyplex electroporation as well as extremely poor transfection (cells had probably died before gene expression). However, AuNPs-polyplex electroporation with various N/P ratios showed an insignificant difference in cell viability while successful transfection was observed in all these groups. Electroporation delivery of the plasmids together with AuNPs and AuNPs-polyplex showed better GFP expression (Figure 4-5 C

and D), which confirmed again our early observation that the enhancement of AuNPs to electroporation performance [254].

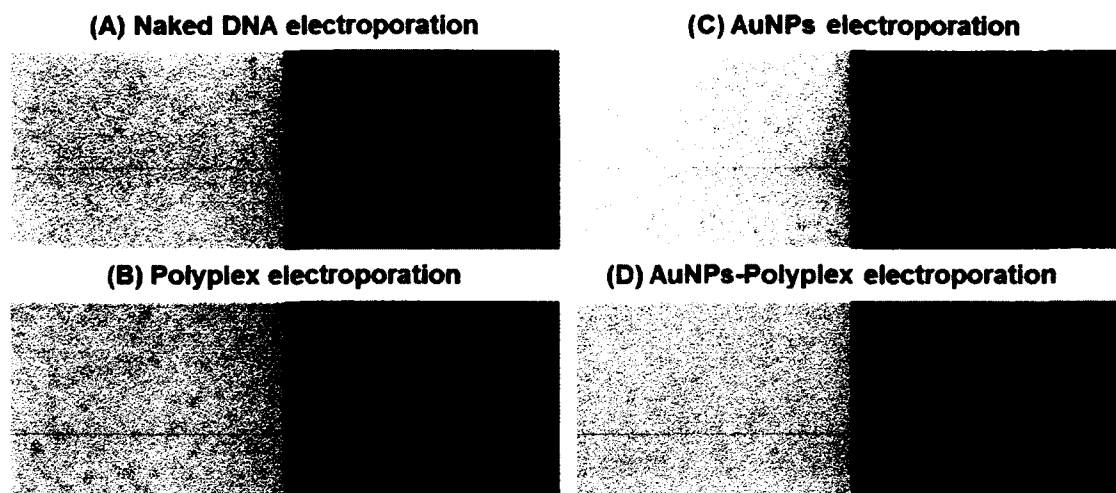


Figure 4-5: Fluorescence and phase contrast microscopic images of pGFP plasmid transfection to NIH 3T3 cells by electroporation.

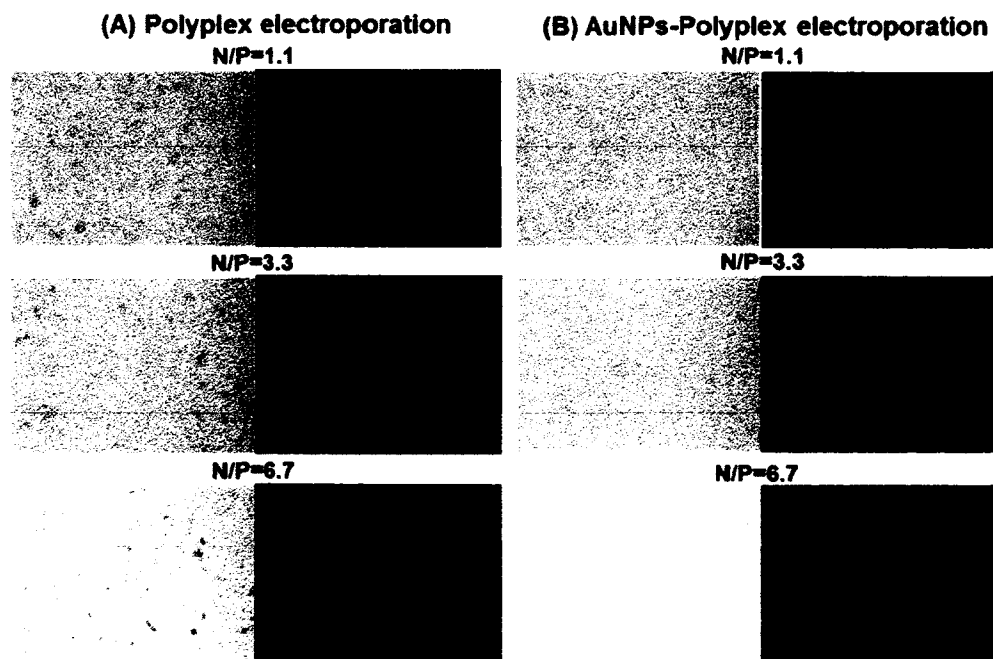


Figure 4-6: Fluorescence and phase contrast microscopic images of pGFP plasmid transfection to NIH 3T3 cells by polyplex and AuNPs-polyplex electroporation.

More quantitative comparison was done by counting the percentage of GFP-positive cells using flow cytometry (Figure 4-7). Efficiency of pGFP transfection from AuNPs-polyplex (using 5 nm AuNPs at a concentration of $1\times$ or 0.1 mg/mL) was about one and a half fold of that using naked plasmids and a simple mixture of DNA and AuNPs (DNA alone: $34.8 \pm 2.0\%$; 5 nm AuNPs and DNA: 44.4% ; 5 nm AuNPs-polyplex: 53.4%). When large sized AuNPs (10–40 nm for their original size) were used, the transfection efficiency was further enhanced to about two-fold of that using naked DNA alone. For comparison, the GFP transfection using electroporation with polyplex was only about one third of that standard electroporation. Greater loss of the cell viability (i.e., 10%) was observed in AuNPs-polyplex electroporation samples than that using naked DNA. However, it is worth the sacrifice of using electroporation to bypass the endocytosis delivery route with direct cytosol delivery and 1.5 - 2 folds increase in the transfection efficiency. When comparing cell viability of 40% (i.e., less than half of the standard electroporation of naked DNA, 90%) with polyplex in electroporation, our approach of introducing AuNPs to fix free or dissociated PEI is effective. This observation was also endorsed with further complex cytotoxicity analysis without electroporation (Figure 4-8).

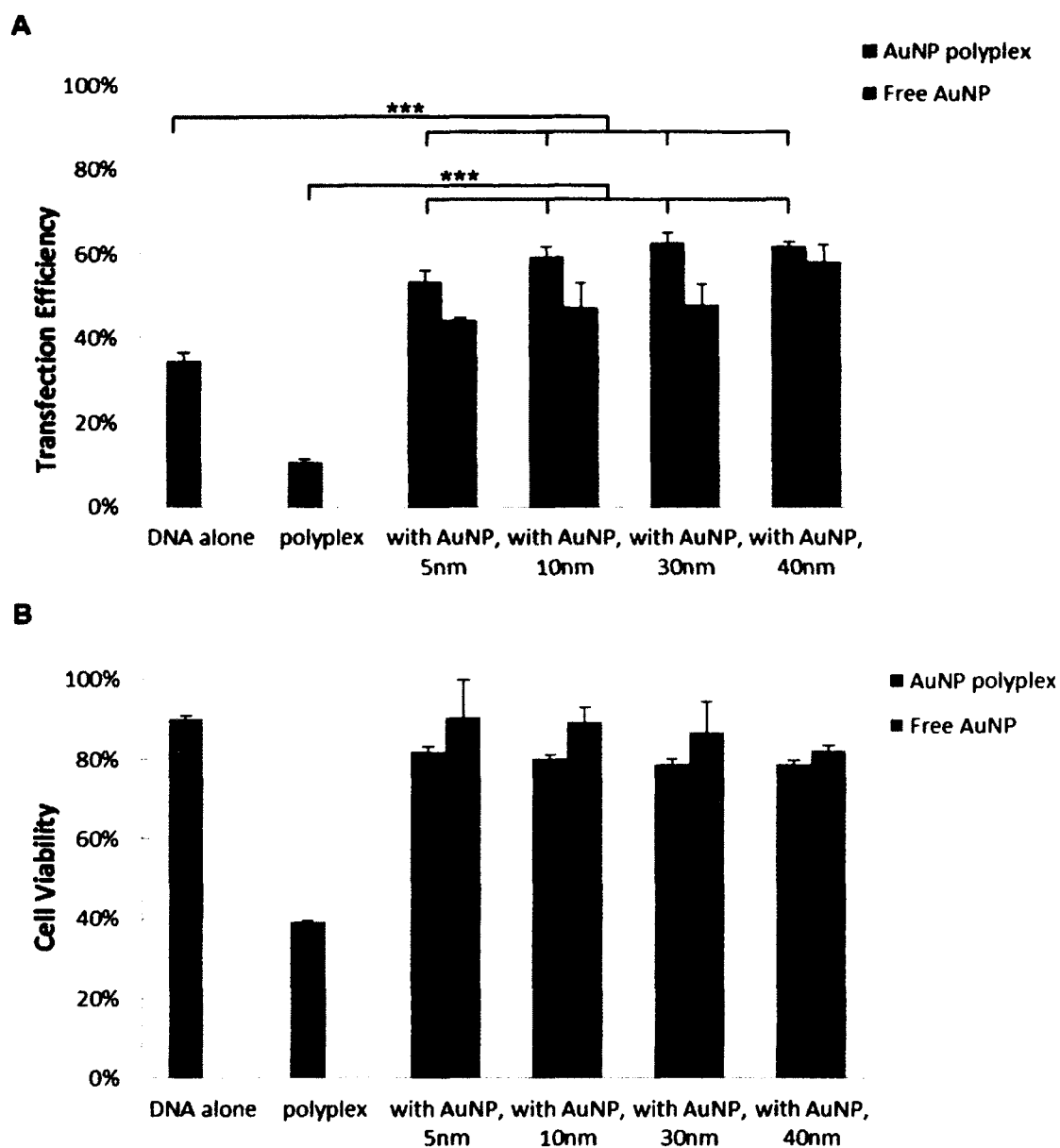


Figure 4-7: Quantitative measurement of electroporation enhanced AuNPs-polyplex delivery performance on 3T3 cells: (A) the flow cytometry results on transfection efficiency and (B) the cell viability via MTS assay. As comparison, results from electroporation with DNA alone, polyplex, and samples of a simple mixing of AuNPs and DNA are also shown. The error bars correspond to triplicate experiments made with independently produced batches. $n = 3$ and (***) represents $p < 0.001$.

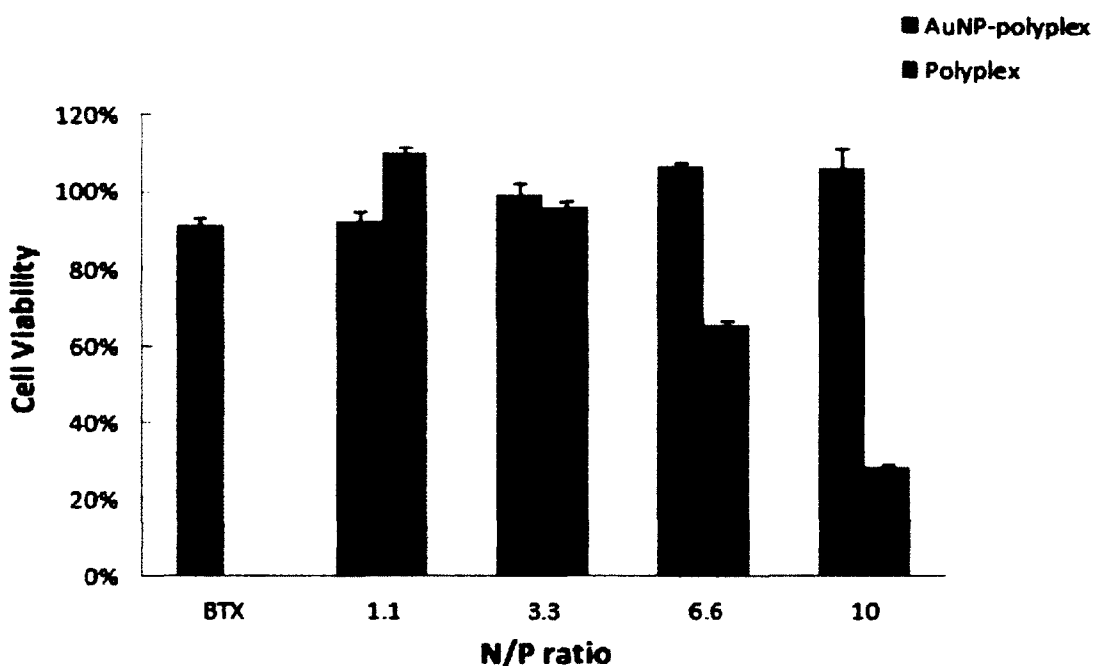


Figure 4-8: The viability of NIH 3T3 cells when incubated with AuNP-polyplex and polyplex determined by MTS assay. PEI is the cationic polymer used here and the incubation was performed at various N/P ratios. The cell viability of commercial bulk electroporation (labeled as “BTX”) is also provided for comparison purpose (n = 3).

In this delivery improvement, the AuNPs core helps enhance the electroporation’s performance from two different aspects [254]: (i) reducing the resistance of the electroporation buffer solution so that the local pulse strength on the cells is enhanced; (ii) serving as virtual microelectrodes to locally porate cells with a limited area from many different sites. Because of their high conductivity (4.5×10^6 S/m), AuNPs dispersed in the buffer and cytoplasm (the conductivity is 0.3 - 1.5 S/m) help greatly reduce the potential drop so that the majority of the electric voltage is imposed on the cell membrane indeed. The cell membrane disruption could therefore be done more effectively without altering the cell physiological conditions (i.e., salt concentration) or losing cell viability. When the electric field converges in the vicinity of AuNPs, they

work like many virtual nanoelectrodes to cause localized poration. Different from the traditional bulk electroporation with two large breakdown locations, multiple small poration sites are formed after adding AuNPs that benefit not only the recovery of the cell membrane, but also the cytosolic delivery of plasmids from multiple sites.

The contribution of AuNPs-polyplex to the transfection improvement of DNA plasmids is also multifactorial: (i) they help fix PEI on the surface of AuNPs to significantly reduce the toxicity caused by the presence of free and/or dissociated cationic polymer molecules in the polyplex (Figure 4-8), (ii) they effectively produce polyplex nanoparticles with smaller average size than the naked DNA plasmids and narrower size distribution when compared to that from the vortex mixing synthesis (Figure 4-2F), (iii) the PEI molecules in AuNPs-polyplex help protect DNA plasmids and condense them near the vicinity of the cell membrane to promote the cytosolic delivery and also later for nuclear transport. These effects offer AuNP-polyplexes advantages over the use of the mixture of AuNP and naked DNA in electroporation (Figure 4-7) as well as many traditional transfection approaches (Figure 4-9) on the transfection efficiency and cell viability. The slight loss on cell viability (Figure 4-7B) probably results from the presence of some free PEI molecules to the electroporated cells.

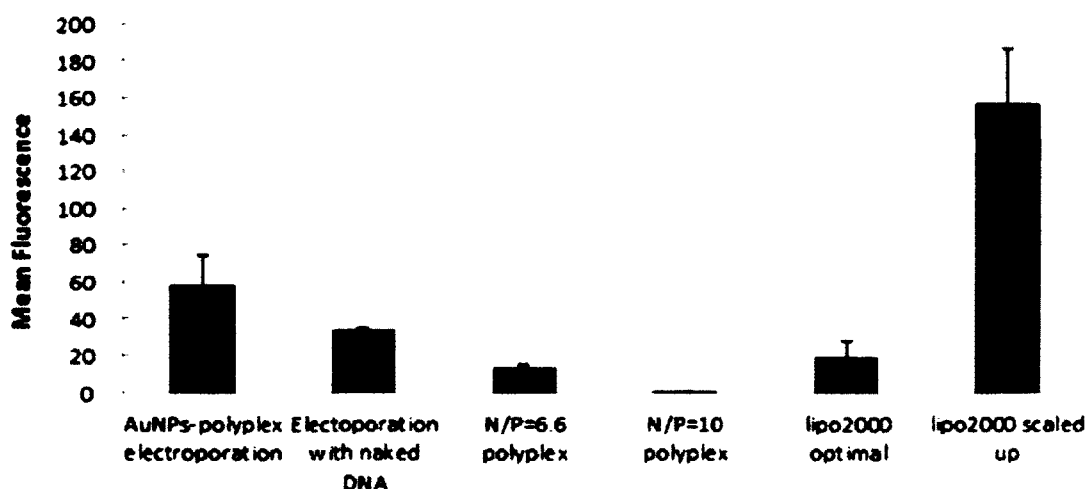


Figure 4-9: Comparison of AuNPs-polyplex electroporation was compared to traditional transfection approaches PEI/DNA polyplex at two different N/P ratios (6.6 and 10) and lipo2000 at two different dosages (“optimal” refers to the protocol recommended dosage; and “scaled up” refers to the case with increased lipo2000 dose to match the actual DNA amount use in electroporation) (n = 3).

4.4 Conclusions

In summary, we immobilized the polyplex on AuNPs and delivered them into the cells through electroporation. Conjugating with AuNPs helps minimize the cytotoxicity concerns from polyplex after cytoplasmic release while still retaining good probe protection. It also avoids poor nanoparticle quality existing in traditional polyplex synthesis, namely large size and broad size variations, by managing molecule interactions and assembly on the surface of AuNPs. Combined with electroporation, conjugated polyplex (AuNPs-Polyplex) showed quick delivery and significant enhancement of the transfection efficiency with no obvious increase of toxicity. Such a combination of physical and chemical delivery concept may stimulate further exploration in the delivery of various therapeutic materials for both *in vitro* and *in vivo* applications.

The choice of AuNPs in the enhancement of polyplex delivery lies on their high conductivity and excellent biocompatibility. Their other potential advantages, such as sensing signal enhancement via localized surface plasmon resonance or surface-enhanced Raman spectrum, have not yet been investigated with this gene delivery approach. Our approach however has a promising potential to integrate both diagnostic and therapeutic functions in one nanosystem (namely nanotheranostics) to accomplish both noninvasively tracking the targeting therapeutic probes and measuring their delivery performance simultaneously. This integration will surely help increase our understanding on the regulation mechanism of many therapeutic probes and quickly establish appropriate strategies to improve their delivery or treatment performance. Other forms of gold nanostructures, such as nanorod, nanoshell, or nanowires, in principle, could also be used for the similar purposes. Their success will accelerate and broaden the applications of these nanomaterials in drug discovery, cancer diagnosis, and treatment, and/or regenerative medicine where quick and precise diagnosis and therapeutics is urgently needed.

CHAPTER 5

GOLD NANOPARTICLE ENHANCED SMALL NUCLEOTIDE MOLECULE DELIVERY BY ELECTROPORATION TO MAMMALIAN CELLS

5.1 Introduction

RNA interference is an endogenous process where small interfering RNA (siRNA) molecules regulate gene expression by silencing mRNA targets. Since the first report from Fire's group that siRNA was responsible for gene silencing in *C. elegans*, RNA interference has been attracting attention in mammalian cell processes and as a treatment for diseases [255-263]. Various carriers, such as cationic polymers, lipids and nanoscale materials, have been investigated for siRNA delivery [74, 264-269]. However, the safety and delivery efficiency still remain as a challenge for clinical application of siRNA [270-273].

MicroRNAs (miRNAs) are small (contains approximately 22 nucleotides) endogenous non-coding RNAs that function in RNA silencing at the posttranscriptional level through base pairing with mRNA molecules [274, 275]. They regulate a broad network of genes since this base pairing is not necessarily perfect. It has been recently demonstrated that down regulation of miR-29 family members in various cancer cells may contribute to the abnormal cell proliferation, apoptosis and migration [276-285]. Therefore, the miR-29 family has become a research focus of miRNA-based therapy and

attracted much attention as a new strategy in cancer treatment. However, delivery of miRNAs encountered critical hurdles including, but not limited to, poor stability, rapid blood clearance, and insufficient cellular uptake.

Polyethylenimine (PEI) has been used as a non-viral carrier for its ability to electrostatically interact with nucleic acids and protect them from intracellular enzymes. While the delivery of plasmids with PEI has been proven to be efficient, siRNA transfection with PEI has been shown to be less satisfying because of the stiffer nature of RNA molecules compared to DNA [4, 286-289]. Moreover, the toxicity of PEI is associated with its positive charges, enabling it to interact strongly with cell membranes and result in damage. Therefore, modification of PEI to reduce the positive charge could be an option to improve its delivery performance.

In our study, we used electroporation to bypass the slow and inefficient endocytosis process by directly delivering therapeutic probes into the cell cytosol. As the followup of our previous study, we applied AuNP to enhance electroporation performance – AuNPs were coated with cationic polymer and further conjugated with negatively charged RNA molecules to form AuNPs-polyplex. The presence of AuNPs helped to focus electric pulses and localize poration, which was proven beneficial for not only the recovery of electroporated cells, but also the uptake of probes from multiple sites to facilitate the cytosolic delivery. The AuNPs enhanced RNA delivery was evaluated by the cell viability and the down regulation of the targeted genes.

5.2 Materials and Methods

5.2.1 Materials and Reagents

Branched PEI (MW = 25 kDa), AuNPs were obtained from Sigma-Aldrich (St. Louis, MO). The concentration of 1 X AuNPs refers to the stock solution, which has 0.01 wt% of Au (0.1 mg/mL) while the actual particle number varies with the size of AuNPs. DNA plasmids with gWiz™GFP and gWiz™Luc reporter genes were purchased from Aldevron (Fargo, ND). siRNA used for silencing GFP (expressed by pMaxGFP purchased from Lonza) and luciferase genes were synthesized by Thermo Scientific (Pittsburgh, PA) and the sequences were as follows: siRNA for GFP silence, sense strand, 5-CGCAUGACCAACAAGAUGAUU-3; antisense strand, 5-UCAUCUUGUUGGUCAUGCGGC-3; luciferase GL3 duplex (Luc-siRNA); sense strand, 5-CUUACGCUGAGUACUUCGA-3; antisense strand, 5-UCGAAGUACUCAGCGUAAG-3. miRIDIAN microRNA human hsa-miR-29b-3p mimic with mature miR sequence: 5-UAGCACCAUUUGAAAUCAGUGUU-3 was purchased from Thermo Scientific (Pittsburgh, PA). All other chemicals were purchased from Sigma-Aldrich (St. Louis, MO); the cell culture reagents, reverse transcription kits, universal master mix for qRT-PCR, and TaqMan® gene expression assays were purchased from Life Technologies (Carlsbad, CA) unless specified.

5.2.2 Preparation of AuNPs-polyplex

To prepare AuNPs/PEI polyplex, 500 µL 0.5 mg/mL PEI (pH 7.0) was added to 500 µL 0.01 wt% of AuNPs. The original citric acid terminated surface of AuNPs facilitated the deposition of PEI molecules through electrostatic interactions. The incubation was performed at room temperature for 20 min and the extra PEI was removed

by centrifuging at $15,000 \times g$ for 10 min. The PEI-coated AuNPs were resuspended in desirable amount of PBS (pH 7.0) and desirable amount of siRNA/miR29b was added to AuNPs/PEI. The resulting mixture was mixed by pipetting and further incubated at room temperature for 20 min.

5.2.3 NIH 3T3 and K562 Cell Culture

NIH 3T3 cells were obtained from American Type Cell Culture (ATCC, Manassas, VA). They were grown and maintained in high-glucose DMEM supplemented with 10% newborn calf serum, 1% penicillin and streptomycin, 1% L-glutamine, and 1% sodium pyruvate. For subculture, culture medium was removed and discarded first. The cell layer was briefly rinsed with DPBS to remove the serum which contains a trypsin inhibitor. Then 1-2 mL trypsin-EDTA was added for a 100 cm² Petri dish. Cell culture was then observed under an inverted microscope until cell layer was dispersed (usually 5-15 min); 8 to 9 mL complete growth medium was added and cells were aspirated by gently pipetting. Appropriate aliquot of the cell suspension was transferred to a new culture dish with the addition of more growth medium to make a total volume of 10 mL for a 100 cm² surface. K562 lymphoblast cells were also obtained from American Type Cell Culture (ATCC, Manassas, VA). K562 cells were cultured and maintained in RPMI 1640 media supplemented with 10% heat-inactivated fetal bovine serum (FBS), 100 U/mL penicillin, 100 g/mL streptomycin, and L-glutamine. For the subculture, a desired amount of K562 cell suspension was transferred to a new Petri dish with the addition of an appropriate amount of fresh culture medium. All cultures were maintained at 37 °C with 5% CO₂ and 100% relative humidity.

5.2.4 Electroporation Setup and Procedure

NIH 3T3 or K562 cells were counted with hemocytometer to determine cell density, centrifuged at $200 \times g$ for 5 min and then resuspended in fresh GIBCO OPTI-MEM I (a serum free medium) at desired densities of 0.5×10^6 to 0.5×10^7 cells/mL. Cell suspensions were then mixed with AuNP-polyplexes of various concentrations and sizes while the amount of DNA plasmids was fixed at 25 μg / sample. Electroporation was done with a commercial instrument (ECM 830, Harvard Apparatus) in cuvettes with a 2-mm gap, each containing a 100 μL sample solution. The standard electroporation condition (single 10 ms pulses of 125 V/2 mm cuvette) was applied with a single unipolar pulse. After electroporation, samples were transferred to 6-well cell culture plates, incubated in a fresh medium for another 24 h, and then harvested for analysis.

5.2.5 Measurements of Cell Viability

The cell viability was evaluated by an MTS cell proliferation assay (Promega, Madison, WI). Briefly, the cells in 100 μL /well of medium were transferred to a 96-well plate and incubated. Twenty microliters of CellTiter 96 AQueous One solution (Promega, Madison, WI) was added to each well and cells were incubated at 37 °C for another 1 h. Absorbance was measured at 492 nm on an automated plate reader (Elx 800, Biotek, VT). Normally grown cell samples were used as negative control whose viability was set to 100%. Data points were represented as the mean \pm SD of triplicates, unless otherwise indicated.

5.2.6 AuNPs-polyplex Delivery Efficiency of Small Interfering RNA

The GFP down regulation efficiency was determined by Agilent 2100 Bioanalyzer (Agilent Technologies, Santa Clara, CA). The fluorescence intensity of GFP

was measured using Cell Assay Module with live cells stained with carboxynaphthofluorescein (CBNF). The results were analyzed with Agilent 2100 Expert Software and 500–1500 events were counted for each sample. The Luc-siRNA down regulation efficiency was quantified by One-Glo™ Luciferase assay system (Promega, Madison, WI). Hundred microliters One-Glo™ reagent was added to the cell growth in 100 μ L of the medium in a 96-well plate. Luminescence was measured with a plate reader (FLUOstar OPTIMA, BMG LABTECH, Germany) after 10 min incubation at room temperature for complete cell lysis.

5.2.7 AuNPs-polyplex Delivery Efficiency of microRNA

The miR29b delivery efficiency was evaluated from two aspects: 1) expression of mature miR29b; 2) expression of target genes including CDK6, DNMT3B and MCL1. To measure expression levels, the total RNA was first transcribed into cDNA and qRT-PCR was conducted. The expression was determined by the $\Delta\Delta$ Ct method and normalized to endogenous controls.

5.2.7.1 Total RNA Extraction

Total RNA was extracted using TRIzol® reagent (Life Technologies, Carlsbad, CA). Cells were harvested by centrifugation and culture media was removed, and 0.75 mL TRIzol® reagent was added to every 0.25 mL sample (containing approximately $5-10 \times 10^6$ cells). Samples were lysed by pipetting up and down several times and incubated for 5 min at room temperature, allowing the nucleoprotein complex to dissociate completely. 0.2 mL chloroform was added to every 1 mL TRIzol® reagent and the tubes were shaken vigorously for 15 s followed by 2-3 min incubation at room temperature. Then centrifugation with $12,000 \times g$ for 15 min at 4 °C was conducted and the samples

were separated into a colorless upper phase, an interphase and a lower red chloroform phase. The upper aqueous phase was transferred into new tubes by gentle pipetting without drawing any of the interphase, and 0.5 mL 100% isopropanol for every 1 mL TRIzol[®] reagent was added to the aqueous phase, followed by 10 min incubation at room temperature. Centrifugation at $12,000 \times g$ for 10 min at 4 °C was conducted and supernatant was removed. To wash the RNA pellet, 1 mL 75% ethanol per 1 mL TRIzol[®] reagent was used. Samples were vortexed briefly and centrifuged at $7500 \times g$ for 5 min at 4 °C. We discarded the supernatant was discarded and air dried the RNA pellet for 5-10 min; 20-50 μ L RNase-free water was added and samples were incubated at 55-60 °C for 10-15 min. Then the RNA was ready for downstream application.

5.2.7.2 Reverse Transcription PCR

The TaqMan[®] microRNA Reverse Transcription Kit (Life Technologies, Carlsbad, CA) was used for miRNAs reverse transcription. The reagents were first allowed to thaw on ice. The total volume of 15 μ L reaction was prepared in a polypropylene tube, including 0.15 μ L dNTP mix (100 mM total), 1 μ L Multiscribe[™] RT enzyme (50 U/ μ L), 1.5 μ L 10X RT buffer, 0.19 μ L RNase inhibitor (20 U/ μ L), 4.16 μ L nuclease free water, 3 μ L primer and 5 μ L RNA sample (1 to 10 ng). The thermal cycler was programmed as follows: 30 min at 16 °C, 30 min at 42 °C, 5 min at 85 °C and finally hold at 4 °C.

The High-Capacity cDNA Reverse Transcription Kit (Life Technologies, Carlsbad, CA) was used to reverse transcribed mRNAs of CDK6, DNMT3B and MCL1. The total volume of 20 μ L reaction was prepared in a polypropylene tube, including 2 μ L 10 X RT buffer, 0.8 μ L dNTP mix (100 mM), 2 μ L 10 X RT random primers, 1 μ L

MultiScribe™ reverse transcriptase, 4.2 µL nuclease free water, and 10 µL RNA sample. The thermal cycler was programmed as follows: 10 min at 25 °C, 120 min at 37 °C, 5 min at 85 °C and finally hold at 4 °C.

5.2.7.3 qRT-PCR Amplification

The resulting cDNA from reverse transcription reaction was amplified by qRT-PCR with TaqMan® Universal Master Mix II (Life Technologies, Carlsbad, CA). The total volume of 20 µL reaction was prepared in a polypropylene tube, including 10 µL 2 X TaqMan® Universal Master Mix II, 1 µL 20 X TaqMan® assay and 9 µL cDNA template (1-100 ng). The thermal cycler was programmed as follows: 10 min at 95 °C for polymerase activation, then 40 PCR cycles with 15 s at 95 °C for denature and 1 min at 60 °C for anneal. The relative gene expression was determined by the $\Delta\Delta C_t$ method. The mature miR-29b expression was normalized to endogenous control RNU48 and relative to the untreated control cells. The expression of CDK6, DNMT3B, and MCL1 mRNAs was normalized to endogenous controlled GAPDH and relative to the untreated controlled cells.

5.3 Results and Discussion

5.3.1 Gold Nanoparticle-Enhanced siRNA Delivery

To demonstrate the effectiveness of AuNPs electroporation on siRNA delivery, we chose siRNA with specific sequences to silence the expression of GFP when cotransfecting with pGFP by electroporation. K562 cells were cotransfected with 5 pmol siRNA and 10 µg pMaxGFP by electroporation, together with free 10 nm AuNPs. The bulk electroporated cells (BTX) were used as negative control. As shown in Figure 5-1A, less GFP expression was seen when codelivering pMaxGFP and the corresponding

siRNA. Electroporation with AuNPs turned off more GFP expressions than electroporation with free siRNA (Figure 5-1B).

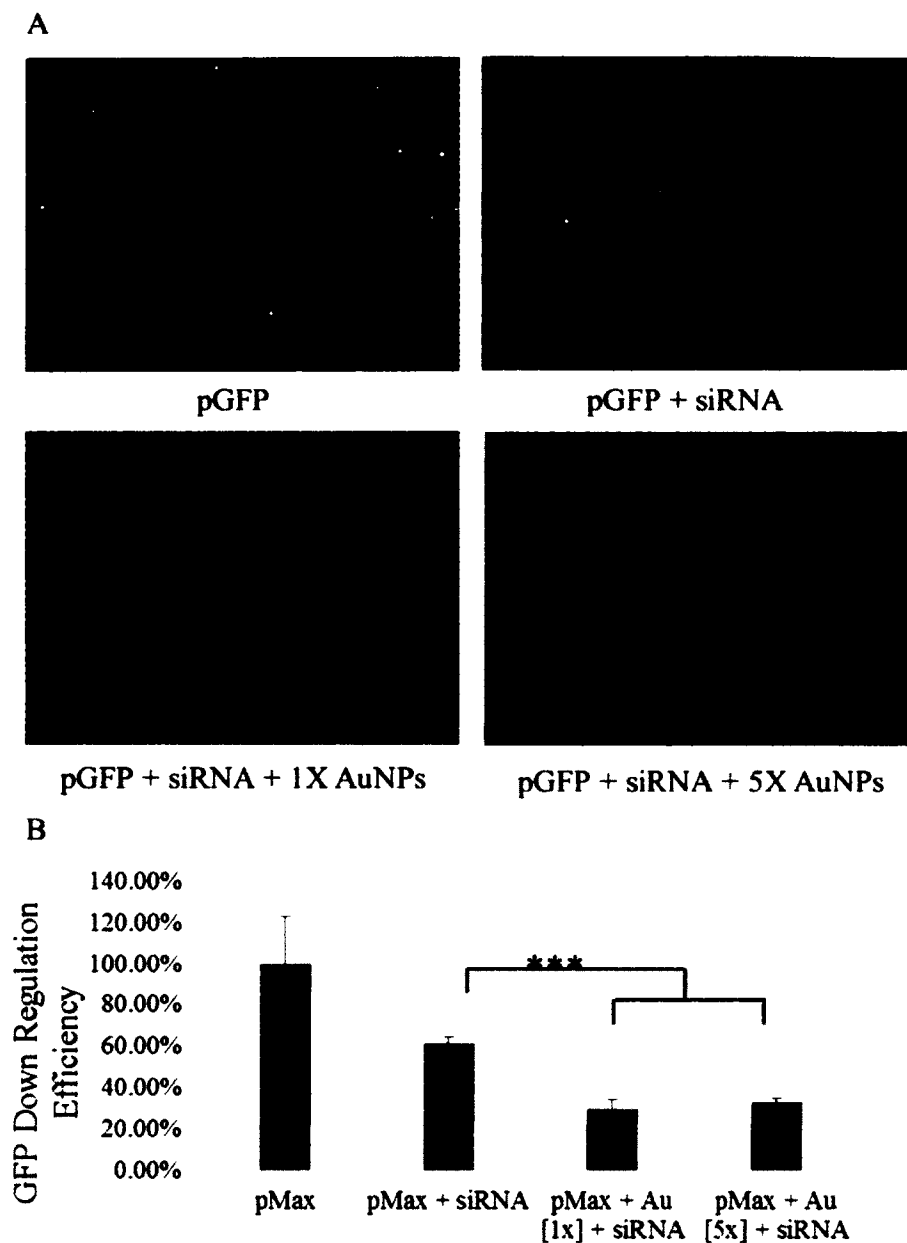


Figure 5-1: AuNPs electroporation enhanced siRNA delivery: (A) fluorescence images and (B) intensity measurement on GFP expression level. $n = 3$ and (***) represents $p < 0.001$.

The enhancement of AuNPs-polyplex to siRNA interference performance should be better than what was shown in Figure 5-1. The presence of AuNPs enhanced the expression level of green fluorescent protein with the same mechanism demonstrated in Figure 4-7 of Chapter 4. This enhanced expression means siRNA with AuNPs must shut off more GPF proteins than that using siRNA only to reach the similar protein expression level. Therefore, the enhancement of AuNPs to siRNA down regulation is better than what was shown in Figure 5-1 for their higher starting protein level.

5.3.2 Gold Nanoparticle-Enhanced miRNA Delivery

K562 cells were electroporated with fluorescent AuNPs (FNP) or transferrin grafted AuNPs (Au-Tf), together with 200 pmol miR-29b. The bulk electroporated cells (BTX) were used as negative control. The cells that were transfected with Lipofectamine2000 (lipo) was used as the positive control. Compared to negative control, the mature miR-29b expression was increased ~1.45 folds in the cells that were electroporated with FNP, and ~1.97 folds in those that were electroporated with Au-Tf at 24 hours after electroporation. This increase demonstrated that both free AuNPs and transferrin-grafted AuNPs have enhanced miR-29b expression (Figure 5-2A). As shown in Figure 5-2B, the expression of targeted genes DNMT3B and MCL-1 was more efficiently down-regulated in the cells electroporated with FNP and Au-TF compared to Lipofectamine2000 transfection. Moreover, the down regulation of the target genes is either more efficient or comparable with bulk electroporation (Figure 5-2B).

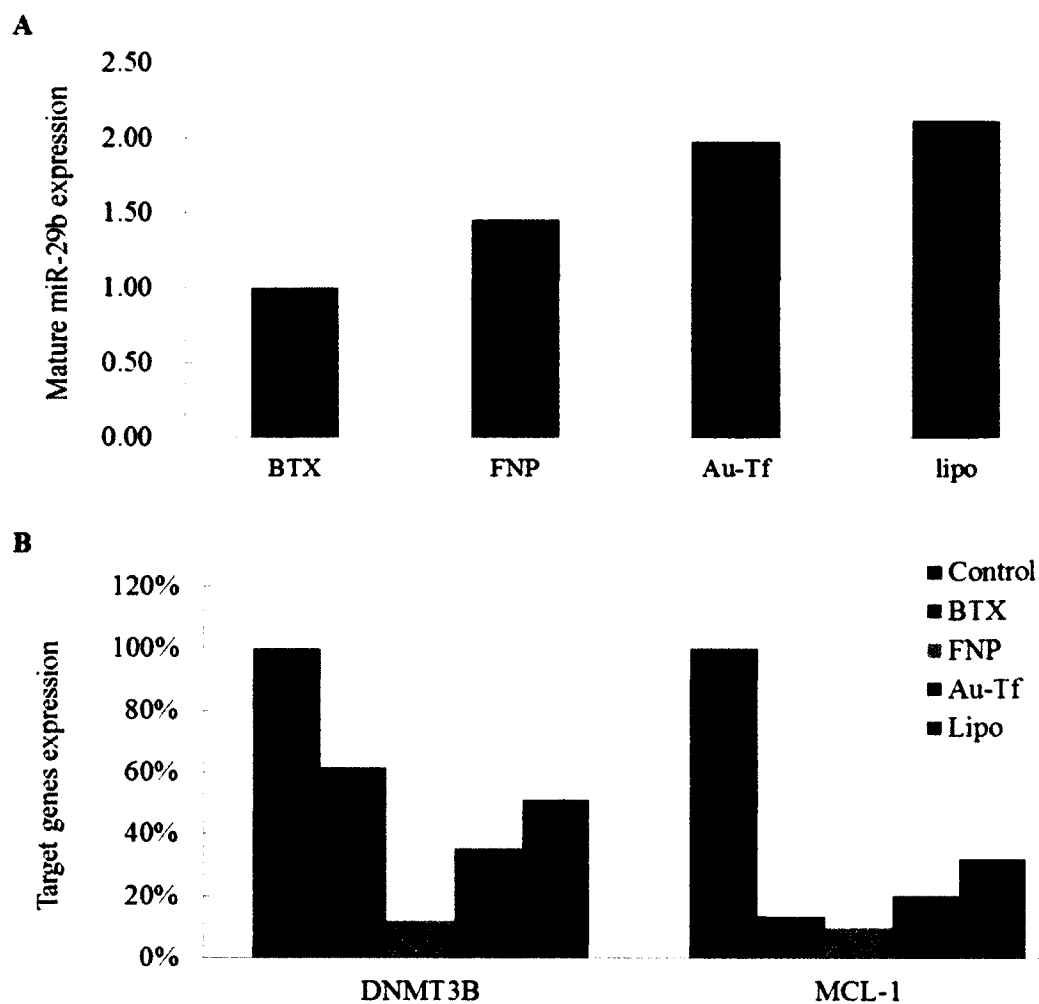


Figure 5-2: Preliminary result for AuNPs enhanced miR-29b delivery in K562 cells: (A) mature miR-29b expression (all expression levels were normalized to bulk electroporation) (B) targeting genes expression.

5.3.3 siRNA Delivery by AuNPs-polyplex

To demonstrate the effectiveness of AuNPs-polyplex electroporation on siRNA delivery, we chose siRNA with specific sequences to silence the expression of GFP and luciferase when cotransfecting with pGFP and pLuc by electroporation. Both adherent cells NIH 3T3 and suspension cells K562 were used for the tests.

As shown in Figure 5-3A and Figure 5-4A, less GFP expression was seen when codelivering pMaxGFP and the corresponding siRNA. Electroporation with AuNPs-polyplex (siRNA) turned off more GFP expressions than electroporation with free siRNA (Figure 5-3B and Figure 5-4B). Similar down regulation performance was found when cotransfecting pLuc and the corresponding siRNA GL3 into K562 cells, as shown in Figure 5-4C. Compared to the interference result of free siRNA GL3, an additional 15% drop of luciferase signal was found when siRNA molecules were conjugated in AuNPs-polyplex. Because siRNA have a much smaller size than plasmid DNA, delivery of neither free siRNA nor AuNPs-polyplex to cell cytosol through electroporation is very challenging. However, because siRNA rapidly denatures, studies of siRNA delivery often focus on their protection from enzyme degradation. Therefore, siRNA delivery with AuNPs-polyplex electroporation could be more beneficial when used for *in vivo* delivery.

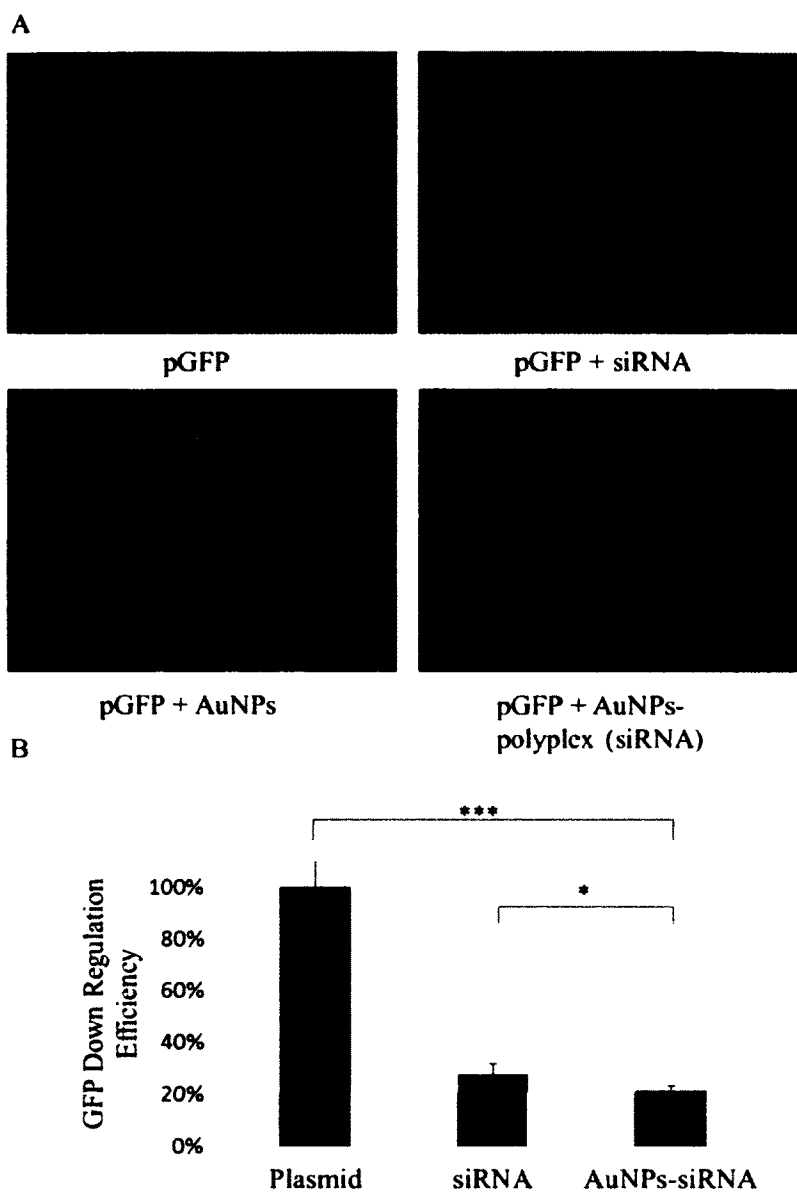


Figure 5-3: AuNPs-polyplex electroporation enhanced siRNA delivery in 3T3 cells: (A) fluorescence images and (B) intensity measurement on GFP expression level. $n = 3$ and (*) represents $p < 0.05$, (***) represents $p < 0.001$.

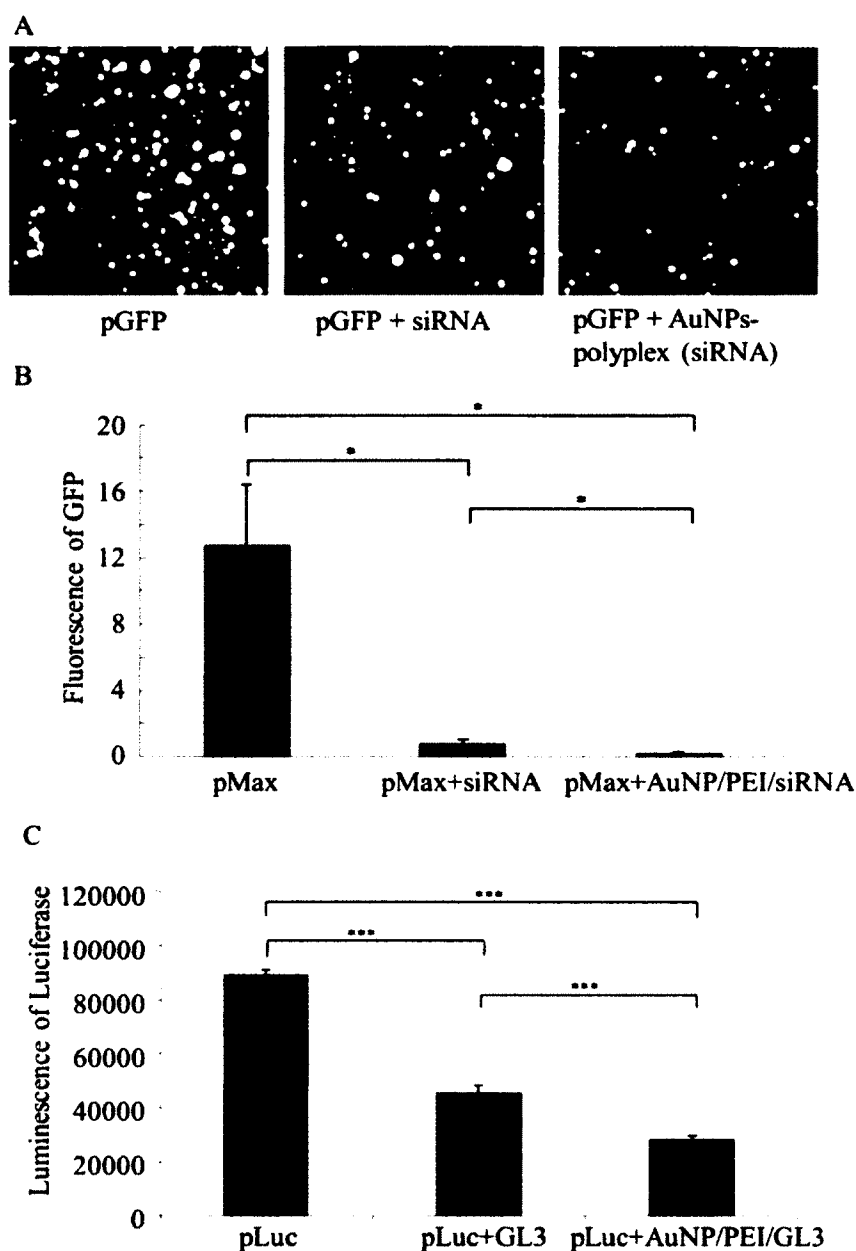


Figure 5-4: AuNPs-polyplex electroporation enhanced siRNA delivery in K562 cells: (A) fluorescence images and (B) intensity measurement on GFP expression level, and (C) the luminescence measurement on luciferase expression level for free siRNA (“pMax + siRNA” and “pLuc + GL3”) and siRNA from AuNPs-polyplex (“pMax + AuNP/PEI/siRNA” and “pLuc + AuNP/PEI/GL3”). $n = 3$ and (*) represents $p < 0.05$, (***) represents $p < 0.001$.

As cotransfection of DNA plasmids and siRNA approach were adopted here, the interference of siRNA to the expression of the targeting reporter gene occurs simultaneously with that particular transgene expression in cells. The early presence of copious siRNA probes could silence the cotransfected targeting genes more efficiently than those that already maintain a sustained expression level in the cells. Therefore, both free siRNA and siRNA from AuNPs-polyplex showed efficient down regulation performance here, which allows only limited room for AuNPs-polyplex to further enhance this interference. Moreover, the presence of AuNPs during polyplex (siRNA) delivery simultaneously enhanced the expression level of green fluorescent protein or luciferase with the same mechanism demonstrated in Figure 4-7 of Chapter 4. This enhanced expression means siRNA molecules in AuNPs-polyplex must shut off more GFP or luciferase proteins than that using free siRNA to reach the similar protein expression level. In other words, the enhancement of AuNPs-polyplex to siRNA down regulation is better than what was shown in Figure 5-3 and Figure 5-4 for their higher starting protein level than that using free siRNA probes.

5.3.4 miRNA Delivery by AuNPs-polyplex

As shown in Figure 5-5A, higher mature miR-29b expression was achieved with AuNPs-polyplex electroporation. At 24 hours after electroporation, the mature miR-29b expression was ~2.7 folds more efficient than bulk electroporation, and ~82 folds more efficient than the expression for the sample in which the cells were incubated with AuNPs-polyplex without electroporation. This result indicates that both AuNPs-polyplex and electroporation contributed in the process of the miR-29b delivery. The expression of the targeted genes, DNMT3B, CDK6, and MCL-1 was more efficiently down regulated

with AuNPs-polyplex electroporation. As shown in Figure 5-5B, for cells that were electroporated with AuNPs-polyplex, the target genes DNMT3B, CDK6 and MCL-1 were down-regulated by 55%, 12%, and 40%, respectively, compared to the untreated cells, and 45%, 34%, and 35%, respectively, compared to the incubation only group.

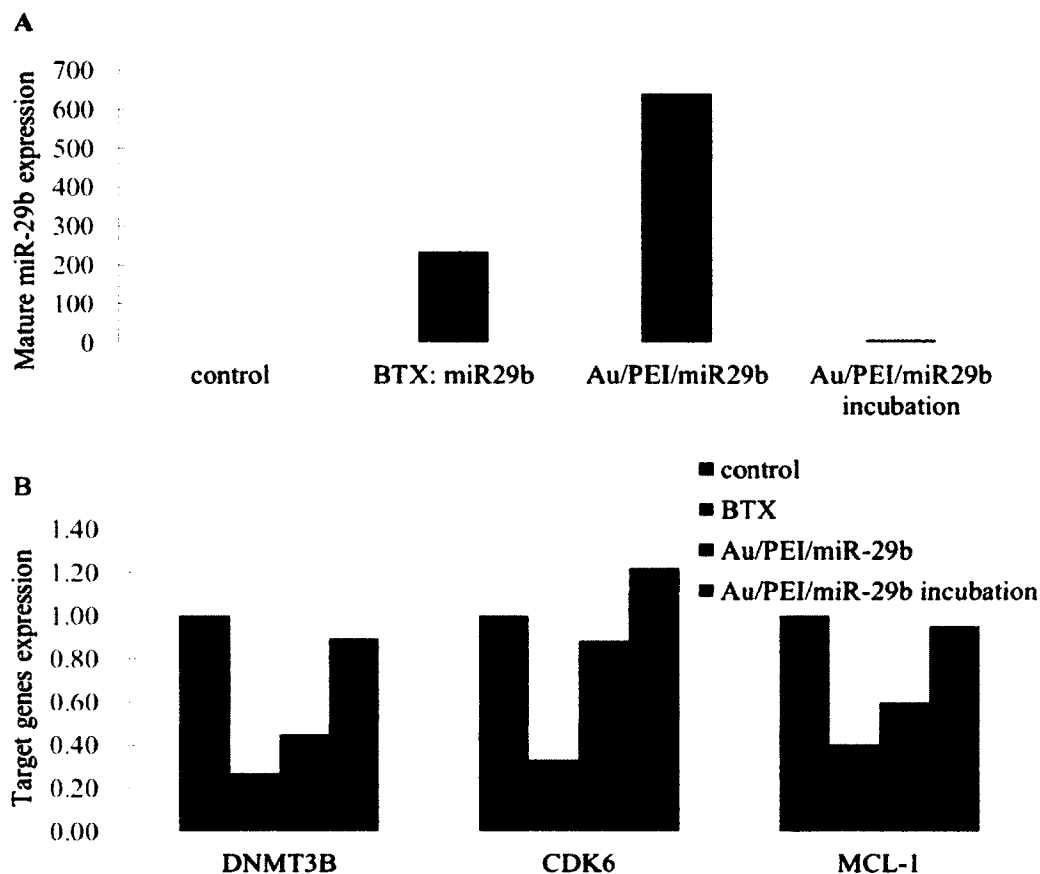


Figure 5-5: Preliminary results for AuNPs-polyplex enhanced miR-29b delivery in K562 cells: (A) mature miR-29b expression (B) targeting genes expression. “Au/PEI/miR29b incubation” stands for transfection with AuNPs-polyplex without electroporation. All expression levels were normalized to untreated cells (control).

5.4 Conclusions

This chapter focuses on the small nucleotide delivery with the AuNP-polyplex electroporation method. AuNPs are used to enhance the strength of the local electric field

and conjugate with the polyplex to reduce the cytotoxicity during electroporation. The RNA release, expression, and their effect to regulate the target genes were justified. Based on the higher expression efficiency of the AuNP-polyplex electroporation, we concluded that this method performs better than bulk electroporation and sole AuNP enhanced electroporation. These findings suggest favorable prospects for the practical application of small nucleotide in genetic therapies. Unlike plasmids, the RNAs are rather fragile and the protections to prevent the RNAs from degrading in the process of delivery are necessary. We expect that our AuNP-polyplex provide a tool for *in vivo* genetic regulation with low toxicity and high delivery efficiency, and therefore serve as resource for novel therapies in regenerative medicine.

CHAPTER 6

CONCLUSIONS AND FUTURE WORK

6.1 Conclusions

Electroporation is an effective nonviral cell transfection approach for its balance on the transfection efficiency and cell viability, no restrictions of probe or cell type, and operation simplicity. In this dissertation, we investigated the improvement of electroporation performance through the introduction of AuNPs, transferrin grafted AuNPs, or AuNP polyplexes. Results are concluded as follows:

With the application of highly conductive AuNPs in electroporation solution, we demonstrated better DNA and RNA delivery efficiency and higher cell viability in mammalian cell electroporation. By adding free AuNPs in the electroporation system, we reduced the resistance of the electroporation solution so that the local pulse strength on the cells was enhanced. We have confirmed the pulse strength focusing effect and investigated its dependence on the particle size, concentration, and electroporation conditions. Transferrin-grafted AuNPs were brought to the cell membrane by affinity binding to TfR receptors to work as virtual microelectrodes to porate cells with a limited area from many different sites. The contributions of localized electroporation with Tf-AuNPs were then evidenced. An equivalent mixture of free AuNPs and Tf-AuNPs exhibited the best enhancement, where the transfection efficiency increased 2-3 folds

with minimum sacrifice of cell viability. These concepts enhanced *in vitro* delivery of DNA probes for both batch-type and flow-through electroporation systems.

We have also used AuNPs as carriers for PEI-DNA and PEI-RNA polyplex while electroporation was applied for fast and direct cytosolic delivery. In this case, cationic polymer molecules condense and/or protect genetic probes as usual, while the AuNPs help in aggregating and fixing polycations. The AuNP fixing helps to minimize the cytotoxicity from polyplex after cytoplasmic release without degrading probe protection. It also avoids the poor nanoparticle quality problem existing in traditional polyplex synthesis, namely oversized particles and broad size variations, by managing molecule interactions and assembly on the surface of AuNPs. This hybrid approach was evaluated with both model anchor cells (i.e., NIH/3T3) and suspension cells (i.e., K562). We found that AuNP-polyplex showed 1.5-2 folds improvement on the transfection efficiency with no significant increase of toxicity when compared to free plasmid delivery by electroporation alone.

6.2 Future Work

It has been demonstrated by several studies that microRNAs are actively involved in tumor development by functioning as tumor suppressors or/and oncogenes. Currently, miRNA-based therapy faces several challenges, including lack of tissue specificity, poor stability, and insufficient cellular uptake. AuNP polyplex can be used to protect microRNA in electroporation therapy by enhancing their intracellular stability. The availability of versatile surface modification technologies for AuNPs allows for great opportunities to use AuNPs-polyplex to deliver miRNA with cell or tissue specificity.

Gold nanomaterials have been widely used in sensing, imaging, diagnosis, and therapeutic applications. In this case, our approaches could be integrated with some diagnostic and therapeutic functions in a single nanosystem. Therefore, they could be used to noninvasively track the target therapeutic probes and to measure their delivery performance simultaneously.

The main objective of this dissertation thesis is to develop AuNPs carriers for electroporation-based therapeutic gene-delivery. Animal models should be used to investigate the *in vivo* behaviors of the therapeutic delivery, such as stability of therapeutic probes, toxicity of the delivered complex, route tracking and clearance rate of AuNPs.

LIST OF PUBLICATIONS AND CONFERENCE PROCEEDINGS

Publications

- Y. Zu, S. Huang, Y. Lu, S. Wang, “Size Specific Transfection to Mammalian Cells by Micropillar Array Electroporation,” *Analytical Chemistry* under revision.
- Y. Zu, S. Huang, W. Liao, Y. Lu, S. Wang, “Gold Nanoparticles Enhanced Electroporation for Mammalian Cell Transfection,” *Journal of Biomedical Nanotechnology* (2014), 10, 982-992. (Impact factor: 7.578)
- S. Huang, H. Deshmukh, K. Rajagopalan, S. Wang, “Enhancing Electroporation Transfection with AuNPs Polyplex,” *Electrophoresis* (2014), 35, 1837-1845. (selected as the cover page, Impact factor: 3.161)
- S. Huang, Y. Zu, S. Wang S. “Gold Nanoparticle-Enhanced Electroporation for Leukemia Cell Transfection,” *Electroporation Protocols*. Springer New York, 2014, 69-77.
- F. Li, S. Huang, L. Wang, J. Yang, H. Zhang, L. Qiu, L. Li, L. Song. “A macrophage migration inhibitory factor like gene from scallop *Chlamys farreri*: Involvement in immune response and wound healing,” *Developmental & Comparative Immunology* (2011), 35(1): 62-71. (Impact factor: 3.705)
- Y. Shi, S. Huang, Z. Zhou. “Constructing a Serial Deletion Vectors of S II Promoter,” *Science Technology and Engineering* (2009), 9(3): 568-571.
- Y. Shi, Z. Zhou, S. Huang, J. Lu. “Construction of HB-S2.S Expression Vector Guided by Carrot Extension Signal Peptide,” *Science Technology and Engineering* (2009), 9(3): 680-683.
- S. Huang, Y. Shi, C. Ji. “Biofuel Alternatives from Microbial Organism,” *Shanghai Chemical Industry* (2009), 2(34): 21-25.
- S. Huang, Y. Shi. “Production of value-added products using biological wastes under solid-state fermentation conditions,” *Journal of Chemical Industry and Engineering* (2009), 4(30): 19-22.
- C. Ji, J. Yu, S. Huang. “Research progress on application of membrane processes in biotechniques,” *Journal of Chemical Industry and Engineering* (2009), 5(30): 24-28.

Conference Proceedings

- S. Huang, Y. Zu, K. Rajapopalan, S. Wang, “Gold Nanoparticle Electroporation Enhanced Polyplex Delivery,” AIChE, Atlanta, GA (Nov., 2014)
- Y. Zu, S. Huang, S. Wang, “Micronanotip Injection Electroporation,” AIChE, Atlanta, GA (Nov., 2014)
- S. Huang, Y. Zu, S. Wang, “Gold Nanoparticle Enhanced DNA and RNA Mediated Therapeutics,” BMES, San Antonio, TX (Oct., 2014)
- F. Ren, S. Huang, K. Rajapopalan, Y. Zu, S. Wang, “Polyplex Synthesis and Delivery by Hybrid-filed Microfluid,” MicroTAS, San Antonio, TX (Oct., 2014)
- S. Huang, Y. Zu, Y. Lu, S. Wang, “Gold nanoparticle-polyplex enhanced electroporation-based therapeutic strategies in leukemia,” ACS, Dallas, TX (Mar., 2014)
- S. Huang, Y. Zu, Y. Lu, S. Wang, “AuNPs-Polyplex Electroporation Enhanced DNA and RNA Delivery,” AIChE, San Francisco, CA (Nov., 2013)
- F. Ren, S. Huang, S. Wang, “Hybrid-Field Microfluidics Enhanced Polyplex Synthesis and Delivery,” AIChE, San Francisco, CA (Nov., 2013)
- A. Pun, Y. Zu, Y. Lu, S. Huang, S. Wang, “Gold Nanoparticles Enhanced Electroporation for Gene Delivery in Mammalian Cells,” BMES, Seattle, WA (Sept., 2013)
- F. Ren, S. Huang, S. Wang, “Hybrid-field Microfluidics Enhanced Polyplex Synthesis and Delivery,” Advances in Microfluidics and Nanofluidics, South Bend, IN (May, 2013)
- S. Huang, Y. Zu, Y. Lu, S. Wang, “Application of AuNPs and AuNRs to enhance electroporation for gene delivery to mammalian cells,” LAS, Grambling, LA (Mar., 2013) selected as **Best Graduate Oral Presentation**
- S. Huang, H. Deshmukh, K. Rajagopalan, S. Wang, “Enhancing Electroporation Transfection with AuNP Polyplex,” AIChE, Pittsburgh, PA (Nov., 2012)
- S. Huang, Y. Zu, Y. Lu, S. Wang, “Enhancing Electroporation with Targeted Gold Nanoparticles,” AIChE, Pittsburgh, PA (Nov., 2012)

BIBLIOGRAPHY

1. Gore, M., *Gene therapy can cause leukaemia: no shock, mild horror but a probe.* GENE THERAPY-BASINGSTOKE-, 2003. **10**(1): p. 4-4.
2. Marshall, E., *Gene therapy death prompts review of adenovirus vector.* Science, 1999. **286**(5448): p. 2244-2245.
3. Wagner, E., et al., *Transferrin-polycation conjugates as carriers for DNA uptake into cells.* Proceedings of the National Academy of Sciences, 1990. **87**(9): p. 3410-3414.
4. Boussif, O., et al., *A versatile vector for gene and oligonucleotide transfer into cells in culture and in vivo: polyethylenimine.* Proceedings of the National Academy of Sciences, 1995. **92**(16): p. 7297-7301.
5. Tang, M. and F. Szoka, *The influence of polymer structure on the interactions of cationic polymers with DNA and morphology of the resulting complexes.* Gene therapy, 1997. **4**(8): p. 823-832.
6. Leong, K., et al., *DNA-polycation nanospheres as non-viral gene delivery vehicles.* Journal of Controlled Release, 1998. **53**(1): p. 183-193.
7. Roy, K., et al., *Oral gene delivery with chitosan-DNA nanoparticles generates immunologic protection in a murine model of peanut allergy.* Nature medicine, 1999. **5**(4): p. 387-391.
8. Abraham, S.A., et al., *The liposomal formulation of doxorubicin.* Methods in enzymology, 2005. **391**: p. 71-97.
9. Kawakami, S., Y. Higuchi, and M. Hashida, *Nonviral approaches for targeted delivery of plasmid DNA and oligonucleotide.* Journal of pharmaceutical sciences, 2008. **97**(2): p. 726-745.
10. Liu, D., A. Mori, and L. Huang, *Role of liposome size and RES blockade in controlling biodistribution and tumor uptake of GM< sub> 1</sub>-containing liposomes.* Biochimica et Biophysica Acta (BBA)-Biomembranes, 1992. **1104**(1): p. 95-101.
11. Pannier, A.K. and L.D. Shea, *Controlled release systems for DNA delivery.* Molecular Therapy, 2004. **10**(1): p. 19-26.
12. Felgner, P.L., et al., *Lipofection: a highly efficient, lipid-mediated DNA-transfection procedure.* Proceedings of the National Academy of Sciences, 1987. **84**(21): p. 7413-7417.

13. Even-Chen, S. and Y. Barenholz, *DOTAP cationic liposomes prefer relaxed over supercoiled plasmids*. *Biochimica et Biophysica Acta (BBA)-Biomembranes*, 2000. **1509**(1): p. 176-188.
14. Gao, X. and L. Huang, *A novel cationic liposome reagent for efficient transfection of mammalian cells*. *Biochemical and biophysical research communications*, 1991. **179**(1): p. 280-285.
15. Leong, K.W., *Polymer design for nonviral gene delivery*, in *BioMEMS and Biomedical Nanotechnology*. 2006, Springer. p. 239-263.
16. Alkilany, A.M., et al., *Cation exchange on the surface of gold nanorods with a polymerizable surfactant: polymerization, stability, and toxicity evaluation*. *Langmuir*, 2010. **26**(12): p. 9328-9333.
17. Baganha, M.F., et al., *Serum and pleural adenosine deaminase. Correlation with lymphocytic populations*. *CHEST Journal*, 1990. **97**(3): p. 605-610.
18. Breyer, B., et al., *Adenoviral vector-mediated gene transfer for human gene therapy*. *Current gene therapy*, 2001. **1**(2): p. 149-162.
19. Scriver, C.R. and J.B. Stanbury, *The metabolic basis of inherited disease*. Vol. 2. 1989: McGraw-Hill New York.
20. Felgner, P.L., *Nonviral strategies for gene therapy*. *Scientific American*, 1997. **276**(6): p. 102-106.
21. Miller, D.G., M.A. Adam, and A.D. Miller, *Gene transfer by retrovirus vectors occurs only in cells that are actively replicating at the time of infection*. *Molecular and cellular biology*, 1990. **10**(8): p. 4239-4242.
22. Fields, B., D. Knipe, and P. Howley, *Virology*, vol. 2. 1996, Lippincott-Raven Publishers, Philadelphia, Pa.
23. Naldini, L., et al., *In vivo gene delivery and stable transduction of nondividing cells by a lentiviral vector*. *Science*, 1996. **272**(5259): p. 263-267.
24. Lewis, P.F. and M. Emerman, *Passage through mitosis is required for oncoretroviruses but not for the human immunodeficiency virus*. *Journal of virology*, 1994. **68**(1): p. 510-516.
25. Li, Q., et al., *Assessment of recombinant adenoviral vectors for hepatic gene therapy*. *Human gene therapy*, 1993. **4**(4): p. 403-409.
26. Quantin, B., et al., *Adenovirus as an expression vector in muscle cells in vivo*. *Proceedings of the National Academy of Sciences*, 1992. **89**(7): p. 2581-2584.
27. Kelly Jr, T.J., *Adenovirus DNA replication*, in *The adenoviruses*. 1984, Springer. p. 271-308.
28. Nahmias, A.J. and B. Roizman, *Infection with herpes-simplex viruses 1 and 2. 1*. *The New England journal of medicine*, 1973. **289**(13): p. 667-674.
29. Parker, J.N., et al., *Engineered herpes simplex virus expressing IL-12 in the treatment of experimental murine brain tumors*. *Proceedings of the National Academy of Sciences*, 2000. **97**(5): p. 2208-2213.

30. Samulski, R., et al., *Targeted integration of adeno-associated virus (AAV) into human chromosome 19*. The EMBO journal, 1991. **10**(12): p. 3941.
31. Buller, R.M., et al., *Herpes simplex virus types 1 and 2 completely help adenovirus-associated virus replication*. Journal of virology, 1981. **40**(1): p. 241-247.
32. Janik, J., et al., *Efficient synthesis of adeno-associated virus structural proteins requires both adenovirus DNA binding protein and VA I RNA*. Virology, 1989. **168**(2): p. 320-329.
33. Zauner, W., M. Ogris, and E. Wagner, *Polylysine-based transfection systems utilizing receptor-mediated delivery*. Advanced drug delivery reviews, 1998. **30**(1): p. 97-113.
34. Wu, G.Y. and C.H. Wu, *Receptor-mediated in vitro gene transformation by a soluble DNA carrier system*. Journal of Biological Chemistry, 1987. **262**(10): p. 4429-4432.
35. Cotten, M., et al., *Transferrin-polycation-mediated introduction of DNA into human leukemic cells: stimulation by agents that affect the survival of transfected DNA or modulate transferrin receptor levels*. Proceedings of the National Academy of Sciences, 1990. **87**(11): p. 4033-4037.
36. Ding, Z.-M., et al., *Malarial circumsporozoite protein is a novel gene delivery vehicle to primary hepatocyte cultures and cultured cells*. Journal of Biological Chemistry, 1995. **270**(8): p. 3667-3676.
37. Müller, M., et al., *Papillomavirus capsid binding and uptake by cells from different tissues and species*. Journal of virology, 1995. **69**(2): p. 948-954.
38. Cristiano, R.J. and J.A. Roth, *Epidermal growth factor mediated DNA delivery into lung cancer cells via the epidermal growth factor receptor*. Cancer gene therapy, 1995. **3**(1): p. 4-10.
39. Chowdhury, N.R., et al., *Fate of DNA targeted to the liver by asialoglycoprotein receptor-mediated endocytosis in vivo. Prolonged persistence in cytoplasmic vesicles after partial hepatectomy*. Journal of Biological Chemistry, 1993. **268**(15): p. 11265-11271.
40. Wu, C.H., J.M. Wilson, and G. Wu, *Targeting genes: delivery and persistent expression of a foreign gene driven by mammalian regulatory elements in vivo*. Journal of Biological Chemistry, 1989. **264**(29): p. 16985-16987.
41. Schaffer, D.V. and D.A. Lauffenburger, *Optimization of cell surface binding enhances efficiency and specificity of molecular conjugate gene delivery*. Journal of Biological Chemistry, 1998. **273**(43): p. 28004-28009.
42. Wagner, E., et al., *Transferrin-polycation-DNA complexes: the effect of polycations on the structure of the complex and DNA delivery to cells*. Proceedings of the National Academy of Sciences, 1991. **88**(10): p. 4255-4259.

43. Ziady, A.-G., et al., *Chain length of the polylysine in receptor-targeted gene transfer complexes affects duration of reporter gene expression both in vitro and in vivo*. Journal of Biological Chemistry, 1999. **274**(8): p. 4908-4916.
44. Nishikawa, M., et al., *Targeted delivery of plasmid DNA to hepatocytes in vivo: optimization of the pharmacokinetics of plasmid DNA/galactosylated poly (L-lysine) complexes by controlling their physicochemical properties*. Journal of Pharmacology and Experimental Therapeutics, 1998. **287**(1): p. 408-415.
45. Stankovics, J., et al., *Overexpression of human methylmalonyl CoA mutase in mice after in vivo gene transfer with asialoglycoprotein/polylysine/DNA complexes*. Human gene therapy, 1994. **5**(9): p. 1095-1104.
46. Dash, P., et al., *Factors affecting blood clearance and in vivo distribution of polyelectrolyte complexes for gene delivery*. Gene therapy, 1999. **6**(4): p. 643-650.
47. Dash, P.R., et al., *Synthetic polymers for vectorial delivery of DNA: characterisation of polymer-DNA complexes by photon correlation spectroscopy and stability to nuclease degradation and disruption by polyanions in vitro*. Journal of controlled release, 1997. **48**(2-3): p. 269-276.
48. Ward, C.M., M.L. Read, and L.W. Seymour, *Systemic circulation of poly (L-lysine)/DNA vectors is influenced by polycation molecular weight and type of DNA: differential circulation in mice and rats and the implications for human gene therapy*. Blood, 2001. **97**(8): p. 2221-2229.
49. Harada-Shiba, M., et al., *Polyion complex micelles as vectors in gene therapy-pharmacokinetics and in vivo gene transfer*. Gene therapy, 2002. **9**(6): p. 407-414.
50. Kwok, K.Y., et al., *Formulation of highly soluble poly (ethylene glycol) - peptide DNA condensates*. Journal of pharmaceutical sciences, 1999. **88**(10): p. 996-1003.
51. Akinc, A., et al., *Exploring polyethylenimine - mediated DNA transfection and the proton sponge hypothesis*. The journal of gene medicine, 2005. **7**(5): p. 657-663.
52. Sonawane, N.D., F.C. Szoka, and A. Verkman, *Chloride accumulation and swelling in endosomes enhances DNA transfer by polyamine-DNA polyplexes*. Journal of Biological Chemistry, 2003. **278**(45): p. 44826-44831.
53. Florea, B.I., et al., *Transfection efficiency and toxicity of polyethylenimine in differentiated Calu-3 and nondifferentiated COS-1 cell cultures*. Aaps Pharmsci, 2002. **4**(3): p. 1-11.
54. Neu, M., D. Fischer, and T. Kissel, *Recent advances in rational gene transfer vector design based on poly (ethylene imine) and its derivatives*. The journal of gene medicine, 2005. **7**(8): p. 992-1009.
55. Gebhart, C.L. and A.V. Kabanov, *Evaluation of polyplexes as gene transfer agents*. Journal of Controlled Release, 2001. **73**(2): p. 401-416.

56. Clamme, J.P., J. Azoulay, and Y. Mély, *Monitoring of the formation and dissociation of polyethylenimine/DNA complexes by two photon fluorescence correlation spectroscopy*. Biophysical journal, 2003. **84**(3): p. 1960-1968.
57. Goula, D., et al., *Size, diffusibility and transfection performance of linear PEI/DNA complexes in the mouse central nervous system*. Gene therapy, 1998. **5**(5): p. 712-717.
58. Ogris, M., et al., *The size of DNA/transferrin-PEI complexes is an important factor for gene expression in cultured cells*. Gene therapy, 1998. **5**(10): p. 1425-1433.
59. Ogris, M., et al., *PEGylated DNA/transferrin-PEI complexes: reduced interaction with blood components, extended circulation in blood and potential for systemic gene delivery*. Gene therapy, 1999. **6**(4): p. 595-605.
60. Fischer, D., et al., *A novel non-viral vector for DNA delivery based on low molecular weight, branched polyethylenimine: effect of molecular weight on transfection efficiency and cytotoxicity*. Pharmaceutical research, 1999. **16**(8): p. 1273-1279.
61. Derouazi, M., et al., *Serum - free large - scale transient transfection of CHO cells*. Biotechnology and Bioengineering, 2004. **87**(4): p. 537-545.
62. Duan, H. and S. Nie, *Cell-penetrating quantum dots based on multivalent and endosome-disrupting surface coatings*. Journal of the American Chemical Society, 2007. **129**(11): p. 3333-3338.
63. Xia, T., et al., *Polyethyleneimine coating enhances the cellular uptake of mesoporous silica nanoparticles and allows safe delivery of siRNA and DNA constructs*. ACS nano, 2009. **3**(10): p. 3273-3286.
64. Mykhaylyk, O., et al., *Generation of magnetic nonviral gene transfer agents and magnetofection in vitro*. Nature protocols, 2007. **2**(10): p. 2391-2411.
65. Kamau, S.W., et al., *Enhancement of the efficiency of non-viral gene delivery by application of pulsed magnetic field*. Nucleic acids research, 2006. **34**(5): p. e40-e40.
66. Huth, S., et al., *Insights into the mechanism of magnetofection using PEI - based magnetofectins for gene transfer*. The journal of gene medicine, 2004. **6**(8): p. 923-936.
67. Gersting, S.W., et al., *Gene delivery to respiratory epithelial cells by magnetofection*. The journal of gene medicine, 2004. **6**(8): p. 913-922.
68. McBain, S., et al., *Polyethyleneimine functionalized iron oxide nanoparticles as agents for DNA delivery and transfection*. Journal of Materials Chemistry, 2007. **17**(24): p. 2561-2565.
69. Thomas, M. and A.M. Klibanov, *Conjugation to gold nanoparticles enhances polyethylenimine's transfer of plasmid DNA into mammalian cells*. Proceedings of the National Academy of Sciences, 2003. **100**(16): p. 9138-9143.

70. Liu, Y. and S. Franzen, *Factors determining the efficacy of nuclear delivery of antisense oligonucleotides by gold nanoparticles*. *Bioconjugate chemistry*, 2008. **19**(5): p. 1009-1016.
71. Rosi, N.L., et al., *Oligonucleotide-modified gold nanoparticles for intracellular gene regulation*. *Science*, 2006. **312**(5776): p. 1027-1030.
72. Lee, S.H., et al., *Amine-functionalized gold nanoparticles as non-cytotoxic and efficient intracellular siRNA delivery carriers*. *International journal of pharmaceutics*, 2008. **364**(1): p. 94-101.
73. Giljohann, D.A., et al., *Gold nanoparticles for biology and medicine*. *Angewandte Chemie International Edition*, 2010. **49**(19): p. 3280-3294.
74. Elbakry, A., et al., *Layer-by-layer assembled gold nanoparticles for siRNA delivery*. *Nano letters*, 2009. **9**(5): p. 2059-2064.
75. Song, W.J., et al., *Gold nanoparticles capped with polyethyleneimine for enhanced siRNA delivery*. *Small*, 2010. **6**(2): p. 239-246.
76. Skaugrud, O., *Chitosan makes the grade*. *Manufacturing Chemist*, 1989. **60**: p. 31.
77. Aspden, T., L. Illum, and Ø. Skaugrud, *Chitosan as a nasal delivery system: evaluation of insulin absorption enhancement and effect on nasal membrane integrity using rat models*. *European journal of pharmaceutical sciences*, 1996. **4**(1): p. 23-31.
78. Henriksen, I., G. Smistad, and J. Karlsen, *Interactions between liposomes and chitosan*. *International journal of pharmaceutics*, 1994. **101**(3): p. 227-236.
79. Schipper, N.G., K.M. Vårum, and P. Artursson, *Chitosans as absorption enhancers for poorly absorbable drugs. 1: Influence of molecular weight and degree of acetylation on drug transport across human intestinal epithelial (Caco-2) cells*. *Pharmaceutical research*, 1996. **13**(11): p. 1686-1692.
80. Hirano, S., et al. *Bio-compatibility of chitosan by oral and intravenous administrations*. in *ABSTRACTS OF PAPERS OF THE AMERICAN CHEMICAL SOCIETY*. 1988. AMER CHEMICAL SOC 1155 16TH ST, NW, WASHINGTON, DC 20036.
81. Artursson, P., et al., *Effect of chitosan on the permeability of monolayers of intestinal epithelial cells (Caco-2)*. *Pharmaceutical research*, 1994. **11**(9): p. 1358-1361.
82. Fernandez-Urrusuno, R., et al., *Enhancement of nasal absorption of insulin using chitosan nanoparticles*. *Pharmaceutical research*, 1999. **16**(10): p. 1576-1581.
83. Mumper, R., et al. *Novel polymeric condensing carriers for gene delivery*. in *Proceedings of the international symposium on controlled release bioactive materials*. 1995.
84. Roy, K., H. Mao, and K. Leong. *DNA-chitosan nanospheres: transfection efficiency and cellular uptake*. in *Proc Int Symp Control Rel Bioact Mater*. 1997.

85. Richardson, S., H. Kolbe, and R. Duncan. *Evaluation of highly purified chitosan as a potential gene delivery vector*. in *Proceed. Int. Symp. Contr. Rel. Bioact. Mater.* 1997.
86. Murata, J.-i., Y. Ohya, and T. Ouchi, *Possibility of application of quaternary chitosan having pendant galactose residues as gene delivery tool*. *Carbohydrate polymers*, 1996. **29**(1): p. 69-74.
87. Lee, K., et al., *Preparation of chitosan self-aggregates as a gene delivery system*. *Journal of Controlled Release*, 1998. **51**(2): p. 213-220.
88. Smith, A.E., *Viral vectors in gene therapy*. *Annual Reviews in Microbiology*, 1995. **49**(1): p. 807-838.
89. Kiang, T., et al., *The effect of the degree of chitosan deacetylation on the efficiency of gene transfection*. *Biomaterials*, 2004. **25**(22): p. 5293-5301.
90. Mao, H.-Q., et al., *Chitosan-DNA nanoparticles as gene carriers: synthesis, characterization and transfection efficiency*. *Journal of controlled release*, 2001. **70**(3): p. 399-421.
91. Erbacher, P., et al., *Chitosan-based vector/DNA complexes for gene delivery: biophysical characteristics and transfection ability*. *Pharmaceutical Research*, 1998. **15**(9): p. 1332-1339.
92. Huang, M., et al., *Transfection efficiency of chitosan vectors: effect of polymer molecular weight and degree of deacetylation*. *Journal of Controlled Release*, 2005. **106**(3): p. 391-406.
93. Rungsardthong, U., et al., *Copolymers of amine methacrylate with poly (ethylene glycol) as vectors for gene therapy*. *Journal of controlled release*, 2001. **73**(2): p. 359-380.
94. Deshpande, M.C., et al., *The effect of poly (ethylene glycol) molecular architecture on cellular interaction and uptake of DNA complexes*. *Journal of controlled release*, 2004. **97**(1): p. 143-156.
95. Piroton, S., et al., *Enhancement of transfection efficiency through rapid and noncovalent post-PEGylation of poly (dimethylaminoethyl methacrylate)/DNA complexes*. *Pharmaceutical research*, 2004. **21**(8): p. 1471-1479.
96. Park, K., *To PEGylate or not to PEGylate, that is not the question*. *Journal of Controlled Release*, 2010. **142**(2): p. 147-148.
97. Jeong, J.H. and T.G. Park, *Poly (L-lysine)-g-poly (D, L-lactic-co-glycolic acid) micelles for low cytotoxic biodegradable gene delivery carriers*. *Journal of controlled release*, 2002. **82**(1): p. 159-166.
98. Katayose, S. and K. Kataoka, *Remarkable increase in nuclease resistance of plasmid DNA through supramolecular assembly with poly (ethylene glycol)—poly (L - lysine) block copolymer*. *Journal of pharmaceutical sciences*, 1998. **87**(2): p. 160-163.

99. Katayose, S. and K. Kataoka, *Water-soluble polyion complex associates of DNA and poly (ethylene glycol)-poly (L-lysine) block copolymer*. *Bioconjugate chemistry*, 1997. **8**(5): p. 702-707.
100. Harada, A., H. Togawa, and K. Kataoka, *Physicochemical properties and nuclease resistance of antisense-oligodeoxynucleotides entrapped in the core of polyion complex micelles composed of poly (ethylene glycol)-poly (L-lysine) block copolymers*. *European journal of pharmaceutical sciences*, 2001. **13**(1): p. 35-42.
101. Petersen, H., et al., *Polyethylenimine-graft-poly (ethylene glycol) copolymers: influence of copolymer block structure on DNA complexation and biological activities as gene delivery system*. *Bioconjugate chemistry*, 2002. **13**(4): p. 845-854.
102. Kabanov, A. and V. Kabanov, *DNA complexes with polycations for the delivery of genetic material into cells*. *Bioconjugate chemistry*, 1995. **6**(1): p. 7-20.
103. Choi, J.S., et al., *Poly (ethylene glycol)-block-poly (L-lysine) dendrimer: novel linear polymer/dendrimer block copolymer forming a spherical water-soluble polyionic complex with DNA*. *Bioconjugate chemistry*, 1999. **10**(1): p. 62-65.
104. Suh, W., et al., *An angiogenic, endothelial-cell-targeted polymeric gene carrier*. *Molecular Therapy*, 2002. **6**(5): p. 664-672.
105. Nah, J.-W., et al., *Artery wall binding peptide-poly (ethylene glycol)-grafted-poly (L-lysine)-based gene delivery to artery wall cells*. *Journal of controlled release*, 2002. **78**(1): p. 273-284.
106. Leamon, C.P., D. Weigl, and R.W. Hendren, *Folate copolymer-mediated transfection of cultured cells*. *Bioconjugate chemistry*, 1999. **10**(6): p. 947-957.
107. Mishra, S., P. Webster, and M.E. Davis, *PEGylation significantly affects cellular uptake and intracellular trafficking of non-viral gene delivery particles*. *European journal of cell biology*, 2004. **83**(3): p. 97-111.
108. Kursa, M., et al., *Novel shielded transferrin-polyethylene glycol-polyethylenimine/DNA complexes for systemic tumor-targeted gene transfer*. *Bioconjugate chemistry*, 2003. **14**(1): p. 222-231.
109. Wakebayashi, D., et al., *Polyion complex micelles of pDNA with acetal-poly (ethylene glycol)-poly (2-(dimethylamino) ethyl methacrylate) block copolymer as the gene carrier system: physicochemical properties of micelles relevant to gene transfection efficacy*. *Biomacromolecules*, 2004. **5**(6): p. 2128-2136.
110. Lin, S., et al., *An acid-labile block copolymer of PDMAEMA and PEG as potential carrier for intelligent gene delivery systems*. *Biomacromolecules*, 2007. **9**(1): p. 109-115.
111. Takae, S., et al., *PEG-detachable polyplex micelles based on disulfide-linked block cationomers as bioresponsive nonviral gene vectors*. *Journal of the American Chemical Society*, 2008. **130**(18): p. 6001-6009.
112. Tao, L., et al., *DNA polyplexes formed using PEGylated biodegradable hyperbranched polymers*. *Macromolecular bioscience*, 2010. **10**(6): p. 632-637.

113. Faraday, M., *The Bakerian lecture: experimental relations of gold (and other metals) to light*. Philosophical Transactions of the Royal Society of London, 1857. **147**: p. 145-181.
114. Graham, T., *Liquid diffusion applied to analysis*. Philosophical transactions of the Royal Society of London, 1861: p. 183-224.
115. Brown, D. and W. Smith, *The chemistry of the gold drugs used in the treatment of rheumatoid arthritis*. Chem. Soc. Rev., 1980. **9**(2): p. 217-240.
116. Frens, G., *Controlled nucleation for the regulation of the particle size in monodisperse gold suspensions*. Nature, 1972(241): p. 20-22.
117. Hayat, M.A., *Colloidal gold: principles, methods, and applications*. 2012: Elsevier.
118. Schmid, G. and L.F. Chi, *Metal clusters and colloids*. Advanced Materials, 1998. **10**(7): p. 515-526.
119. Schmid, G., *Large clusters and colloids. Metals in the embryonic state*. Chemical Reviews, 1992. **92**(8): p. 1709-1727.
120. Fendler, J.H. and F.C. Meldrum, *The Colloid Chemical Approach to Nanostructured Materials***. Advanced Materials, 1995. **7**(7): p. 607-632.
121. Edelstein, A.S. and R. Cammaratra, *Nanomaterials: synthesis, properties and applications*. 1998: CRC Press.
122. Bethell, D., et al., *From monolayers to nanostructured materials: an organic chemist's view of self-assembly*. Journal of Electroanalytical Chemistry, 1996. **409**(1): p. 137-143.
123. Matijević, E., *Controlled colloid formation*. Current Opinion in Colloid & Interface Science, 1996. **1**(2): p. 176-183.
124. Ung, T., L.M. Liz-Marzan, and P. Mulvaney, *Gold nanoparticle thin films*. Colloids and Surfaces A: Physicochemical and Engineering Aspects, 2002. **202**(2): p. 119-126.
125. Brust, M. and C.J. Kiely, *Some recent advances in nanostructure preparation from gold and silver particles: a short topical review*. Colloids and Surfaces A: Physicochemical and Engineering Aspects, 2002. **202**(2): p. 175-186.
126. Quinn, B.M., et al., *Electrochemical resolution of 15 oxidation states for monolayer protected gold nanoparticles*. Journal of the American Chemical Society, 2003. **125**(22): p. 6644-6645.
127. Yonezawa, T. and T. Kunitake, *Practical preparation of anionic mercapto ligand-stabilized gold nanoparticles and their immobilization*. Colloids and Surfaces A: Physicochemical and Engineering Aspects, 1999. **149**(1): p. 193-199.
128. Papasani, M.R., G. Wang, and R.A. Hill, *Gold nanoparticles: the importance of physiological principles to devise strategies for targeted drug delivery*. Nanomedicine: Nanotechnology, Biology and Medicine, 2012. **8**(6): p. 804-814.

129. Shan, Y., et al., *Gene delivery using dendrimer-entrapped gold nanoparticles as nonviral vectors*. Biomaterials, 2012. **33**(10): p. 3025-3035.
130. Shukla, R., et al., *Biocompatibility of gold nanoparticles and their endocytotic fate inside the cellular compartment: a microscopic overview*. Langmuir, 2005. **21**(23): p. 10644-10654.
131. Connor, E.E., et al., *Gold nanoparticles are taken up by human cells but do not cause acute cytotoxicity*. Small, 2005. **1**(3): p. 325-327.
132. Sandhu, K.K., et al., *Gold nanoparticle-mediated transfection of mammalian cells*. Bioconjugate chemistry, 2002. **13**(1): p. 3-6.
133. Sullivan, M.O., J. Green, and T. Przybycien, *Development of a novel gene delivery scaffold utilizing colloidal gold-polyethylenimine conjugates for DNA condensation*. Gene therapy, 2003. **10**(22): p. 1882-1890.
134. Jen, C.-P., et al., *A nonviral transfection approach in vitro: the design of a gold nanoparticle vector joint with microelectromechanical systems*. Langmuir, 2004. **20**(4): p. 1369-1374.
135. Daniel, M.-C. and D. Astruc, *Gold nanoparticles: assembly, supramolecular chemistry, quantum-size-related properties, and applications toward biology, catalysis, and nanotechnology*. Chemical reviews, 2004. **104**(1): p. 293-346.
136. Bauer, L.A., N.S. Birenbaum, and G.J. Meyer, *Biological applications of high aspect ratio nanoparticles*. Journal of Materials Chemistry, 2004. **14**(4): p. 517-526.
137. Yang, P.-H., et al., *Transferrin-mediated gold nanoparticle cellular uptake*. Bioconjugate chemistry, 2005. **16**(3): p. 494-496.
138. Chithrani, B.D., A.A. Ghazani, and W.C. Chan, *Determining the size and shape dependence of gold nanoparticle uptake into mammalian cells*. Nano letters, 2006. **6**(4): p. 662-668.
139. Pan, Y., et al., *Size - dependent cytotoxicity of gold nanoparticles*. Small, 2007. **3**(11): p. 1941-1949.
140. Chithrani, B.D. and W.C. Chan, *Elucidating the mechanism of cellular uptake and removal of protein-coated gold nanoparticles of different sizes and shapes*. Nano letters, 2007. **7**(6): p. 1542-1550.
141. Ghosh, P., et al., *Gold nanoparticles in delivery applications*. Advanced drug delivery reviews, 2008. **60**(11): p. 1307-1315.
142. Murphy, C.J., et al., *Gold nanoparticles in biology: beyond toxicity to cellular imaging*. Accounts of Chemical Research, 2008. **41**(12): p. 1721-1730.
143. Guo, S., et al., *Enhanced gene delivery and siRNA silencing by gold nanoparticles coated with charge-reversal polyelectrolyte*. Acs Nano, 2010. **4**(9): p. 5505-5511.
144. Enustun, B. and J. Turkevich, *Coagulation of colloidal gold*. Journal of the American chemical society, 1963. **85**(21): p. 3317-3328.

145. Cho, E.C., et al., *Understanding the role of surface charges in cellular adsorption versus internalization by selectively removing gold nanoparticles on the cell surface with a I2/KI etchant*. Nano letters, 2009. **9**(3): p. 1080-1084.
146. Tkachenko, A.G., et al., *Multifunctional gold nanoparticle-peptide complexes for nuclear targeting*. Journal of the American Chemical Society, 2003. **125**(16): p. 4700-4701.
147. Nativo, P., I.A. Prior, and M. Brust, *Uptake and intracellular fate of surface-modified gold nanoparticles*. ACS nano, 2008. **2**(8): p. 1639-1644.
148. Brust, M., et al., *Synthesis of thiol-derivatised gold nanoparticles in a two-phase liquid-liquid system*. J. Chem. Soc., Chem. Commun., 1994(7): p. 801-802.
149. Tkachenko, A.G., et al., *Cellular trajectories of peptide-modified gold particle complexes: comparison of nuclear localization signals and peptide transduction domains*. Bioconjugate chemistry, 2004. **15**(3): p. 482-490.
150. Liu, Y., et al., *Synthesis, stability, and cellular internalization of gold nanoparticles containing mixed peptide-poly (ethylene glycol) monolayers*. Analytical chemistry, 2007. **79**(6): p. 2221-2229.
151. El-Sayed, I.H., X. Huang, and M.A. El-Sayed, *Surface plasmon resonance scattering and absorption of anti-EGFR antibody conjugated gold nanoparticles in cancer diagnostics: applications in oral cancer*. Nano letters, 2005. **5**(5): p. 829-834.
152. Luo, D. and W.M. Saltzman, *Synthetic DNA delivery systems*. Nature biotechnology, 2000. **18**(1): p. 33-37.
153. Templeton, N.S., *Gene and Cell Therapy: Therapeutic Mechanisms and Strategies, Revised and Expanded*. 2003: CRC Press.
154. Hamer, D.H. and P. Leder, *Splicing and the formation of stable RNA*. Cell, 1979. **18**(4): p. 1299-1302.
155. Verma, I.M. and N. Somia, *Gene therapy-promises, problems and prospects*. Nature, 1997. **389**(6648): p. 239-242.
156. Lungwitz, U., et al., *Polyethylenimine-based non-viral gene delivery systems*. European Journal of Pharmaceutics and Biopharmaceutics, 2005. **60**(2): p. 247-266.
157. Boussif, O., M.A. Zanta, and J.-P. Behr, *Optimized galenics improve in vitro gene transfer with cationic molecules up to 1000-fold*. Gene Therapy, 1996. **3**(12): p. 1074-1080.
158. Felgner, P., et al., *Nomenclature for synthetic gene delivery systems*. Human gene therapy, 1997. **8**(5): p. 511-512.
159. Li, S. and Z. Ma, *Nonviral gene therapy*. Current gene therapy, 2001. **1**(2): p. 201-226.
160. Yu, B., et al., *Targeted delivery systems for oligonucleotide therapeutics*. The AAPS journal, 2009. **11**(1): p. 195-203.

161. Schakowski, F., et al., *Novel non-viral method for transfection of primary leukemia cells and cell lines*. Genetic vaccines and therapy, 2004. 2(1): p. 1.
162. Patra, C.R., et al., *Application of gold nanoparticles for targeted therapy in cancer*. Journal of Biomedical Nanotechnology, 2008. 4(2): p. 99-132.
163. Cai, W., et al., *Applications of gold nanoparticles in cancer nanotechnology*. Nanotechnology, science and applications, 2008. 1: p. 17.
164. Viator, J.A., et al., *Gold nanoparticle mediated detection of prostate cancer cells using photoacoustic flowmetry with optical reflectance*. Journal of biomedical nanotechnology, 2010. 6(2): p. 187-191.
165. Cutler, J.I., E. Auyeung, and C.A. Mirkin, *Spherical nucleic acids*. Journal of the American Chemical Society, 2012. 134(3): p. 1376-1391.
166. Verma, A., et al., *Surface-structure-regulated cell-membrane penetration by monolayer-protected nanoparticles*. Nature materials, 2008. 7(7): p. 588-595.
167. Ahmed, M., Z. Deng, and R. Narain, *Study of transfection efficiencies of cationic glyconanoparticles of different sizes in human cell line*. ACS applied materials & interfaces, 2009. 1(9): p. 1980-1987.
168. Yang, N.-S. and W.H. Sun, *Gene gun and other non-viral approaches for cancer gene therapy*. Nature medicine, 1995. 1(5): p. 481-483.
169. Salem, A.K., P.C. Searson, and K.W. Leong, *Multifunctional nanorods for gene delivery*. Nature materials, 2003. 2(10): p. 668-671.
170. Neumann, E., et al., *Gene transfer into mouse lymphoma cells by electroporation in high electric fields*. The EMBO journal, 1982. 1(7): p. 841.
171. Toneguzzo, F. and A. Keating, *Stable expression of selectable genes introduced into human hematopoietic stem cells by electric field-mediated DNA transfer*. Proceedings of the National Academy of Sciences, 1986. 83(10): p. 3496-3499.
172. Chang, D.C., et al., *Guide to electroporation and electrofusion*. 1992: Academic Press.
173. Teissie, J. and M.-P. Rols, *An experimental evaluation of the critical potential difference inducing cell membrane electropermeabilization*. Biophysical journal, 1993. 65(1): p. 409-413.
174. Neumann, E. and S. Kakorin, *Digression on membrane electroporation and electroporative delivery of drugs and genes*. Radiol Oncol, 1998. 32.
175. Gehl, J., *Electroporation: theory and methods, perspectives for drug delivery, gene therapy and research*. Acta Physiologica Scandinavica, 2003. 177(4): p. 437-447.
176. Lorenz, P., U. Harnack, and R. Morgenstern, *Efficient gene transfer into murine embryonic stem cells by nucleofection*. Biotechnology letters, 2004. 26(20): p. 1589-1592.

177. Rubinsky, B., G. Onik, and P. Mikus, *Irreversible electroporation: a new ablation modality—clinical implications*. *Technology in cancer research & treatment*, 2007. 6(1): p. 37-48.
178. Daud, A.I., et al., *Phase I trial of interleukin-12 plasmid electroporation in patients with metastatic melanoma*. *Journal of Clinical Oncology*, 2008. 26(36): p. 5896-5903.
179. Spanggaard, I., et al., *Gene electrotransfer of plasmid antiangiogenic metargidin peptide (AMEP) in disseminated melanoma: safety and efficacy results of a phase I first-in-man study*. *Human Gene Therapy Clinical Development*, 2013. 24(3): p. 99-107.
180. Belehradec, M., et al., *Electrochemotherapy, a new antitumor treatment. First clinical phase I - II trial*. *Cancer*, 1993. 72(12): p. 3694-3700.
181. Mir, L.M., *Bases and rationale of the electrochemotherapy*. *European Journal of Cancer Supplements*, 2006. 4(11): p. 38-44.
182. Huang, Y. and B. Rubinsky, *Flow-through micro-electroporation chip for high efficiency single-cell genetic manipulation*. *Sensors and Actuators A: Physical*, 2003. 104(3): p. 205-212.
183. Lin, Y.-C., M. Li, and C.-C. Wu, *Simulation and experimental demonstration of the electric field assisted electroporation microchip for in vitro gene delivery enhancement*. *Lab on a Chip*, 2004. 4(2): p. 104-108.
184. Lu, H., M.A. Schmidt, and K.F. Jensen, *A microfluidic electroporation device for cell lysis*. *Lab on a Chip*, 2005. 5(1): p. 23-29.
185. Khine, M., et al., *A single cell electroporation chip*. *Lab on a Chip*, 2005. 5(1): p. 38-43.
186. Fei, Z., et al., *Gene transfection of mammalian cells using membrane sandwich electroporation*. *Analytical chemistry*, 2007. 79(15): p. 5719-5722.
187. Kim, J.A., et al., *A multi-channel electroporation microchip for gene transfection in mammalian cells*. *Biosensors and Bioelectronics*, 2007. 22(12): p. 3273-3277.
188. Valero, A., et al., *Gene transfer and protein dynamics in stem cells using single cell electroporation in a microfluidic device*. *Lab on a Chip*, 2008. 8(1): p. 62-67.
189. Wang, H.Y. and C. Lu, *Microfluidic electroporation for delivery of small molecules and genes into cells using a common DC power supply*. *Biotechnology and bioengineering*, 2008. 100(3): p. 579-586.
190. Wang, S., et al., *Semicontinuous flow electroporation chip for high-throughput transfection on mammalian cells*. *Analytical chemistry*, 2009. 81(11): p. 4414-4421.
191. Fei, Z., et al., *Micronozzle array enhanced sandwich electroporation of embryonic stem cells*. *Analytical chemistry*, 2009. 82(1): p. 353-358.

192. Geng, T., et al., *Flow-through electroporation based on constant voltage for large-volume transfection of cells*. Journal of Controlled Release, 2010. **144**(1): p. 91-100.
193. Boukany, P.E., et al., *Nanochannel electroporation delivers precise amounts of biomolecules into living cells*. Nature nanotechnology, 2011. **6**(11): p. 747-754.
194. Chang, D. and T.S. Reese, *Changes in membrane structure induced by electroporation as revealed by rapid-freezing electron microscopy*. Biophysical journal, 1990. **58**(1): p. 1-12.
195. Wang, S. and L.J. Lee, *Micro-/nanofluidics based cell electroporation*. Biomicrofluidics, 2013. **7**(1): p. 011301.
196. Rojas-Chapana, J.A., et al., *Enhanced introduction of gold nanoparticles into vital Acidithiobacillus ferrooxidans by carbon nanotube-based microwave electroporation*. Nano Letters, 2004. **4**(5): p. 985-988.
197. Raffa, V., et al., *Carbon nanotube-enhanced cell electropermeabilisation*. Bioelectrochemistry, 2010. **79**(1): p. 136-141.
198. Kinoshita, K. and T.Y. Tsong, *Voltage-induced pore formation and hemolysis of human erythrocytes*. Biochimica et Biophysica Acta (BBA)-Biomembranes, 1977. **471**(2): p. 227-242.
199. Bernhardt, J. and H. Pauly, *On the generation of potential differences across the membranes of ellipsoidal cells in an alternating electrical field*. Biophysik, 1973. **10**(1): p. 89-98.
200. Schwan, H.P., *Electrical properties of tissue and cell suspensions*. Advances in biological and medical physics, 1956. **5**: p. 147-209.
201. Kotnik, T. and D. Miklavčič, *Analytical description of transmembrane voltage induced by electric fields on spheroidal cells*. Biophysical Journal, 2000. **79**(2): p. 670-679.
202. Gimsa, J. and D. Wachner, *Analytical description of the transmembrane voltage induced on arbitrarily oriented ellipsoidal and cylindrical cells*. Biophysical Journal, 2001. **81**(4): p. 1888-1896.
203. Kotnik, T., et al., *Cell membrane electroporation-Part 1: The phenomenon*. Electrical Insulation Magazine, IEEE, 2012. **28**(5): p. 14-23.
204. Tekle, E., R.D. Astumian, and P.B. Chock, *Electro-permeabilization of cell membranes: effect of the resting membrane potential*. Biochemical and biophysical research communications, 1990. **172**(1): p. 282-287.
205. Stämpfli, R., *Reversible electrical breakdown of the excitable membrane of a Ranvier node*. Ann. Acad. Brasil. Ciens, 1958. **30**: p. 57-63.
206. Neumann, E. and K. Rosenheck, *Permeability changes induced by electric impulses in vesicular membranes*. The Journal of membrane biology, 1972. **10**(1): p. 279-290.

207. Benz, R. and U. Zimmermann, *376-Relaxation studies on cell membranes and lipid bilayers in the high electric field range*. Bioelectrochemistry and Bioenergetics, 1980. 7(4): p. 723-739.
208. Benz, R. and U. Zimmermann, *Pulse-length dependence of the electrical breakdown in lipid bilayer membranes*. Biochimica et Biophysica Acta (BBA)-Biomembranes, 1980. 597(3): p. 637-642.
209. Benz, R. and U. Zimmermann, *The resealing process of lipid bilayers after reversible electrical breakdown*. Biochimica et Biophysica Acta (BBA)-Biomembranes, 1981. 640(1): p. 169-178.
210. Benz, R. and F. Conti, *Reversible electrical breakdown of squid giant axon membrane*. Biochimica et Biophysica Acta (BBA)-Biomembranes, 1981. 645(1): p. 115-123.
211. Chemomordik, L., et al., *The study of the BLM reversible electrical breakdown mechanism in the presence of UO_2^{2+}* . Bioelectrochem. Bioenerg, 1982. 9: p. 149-155.
212. Teissie, J., et al., *Electric pulse-induced fusion of 3T3 cells in monolayer culture*. Science, 1982. 216(4545): p. 537-538.
213. Mir, L.M., H. Banoun, and C. Paoletti, *Introduction of definite amounts of nonpermeant molecules into living cells after electroporation: direct access to the cytosol*. Experimental cell research, 1988. 175(1): p. 15-25.
214. Silve, A. and L.M. Mir, *Cell electroporation and cellular uptake of small molecules: the electrochemotherapy concept*, in *Clinical aspects of electroporation*. 2011, Springer. p. 69-82.
215. Pron, G., J. Belehradek, and L. Mir, *Identification of a plasma membrane protein that specifically binds bleomycin*. Biochemical and biophysical research communications, 1993. 194(1): p. 333-337.
216. Tieleman, D.P., et al., *Simulation of pore formation in lipid bilayers by mechanical stress and electric fields*. Journal of the American Chemical Society, 2003. 125(21): p. 6382-6383.
217. Tarek, M., *Membrane electroporation: a molecular dynamics simulation*. Biophysical journal, 2005. 88(6): p. 4045-4053.
218. Fernández, M.L., et al., *Size-controlled nanopores in lipid membranes with stabilizing electric fields*. Biochemical and biophysical research communications, 2012. 423(2): p. 325-330.
219. Levine, Z.A. and P.T. Vernier, *Life cycle of an electropore: field-dependent and field-independent steps in pore creation and annihilation*. The Journal of membrane biology, 2010. 236(1): p. 27-36.
220. Tokman, M., et al., *Electric field-driven water dipoles: nanoscale architecture of electroporation*. PloS one, 2013. 8(4): p. e61111.

221. Teissie, J., M. Golzio, and M. Rols, *Mechanisms of cell membrane electropermeabilization: a minireview of our present (lack of?) knowledge*. Biochimica et Biophysica Acta (BBA)-General Subjects, 2005. **1724**(3): p. 270-280.
222. Lopez, A., M. Rols, and J. Teissie, *Phosphorus-31 NMR analysis of membrane phospholipid organization in viable, reversibly electropermeabilized Chinese hamster ovary cells*. Biochemistry, 1988. **27**(4): p. 1222-1228.
223. Rols, M.-P. and J. Teissie, *Electropermeabilization of mammalian cells to macromolecules: control by pulse duration*. Biophysical journal, 1998. **75**(3): p. 1415-1423.
224. Teissie, J. and C. Ramos, *Correlation between electric field pulse induced long-lived permeabilization and fusogenicity in cell membranes*. Biophysical journal, 1998. **74**(4): p. 1889-1898.
225. Escoffre, J.-M., et al., *Electromediated formation of DNA complexes with cell membranes and its consequences for gene delivery*. Biochimica et Biophysica Acta (BBA)-Biomembranes, 2011. **1808**(6): p. 1538-1543.
226. Dean, D., D. Strong, and W. Zimmer, *Nuclear entry of nonviral vectors*. Gene therapy, 2005. **12**(11): p. 881-890.
227. Breton, M., et al., *Nanosecond pulsed electric field driven transport of siRNA molecules through lipid membranes: an experimental and computational study*. J Am Chem Soc, 2012. **134**: p. 13938-13941.
228. Mir, L.M., et al., *[Electrochemotherapy, a new antitumor treatment: first clinical trial]*. Comptes Rendus de l'Academie des Sciences. Serie III, Sciences de la vie, 1990. **313**(13): p. 613-618.
229. Satkauskas, S., et al., *Mechanisms of in vivo DNA electrotransfer: respective contributions of cell electropermeabilization and DNA electrophoresis*. Molecular Therapy, 2002. **5**(2): p. 133-140.
230. Šatkauskas, S., et al., *Electrophoretic component of electric pulses determines the efficacy of in vivo DNA electrotransfer*. Human gene therapy, 2005. **16**(10): p. 1194-1201.
231. Spath, K., S. Heintl, and R. Grabherr, *Direct cloning in Lactobacillus plantarum: Electroporation with non-methylated plasmid DNA enhances transformation efficiency and makes shuttle vectors obsolete*. Microb Cell Fact, 2012. **11**: p. 141.
232. Lin, S.-Y., et al., *Promoter CpG methylation of tumor suppressor genes in colorectal cancer and its relationship to clinical features*. Oncology reports, 2004. **11**(2): p. 341-348.
233. Chen, Y., A. Dhupelia, and C.J. Schoenherr, *The Igf2/H19 imprinting control region exhibits sequence-specific and cell-type-dependent DNA methylation-mediated repression*. Nucleic acids research, 2009. **37**(3): p. 793-803.
234. Li, S., *Electroporation gene therapy: new developments in vivo and in vitro*. Current gene therapy, 2004. **4**(3): p. 309-316.

235. Nicol, F., et al., *Poly-L-glutamate, an anionic polymer, enhances transgene expression for plasmids delivered by intramuscular injection with in vivo electroporation*. *Gene therapy*, 2002. **9**(20): p. 1351-1358.
236. Draghia-Akli, R., et al., *Electrical enhancement of formulated plasmid delivery in animals*. *Technology in cancer research & treatment*, 2002. **1**(5): p. 365-371.
237. Fewell, J.G., et al., *Gene therapy for the treatment of hemophilia B using PINC-formulated plasmid delivered to muscle with electroporation*. *Molecular Therapy*, 2001. **3**(4): p. 574-583.
238. Barbon, C.M., et al., *In vivo electroporation enhances the potency of poly-lactide co-glycolide (PLG) plasmid DNA immunization*. *Vaccine*, 2010. **28**(50): p. 7852-7864.
239. Gopalakrishnan, A.M., et al., *Novel nanosomes for gene delivery to plasmodium falciparum-infected red blood cells*. *Scientific reports*, 2013. **3**.
240. Mignet, N., et al., *Cationic and anionic lipoplexes inhibit gene transfection by electroporation in vivo*. *The journal of gene medicine*, 2010. **12**(6): p. 491-500.
241. Flanagan, M., et al., *Competitive electroporation formulation for cell therapy*. *Cancer gene therapy*, 2011. **18**(8): p. 579-586.
242. Flanagan, M., et al., *Competitive DNA transfection formulation via electroporation for human adipose stem cells and mesenchymal stem cells*. *Biol Proced Online*, 2012. **14**(7).
243. Wang, H.-Y. and C. Lu, *Electroporation of mammalian cells in a microfluidic channel with geometric variation*. *Analytical chemistry*, 2006. **78**(14): p. 5158-5164.
244. Wang, H.Y. and C. Lu, *High - throughput and real - time study of single cell electroporation using microfluidics: Effects of medium osmolarity*. *Biotechnology and bioengineering*, 2006. **95**(6): p. 1116-1125.
245. Guignet, E.G. and T. Meyer, *Suspended-drop electroporation for high-throughput delivery of biomolecules into cells*. *Nature methods*, 2008. **5**(5): p. 393-395.
246. Wei, Z., et al., *A laminar flow electroporation system for efficient DNA and siRNA delivery*. *Analytical chemistry*, 2011. **83**(15): p. 5881-5887.
247. Wang, S., et al., *Targeted nanoparticles enhanced flow electroporation of antisense oligonucleotides in leukemia cells*. *Biosensors and Bioelectronics*, 2010. **26**(2): p. 778-783.
248. Yang, X., et al., *Transferrin receptor-targeted lipid nanoparticles for delivery of an antisense oligodeoxyribonucleotide against Bcl-2*. *Molecular pharmaceuticals*, 2008. **6**(1): p. 221-230.
249. DA Stewart, J., et al., *Cylindrical cell membranes in uniform applied electric fields: validation of a transport lattice method*. *Biomedical Engineering, IEEE Transactions on*, 2005. **52**(10): p. 1643-1653.

250. Wagner, E., D. Curiel, and M. Cotten, *Delivery of drugs, proteins and genes into cells using transferrin as a ligand for receptor-mediated endocytosis*. *Advanced Drug Delivery Reviews*, 1994. **14**(1): p. 113-135.
251. Laibinis, P.E., et al., *Orthogonal self-assembled monolayers: alkanethiols on gold and alkane carboxylic acids on alumina*. *Science*, 1989. **245**(4920): p. 845-847.
252. Brown, P.K., et al., *Silver nanoscale antisense drug delivery system for photoactivated gene silencing*. *ACS nano*, 2013. **7**(4): p. 2948-2959.
253. Weecharangsan, W., P. Opanasopit, and R.J. Lee, *In vitro gene transfer using cationic vectors, electroporation and their combination*. *Anticancer research*, 2007. **27**(1A): p. 309-313.
254. Zu, Y., et al., *Gold Nanoparticles Enhanced Electroporation for Mammalian Cell Transfection*. *Journal of biomedical nanotechnology*, 2014. **10**(6): p. 982-992.
255. Fire, A., et al., *Potent and specific genetic interference by double-stranded RNA in *Caenorhabditis elegans**. *nature*, 1998. **391**(6669): p. 806-811.
256. Meyer, M. and E. Wagner, *Recent developments in the application of plasmid DNA-based vectors and small interfering RNA therapeutics for cancer*. *Human gene therapy*, 2006. **17**(11): p. 1062-1076.
257. Behlke, M.A., *Progress towards in vivo use of siRNAs*. *Molecular Therapy*, 2006. **13**(4): p. 644-670.
258. Elbashir, S.M., et al., *Duplexes of 21-nucleotide RNAs mediate RNA interference in cultured mammalian cells*. *nature*, 2001. **411**(6836): p. 494-498.
259. Li, B.-j., et al., *Using siRNA in prophylactic and therapeutic regimens against SARS coronavirus in Rhesus macaque*. *Nature medicine*, 2005. **11**(9): p. 944-951.
260. Zimmermann, T.S., et al., *RNAi-mediated gene silencing in non-human primates*. *Nature*, 2006. **441**(7089): p. 111-114.
261. Dorsett, Y. and T. Tuschl, *siRNAs: applications in functional genomics and potential as therapeutics*. *Nature Reviews Drug Discovery*, 2004. **3**(4): p. 318-329.
262. Kim, D.H. and J.J. Rossi, *Strategies for silencing human disease using RNA interference*. *Nature Reviews Genetics*, 2007. **8**(3): p. 173-184.
263. Jacque, J.-M., K. Triques, and M. Stevenson, *Modulation of HIV-1 replication by RNA interference*. *Nature*, 2002. **418**(6896): p. 435-438.
264. Jeong, J.H., et al., *siRNA conjugate delivery systems*. *Bioconjugate chemistry*, 2008. **20**(1): p. 5-14.
265. Akinc, A., et al., *A combinatorial library of lipid-like materials for delivery of RNAi therapeutics*. *Nature biotechnology*, 2008. **26**(5): p. 561-569.
266. Oishi, M., et al., *Smart PEGylated gold nanoparticles for the cytoplasmic delivery of siRNA to induce enhanced gene silencing*. *Chemistry Letters*, 2006. **35**(9): p. 1046-1047.

267. Giljohann, D.A., et al., *Gene regulation with polyvalent siRNA– nanoparticle conjugates*. Journal of the American Chemical Society, 2009. **131**(6): p. 2072-2073.
268. Jere, D., et al., *Poly (β -amino ester) as a carrier for si/shRNA delivery in lung cancer cells*. Biomaterials, 2008. **29**(16): p. 2535-2547.
269. Medarova, Z., et al., *In vivo imaging of siRNA delivery and silencing in tumors*. Nature medicine, 2007. **13**(3): p. 372-377.
270. Whitehead, K.A., R. Langer, and D.G. Anderson, *Knocking down barriers: advances in siRNA delivery*. Nature reviews Drug discovery, 2009. **8**(2): p. 129-138.
271. Heidel, J.D., et al., *Administration in non-human primates of escalating intravenous doses of targeted nanoparticles containing ribonucleotide reductase subunit M2 siRNA*. Proceedings of the National Academy of Sciences, 2007. **104**(14): p. 5715-5721.
272. Kumar, P., et al., *Transvascular delivery of small interfering RNA to the central nervous system*. Nature, 2007. **448**(7149): p. 39-43.
273. Peer, D., et al., *Systemic leukocyte-directed siRNA delivery revealing cyclin D1 as an anti-inflammatory target*. Science, 2008. **319**(5863): p. 627-630.
274. Chen, K. and N. Rajewsky, *The evolution of gene regulation by transcription factors and microRNAs*. Nature Reviews Genetics, 2007. **8**(2): p. 93-103.
275. He, L. and G.J. Hannon, *MicroRNAs: small RNAs with a big role in gene regulation*. Nature Reviews Genetics, 2004. **5**(7): p. 522-531.
276. Li, Y., et al., *Progressive miRNA expression profiles in cervical carcinogenesis and identification of HPV - related target genes for miR - 29*. The Journal of pathology, 2011. **224**(4): p. 484-495.
277. Garzon, R., et al., *MicroRNA 29b functions in acute myeloid leukemia*. Blood, 2009. **114**(26): p. 5331-5341.
278. Nguyen, T., et al., *Downregulation of microRNA-29c is associated with hypermethylation of tumor-related genes and disease outcome in cutaneous melanoma*. Epigenetics, 2011. **6**(3): p. 388-394.
279. Kriegel, A.J., et al., *The miR-29 family: genomics, cell biology, and relevance to renal and cardiovascular injury*. Physiological genomics, 2012. **44**(4): p. 237-244.
280. Xiong, Y., et al., *Effects of MicroRNA - 29 on apoptosis, tumorigenicity, and prognosis of hepatocellular carcinoma*. Hepatology, 2010. **51**(3): p. 836-845.
281. Calin, G.A., et al., *A MicroRNA signature associated with prognosis and progression in chronic lymphocytic leukemia*. New England Journal of Medicine, 2005. **353**(17): p. 1793-1801.

282. Cummins, J.M., et al., *The colorectal microRNAome*. Proceedings of the National Academy of Sciences of the United States of America, 2006. **103**(10): p. 3687-3692.
283. Pekarsky, Y., et al., *Tcl1 expression in chronic lymphocytic leukemia is regulated by miR-29 and miR-181*. Cancer research, 2006. **66**(24): p. 11590-11593.
284. Garzon, R., et al., *Distinctive microRNA signature of acute myeloid leukemia bearing cytoplasmic mutated nucleophosmin*. Proceedings of the National Academy of Sciences, 2008. **105**(10): p. 3945-3950.
285. Schmitt, M., et al., *MiRNA-29: a microRNA family with tumor-suppressing and immune-modulating properties*. Current molecular medicine, 2013. **13**(4): p. 572-585.
286. Gary, D.J., N. Puri, and Y.-Y. Won, *Polymer-based siRNA delivery: perspectives on the fundamental and phenomenological distinctions from polymer-based DNA delivery*. Journal of Controlled Release, 2007. **121**(1): p. 64-73.
287. Hassani, Z., et al., *Lipid - mediated siRNA delivery down - regulates exogenous gene expression in the mouse brain at picomolar levels*. The journal of gene medicine, 2005. **7**(2): p. 198-207.
288. Grayson, A.C.R., A.M. Doody, and D. Putnam, *Biophysical and structural characterization of polyethylenimine-mediated siRNA delivery in vitro*. Pharmaceutical research, 2006. **23**(8): p. 1868-1876.
289. Zou, S.M., et al., *Systemic linear polyethylenimine (L - PEI) - mediated gene delivery in the mouse*. The Journal of Gene Medicine, 2000. **2**(2): p. 128-134.